Aus dem Universitätsklinikum Schleswig-Holstein
Institut für Diabetologie und klinische Stoffwechselforschung
der Christian-Albrechts-Universität zu Kiel

The role of nicotinuric acid in metabolic inflammation and type 2 diabetes

Dissertation

Zur Erlangung des Doktorgrades
der Agrar- und Ernährungswissenschaftlichen Fakultät
der Christian-Albrechts-Universität zu Kiel

vorgelegt von

M.Sc. Juliane Brandes
aus Paderborn

Kiel, 2022

Dekan: Prof. Dr. Karl H. Mühling

1. Berichterstatter: Prof. Dr. Matthias Laudes
2. Berichterstatter: Prof. Dr. Gerald Rimbach

Tag der mündlichen Prüfung: 04. Mai 2022

Zusammenfassung

Die Prävalenz für Adipositas hat sich in den letzten Jahrzehnten verdoppelt und stellt eine ernstzunehmende Herausforderung für das Gesundheitswesen dar. Adipositas wird durch eine übermäßige Kalorienaufnahme mit massiver Ansammlung von Fettgewebe im Körper charakterisiert. Dies kann Insulinresistenz (IR) und Typ 2 Diabetes (T2D) zur Folge haben. Eine chronisch niederschwellige Entzündung kann mit einem Ungleichgewicht im Stoffwechsel der essentiellen Aminosäure Tryptophan (TRP) und des Vitamins Nikotinsäure (NA) einhergehen. NA ist bekannt für seine lipidsenkenden und anti-entzündlichen Wirkungen, die es über den GPR109A Rezeptor vermittelt. Nikotinursäure (NUA) ist das Hauptabbauprodukt von NA. Jedoch ist seine Funktion im menschlichen Körper wenig erforscht. Ziel dieser Arbeit ist mehr Einblicke in die Rolle der NUA bei metabolischer Entzündung und T2D zu erlangen.

Eine Metabolom Untersuchung wurde bei Probanden der Food Chain Plus (FoCus) Subkohorte durchgeführt, um festzustellen, ob die NUA-Intensitäten im Serum mit T2D und dem BMI assoziiert sind. Probanden mit Prädiabetes (PreD) oder T2D zeigten im Vergleich zu gesunden Probanden höhere NUA-Intensitäten. Erhöhte NUA-Intensitäten wurden bei Probanden mit einem hohen BMI im Vergleich zu den Kontrollen festgestellt. Bei den Probanden aus der gesamten FoCus-Kohorte zeigte sich eine positive Korrelation zwischen den NUA-Intensitäten im Serum und klinischen Markern wie C-reaktives Protein (CRP), Triglyceride (TG) und Lipoprotein (a) (Lp(a)). Es wurde kein Zusammenhang mit anderen Krankheiten, Nahrungsaufnahme und dem Darmmikrobiom festgestellt.

In vitro Experimente wurden durchgeführt, um den Zusammenhang zwischen NUA und metabolischer Inflammation zu untersuchen. THP-1-Zellen, die mit NUA behandelt wurden, zeigten keine Veränderungen in der Expression des Nuclear factor-κB (NF-κB) p50 Proteins. Untersuchungen mit menschlichen primären Immunzellen zeigten, dass NUA den intrazellulären Ca^{2+} Fluss in Neutrophilen induzierte und die Synthese von zyklischem Adenosinmonophosphat (cAMP) in Neutrophilen und Monozyten reduzierte. Eine Stimulierung mit NUA führte zu einer verminderten Expression des NF-κB p65-Proteins und einer geringeren Aktivierung von mitogenaktivierten Proteinkinasen (MAPK) und anderen Proteinkinasen in Monozyten.

Darüber hinaus wurden $GPR109A^{+/+}$ und $GPR109A^{-/-}$ Immunzellen von Mäusen verwendet, um zu untersuchen, ob die Auswirkungen von NUA auf die intrazelluläre Signalübertragung

von GPR109A abhängig sind. Es wurde beobachtet, dass NUA den intrazellulären Ca^{2+} Fluss in $GPR109A^{+/+}$ Neutrophilen induzierte, während dieser Effekt in $GPR109A^{-/-}$ Neutrophilen aufgehoben war. Eine Verringerung des cAMP-Spiegels durch NUA wurde in Neutrophilen und Makrophagen von $GPR109A^{+/+}$ und $GPR109A^{-/-}$ Mäusen beobachtet.

Diese Arbeit zeigt zum ersten Mal einen Zusammenhang zwischen NUA-Serumspiegeln und Stoffwechselkrankheiten wie Adipositas und T2D. Es lässt vermuten, dass die Funktion von NUA im menschlichen Körper über die eines Abbauproduktes hinausgehen könnte.

Abstract

The prevalence of obesity has doubled in the past decades and displays a severe public health issue. Obesity is characterized by an excessive calorie intake with abnormal body fat accumulation and can lead to insulin resistance (IR) and type 2 diabetes (T2D). Chronic low-grade inflammation is associated with an imbalance in metabolism of the essential amino acid tryptophan (TRP) and the vitamin nicotinic acid (NA). NA is known for its lipid modifying and anti-inflammatory characteristics via the G protein-coupled receptor 109A (GPR109A). Nicotinuric acid (NUA) exhibits the major catabolic product of NA. However, the function of NUA in the human organism is poorly studied. The aim of this thesis is to gain more insights in the role of NUA in metabolic inflammation and T2D.

A metabolomics-based approach in subjects of the Food Chain Plus (FoCus) sub-cohort was performed to evaluate if serum NUA intensities are associated with T2D and BMI. Subjects with prediabetes (PreD) or T2D showed higher NUA intensities compared to healthy subjects. Increased NUA intensities were found in subjects with a high BMI compared to controls. Subjects from the total FoCus cohort revealed a positive correlation between serum NUA intensities and clinical markers such as c-reactive protein (CRP), triglycerides (TG) and lipoprotein (a) (Lp(a)). No association with other diseases, nutritional intake and gut microbiome was observed.

In vitro experiments were performed to evaluate the association between NUA and metabolic inflammation. THP-1 cells, treated with NUA, showed no alterations in nuclear factor-κB (NF-κB) p50 protein expression. Investigations with human primary immune cells demonstrated that NUA induced intracellular Ca^{2+} flux in neutrophils and reduced cyclic adenosine monophosphate (cAMP) levels in neutrophils and monocytes. NUA treatment led to extenuated NF-κB p65 protein expression and decreased activation of mitogen-activated protein kinases (MAPK) and other protein kinases in monocytes.

Furthermore, $GPR109A^{+/+}$ and $GPR109A^{-/-}$ murine immune cells were used to examine if the effects of NUA on intracellular signalling are GPR109A-dependent. It was observed that NUA induced intracellular Ca^{2+} flux in $GPR109A^{+/+}$ neutrophils while this effect was abrogated in $GPR109A^{-/-}$ neutrophils. Reduction of cAMP levels by NUA was observed in neutrophils and macrophages of $GPR109A^{+/+}$ as well as $GPR109A^{-/-}$ mice.

This thesis shows for the first time an association between serum NUA levels and metabolic diseases such as obesity and T2D and gives an estimation that NUA`s function in the human body might be more than acting as catabolic product.

Table of content

Abbreviations

Adipocyte triglyceride lipase	ATGL
Arachidonic acid	AA
Aryl hydrocarbon receptor	AhR
Bcl-2 associated agonist of cell death	BAD
Body weight	BW
Bone marrow derived	BMD
Bovine serum albumin	BSA
c-Jun N-terminal kinases	JNK
C-reactive protein	CRP
Cyclooxygenase-1	COX-1
Cyclic adenosine monophosphate	cAMP
Dimethyl fumarate	DMF
Dulbecco’s Modified Eagle’s Medium	DMEM
Extracellular signal-regulated kinases 1 and 2	ERK1/2
False discovery rate	FDR
Fetal calf serum	FCS
N-formyl-methionyl-leucyl-phenylalanine	fMLF
Food Frequency Questionnaire	FFQ
Fourier-transform ion cyclotron resonance mass spectrometry	FT-ICR-MS
Free fatty acids	FFA
Glyceraldehyde 3-phosphate dehydrogenase	GAPDH
G protein-coupled receptor	GPCR
G protein-coupled receptor 109A	GPR109A
Hanks' Balanced Salt Solution	HBSS
High-density lipoprotein cholesterol	HDL-C
High-sensitivity C-reactive protein	hs-CRP
Hormone sensitive lipase	HSL
Human metabolome database	HMDB
Hydroxy-carboxylic acid receptor 2	HCA_2
Indoleamine 2,3-dioxygenase	IDO1
Indoleamine 2,3-dioxygenase 2	IDO2

Institute of Clinical Molecular Biology	IKMB
Insulin resistance	IR
Interleukin-1β	IL-1β
Interleukin-6	IL-6
Interleukin-4	IL-4
Kyoto Encyclopedia of genes and genomes	KEGG
Low-density lipoprotein cholesterol	LDL-C
Lipoprotein (a)	Lp(a)
Lipopolysaccharide	LPS
Level of detection	LOD
Magnetic-activated cell sorting	MACS
Mitogen-activated protein kinase	MAPK
MAPK kinase 1	MAPKK1
MAPK kinase 2	MAPKK2
MAPK kinase 3	MAPKK3
MAPK kinase 4	MAPKK4
MAPK kinase 6	MAPKK6
MAPK kinase 7	MAPKK7
MAPK kinase kinase	MAPKKK
Monocyte chemoattractant protein-1	MCP-1
Nicotinic acid	NA
Nicotinamide	NAM
Nicotinamide adenine dinucleotide	NAD
Nicotinamide adenine dinucleotide (phosphate)	NAD(P)
Nicotinuric acid	NUA
N-methylnicotinamide	NMA
N-methyl-2-pyridone-5-carboxymide	2PY
N-methyl-4-pyridone-5-carboxamide	4PY
Nuclear factor-κB	NF-κB
Operational taxonomic unit	OTU
Phosphate buffered saline	PBS
Phospholipase A_2	PLA_2
Peripheral blood mononuclear cells	PBMCs
Peritoneal macrophages	PEMs

Phorbol 12-myristate 13-acetate	PMA
Phosphoinositide-3 kinase	PI3K
Polymerase chain reaction	PCR
Prediabetes	PreD
Prostaglandin D_2	PGD_2
Prostaglandin E_2	PGE_2
Protein kinase A	PKA
Protein kinase B	Akt
Radioimmunoprecipitation assay	RIPA
Red fluorescent protein	RFP
Room Temperature	RT
Sodium Dodecyl Sulphate Polyacrylamide Gel Electrophoresis	SDS-PAGE
Specific pathogen free	SPF
Tumor necrosis factor-α	TNF-α
Transcription factor	TF
Triglycerides	TG
Tryptophan	TRP
Tryptophan 2,3-dioxygenase	TDO2
Type 2 diabetes	T2D
Very low-density lipoprotein cholesterol	VLDL-C
World Health Organisation	WHO
Zentrale Tierhaltung	ZTH
5`AMP-activated protein kinase	AMPK
5`AMP-activated protein kinase α	AMPKα

List of figures

List of tables

1 Introduction

Obesity and T2D display a global health issue which rises continuously and affects adults as well as children (1, 2). Obesity results from excessive caloric intake and is associated with metabolic inflammation, which can spread from the adipose tissue to other organs such as liver, muscle and hypothalamus (3, 4, 1).

Niacin, which is the general term for NA and nicotinamide (NAM), is a fundamental vitamin in energy metabolism and oxidative phosphorylation in all cells. It is involved in ATP synthesis, DNA repair and detoxification of reactive oxygen species (ROS) by being a nutritional precursor of nicotinamide adenine dinucleotide (NAD) (5–7). As endogenous source, niacin is metabolized from the amino acid TRP via the kynurenine pathway while animal and plant based foods enable exogenous niacin uptake (8–11). Niacin displays the major factor in preventing pellagra disease. Causes for niacin deficiency are a low niacin/ TRP diet, genetic diseases, malignant events, infections and metabolic diseases (6). Obesity is linked to a shift in the kynurenine pathway. While the conversion of TRP to niacin is downregulated, leading to niacin deficiency, the synthesis of other TRP metabolites, such as xanthurenic acid, is increased which reinforces low-grade inflammation. However, the exact mechanism are still elusive (12).

NA is well-known for its broad spectrum of beneficial effects such as amelioration of the lipid profile when co-administered with statins. Studies showed that NA is able to enhance high-density lipoprotein cholesterol (HDL-C) levels and at the same time it reduces levels of Lp(a), very low-density lipoprotein cholesterol (VLDL-C) and low-density lipoprotein cholesterol (LDL-C). Furthermore, NA decreases the expression of adhesion molecules in endothelial cells which reduces the progression of atherosclerosis (13). Several studies also confirmed a markedly reduction of inflammatory markers like high-sensitivity C-reactive protein (hs-CRP) and tumor necrosis factor-α (TNF-α) by NA in human monocytes. These findings have emerged to be GPR109A dependently which represents the receptor of NA (14). A growing body of evidence supports that NA positively affects metabolic inflammation by changing the composition of the gut microbiome. It was shown that low dietary NA intake in obese subjects is associated with a reduced α-diversity and *Bacteriodetes* abundance. In another study, it was observed that 6-week administration of NA microcapsules raised *Bacteriodetes* abundance in the gut of healthy subjects and enhanced insulin sensitivity in liver and muscle tissue (7).

NUA represents the main catabolic product of NA (15). After oral uptake, NA is rapidly converted into NAM/NAD in the intestine and liver. Saturation of the NAD pathway leads to

transformation of NA into NUA by glycine conjugation and excretion via the kidneys (16–18). Although, NA is well-known for its pleotropic effects in the human organism, the functionality of NUA is hardly explored. In 1960, a clinical study showed that subjects treated with NUA had markedly reduced serum cholesterol levels compared to controls (19) and a metabolomics-based approach showed a positive association between urinary NUA levels and markers of metabolic inflammation such as hypertension and LDL-C (15). So far, data from *in vitro* studies, investigating the functionality of NUA, barely exist. It was shown that NUA affects polarisation capacity of healthy human monocytes. While NA and NAM induced a shift towards anti-inflammatory M_2-macrophages, NUA initiated the formation of pro-inflammatory M_1-macrophages (20). Based on these results, it might be assumed that NUA displays more than just a degradation product.

With special focus on NUA, the aim of this thesis was to gain more insights into the association between TRP - NA metabolites and metabolic diseases such as obesity and T2D. (I) A metabolomics-based approach in subjects of the FoCus sub-cohort was performed to compare the abundance of TRP-NA metabolites between healthy subjects and diabetic or obese subjects. Furthermore, the association of NUA with clinical markers, nutritional intake and gut microbiome was examined in the total FoCus cohort. (II) *In vitro* studies were performed to evaluate the effects of NUA on intracellular immune signalling and its GPR109A-dependence. (III) Furthermore, the expression of GPR109A in the metabolic active tissues liver and hypothalamus was investigated by immunohistochemistry.

2 Theoretical background

2.1 The complexity of obesity, IR and metabolic inflammation

Obesity reveals a complex multifactorial disease and it is known to be a major risk factor for development of a PreD and T2D. The prevalence of obesity has doubled in the past 40 years, with a third of the world`s population which has been diagnosed with overweight or obesity. Obesity is characterized by a higher energy intake compared to energy expenditure and is accompanied with diverse endocrine abnormalities such as IR and hypothalamic inflammation. Obesity affects all ages and both sexes. Older people and women exhibit a higher prevalence in obesity (21–25, 4).

Insulin induces the uptake of glucose from blood into muscle cells by translocation of glucose transporter 4 to the plasma membrane. Insulin regulates levels of free fatty acids (FFA) by reducing lipolysis and inhibits gluconeogenesis in the liver. IR is defined as impaired insulin sensitivity of target organs like liver, adipose tissue and muscle tissue which can result in T2D (26).

Obesity is associated with increased levels of TG which accumulate in adipocytes as energy storage. Increased TG accumulation leads to hypertrophy and hyperplasia of adipocytes (25). In this condition, adipocytes are poorly oxygenated which induces stress in the endoplasmatic reticulum. Thus, cell apoptosis is initiated, pro-inflammatory M_1-macrophages infiltrate the adipose tissue and the G_0/G_1-phase cell cycle is stopped by the MAPKs protein kinase B (Akt) and c-Jun N-terminal kinases (JNK). Consequently, adipocytes secret increased levels of pro-inflammatory adipokines such as leptin and interleukin-6 (IL-6). Furthermore, they express reduced concentrations of anti-inflammatory adipokines as adiponectin (3, 26). Adiponectin physiologically ameliorates insulin sensitivity and is negatively correlated with abdominal obesity, IR and T2D (27). Consequently, IR leads to elevated levels of FFA, followed by ectopic fat deposition forming the visceral adipose tissue. Thus, metabolic inflammation takes over from adipose tissue to other metabolic active organs like liver, skeletal muscle and pancreas which deteriorates IR (26, 3). Obesity is often characterized as a neuroendocrine disease. Leptin, a major anorexigenic hormone, released from adipose tissue, physiologically mediates signal of satiety in mediobasal hypothalamus. However, chronic low-grade inflammation can cause hypothalamic inflammation followed by leptin resistance which further reinforces the development of obesity (4).

The association between the human gut microbiome and obesity is also of high interest in medical research. It was observed that obese patients show alterations in α-diversity and β-diversity of their gut microbiome which can reinforce disease progression. *Bacteriodetes* and *Firmicutes* belong to the main bacterial phyla in the human gut and it is described that obese subjects reveal a lower *Bacteriodetes* and a higher *Firmicutes* abundance compared to lean subjects (28, 29, 7).

2.2 Metabolic inflammation and TRP metabolism

TRP is an essential amino acid and is ingested from protein-based food such as meat, dairy products and seeds. It displays a key factor in metabolism as it is converted into pleiotropic compounds for various metabolic pathways besides its important part in protein synthesis (8, 30). There are four pathways of TRP degradation: In small amounts, TRP is decarboxylated to tryptamine, transaminated for indole-pathway or hydroxylated to serotonin which is an important neurotransmitter for regulation of cognition, mood-anxiety and feeding behaviour. However, 95% of TRP is degradated to kynurenine via the kynurenine pathway which primarily takes place in the liver and is initiated by the enzymes TRP 2,3-dioxygenase (TDO2) and indoleamine 2,3-dioxygenase 2 (IDO2). To a small percentage, the kynurenine pathway also exists in extrahepatic tissues such as adipose tissue. In these tissues, TRP degradation is induced by the enzyme indoleamine 2,3-dioxygenase (IDO1). The serum kynurenine/TRP ratio is used to determine IDO1 activity (9, 12, 8). Along the kynurenine pathway, TRP is metabolised to 3-hydroxykynurenine, 3-hydroxyanthranilic acid and quinolinic acid which are precursors of NA, NAM and nicotinamide adenine dinucleotide (phosphate) (NAD(P)). In another branch of the kynurenine pathway, TRP is transformed into kynurenic acid and xanthurenic acid (31).

Alterations in TRP-downstream pathways are associated with several diseases. A diminished serotonin production can lead to mood affective disorders, obesity and anorexia (8). The extrahepatic kynurenine pathway is known to be associated with immune dysfunction (9). Hypertrophy of adipocytes results in a polarization from anti-inflammatory M_2-macrophages to pro-inflammatory M_1-macrophages with an increase of pro-inflammatory cytokines such as TNF-α and interleukin 1β (IL-1β) (3, 26, 32). This shift leads to enhanced IDO1 activation with an increase of the kynurenine/TRP ratio in adipose tissue. Elevated IDO1 induces increased kynurenic acid and xanthurenic acid production by the enzymes kynurenine aminotransferase III (CCBL2) and kynurenine 3-monooxygenase (KMO). Due to this shift, niacin synthesis via kynureninase (KYNU) is diminished **(Fig 1)**. While kynurenic acid exhibits neuroprotective

and anti-inflammatory properties, xanthurenic acid reveals neurotoxic and zinc-chelating characteristics leading to disturbance of insulin secretion (33, 12). To build up NA, the enzymes of the kynurenine pathway require the active form of pyridoxal-5-phosphate (Vit B6) which is often deficient in obesity and T2D. Thus, NA depletion is further reinforced (34, 33).

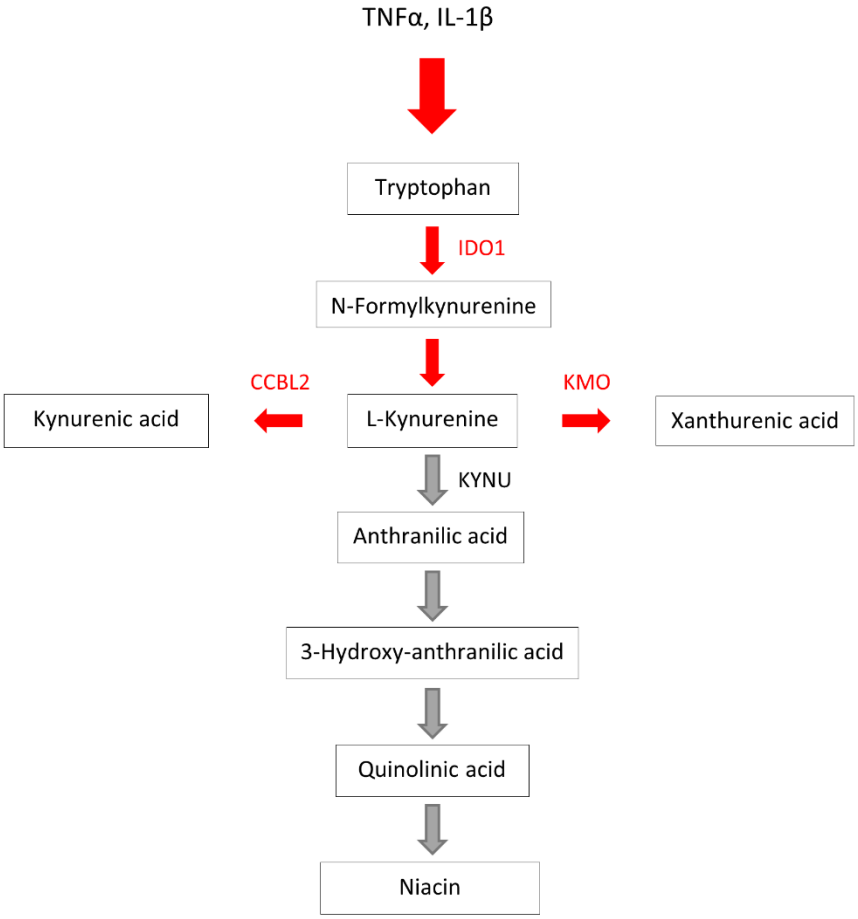

Figure 1: Degradation of TRP via the kynurenine pathway in obesity: Hypertrophy and hyperplasia of the adipose tissue lead to increased levels of pro-inflammatory cytokines (TNF-α, IL-1β) followed by the activation of the enzymes IDO1, CCBL2, KMO. TRP is increasingly converted into kynurenic acid and xanthurenic acid. Formation of niacin is reduced. (Own illustration)

2.3 Niacin – general background

Niacin is a general term for the two vitamers NA and NAM. It is also called Vitamin B3 or Vitamin PP (Pellagra preventing) (35, 36). NAM represents the active form of Vitamin B3 (37). In human organism, NA and NAM can be converted into each other and they are quantitatively and qualitatively equivalent regarding their biological properties (36). They both are precursors for the biologically active coenzymes NAD and its phosphorylated derivative NADP which are essential for energy production and anabolism (35, 38).

The kynurenine pathway is the endogenous source for niacin synthesis (35). However, NA synthesis from TRP is not efficient since 60mg TRP results in 1mg niacin. A daily niacin intake of 8-17 mg-equivalent for children/adolescents and 11-16 mg-equivalent for adults is recommended (10). The European Food Safety Authority suggests an intake of 5.5-6.6mg niacin equivalent/1000kcal to maintain anabolic and catabolic processes (39, 20). Animal based products such as fatty fish, lean meat and dairy products are rich in niacin. But also plant based food like legumes, nuts, green leafy vegetables, mushrooms, bread and coffee offer great amounts of NA and NAM. Niacin digested from animal based food shows better absorption than from plant based products. In grains, NA and NAM are largely bound and bioavailability is small (37, 40).

NA deficiency can lead to the nutritional disorder pellagra with clinical manifestations from skin (e.g. skin lesions), nervous system (e.g. disorientation) and the gastrointestinal tract (e.g. diarrhea) (41). In contrast, pharmacological doses of NUA can also elicit several adverse reactions. It is well documented that administration of NA can induce insulin resistance and increased $HbA1_c$ levels in diabetic patients. However, flush symptomatic exhibits the most common side effect of NA. Patients often complain about burning and itching skin in the upper half of the body. It is induced by prostaglandin D_2 (PGD_2) release in skin cells which can be attenuated by application of the PGD_2 selective antagonist Laropiprant (13, 42).

2.4 Metabolism of NA

NA is absorbed from stomach and the upper small intestine via sodium-dependent diffusion and by passive diffusion (43, 37). Furthermore, the microbiome in the large intestine is able to synthesize NA from TRP (44, 45). After intestinal absorption, NA undergoes a first pass metabolism in the liver which includes two pathways (46, 17): Initially, NA is converted into NAM, NAD, N-methylnicotinamide (MNA), N-methyl-2-pyridone-5-carboxymide (2PY) and

N-methyl-4-pyridone-5-carboxamide (4PY). This pathway is characterized by a low capacity and high affinity for NA conversion and is associated with hepatotoxicity because of long-acting systemic niacin compounds. When the first pathway is saturated, the second pathway is activated and NA is conjugated with glycine to form NUA. This pathway exhibits a high capacity but low affinity (17) **(Fig. 2)**. The formation of NUA is discussed to be responsible for flushing effects. All niacin metabolites are excreted via the urine (46).

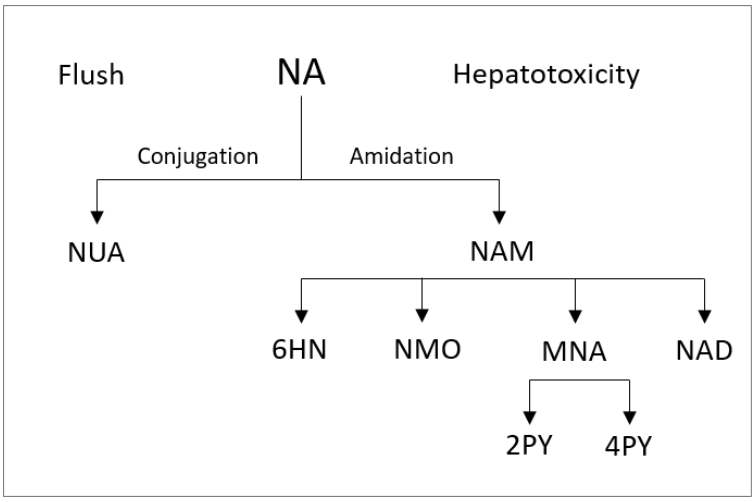

Figure 2: Hepatic metabolism of NA: Via the first pathway, NA is metabolised into NAM for energy metabolism. In the second pathway, NA is converted into NUA for renal excretion (based on (17)).

2.5 NA as a lipid modifying drug

Lipid disorders, such as extenuated HDL-C levels, are highly associated with the risk for cardiovascular diseases (46, 47). Pharmacological doses of NA (1500-3000 mg/day) reveal a broad-spectrum lipid drug since it elevates HDL-C levels in the blood (46, 20). NA increases the stability and function of ApoA-I, an important constituent of HDL-C via the liver x receptor. NA downregulates the surface expression of the hepatic HDL receptor β-chain ATP synthase. Accordingly, HDL-C uptake in the liver is reduced which enhances HDL-C availability for cholesterol scavenging in the blood (47). While HMG-CoA-reductase inhibitors (statins) raise HDL-C levels up to 10%, NA induces an elevation up to 35%. NA also reduces serum levels of VLDL-C, TG and Lp(a). It also leads to a decrease of plasma FFA within minutes after administration while VLDL-C and TG are diminished after a few hours. Regulation of LDL-C

and HDL-C takes several days of treatment. Thus, NA treatment contributes to the reduction of cardio vascular morbidity and mortality (46).

2.6 NA mediates its effects via GPR109A

The G protein-coupled receptors (GPCRs) encompass a protein family of transmembrane receptors with a key role in the research of cancer and diabetes treatment. GPR109A, also known as hydroxy-carboxylic acid receptor 2 (HCA_2), is a receptor for the predominate ketone body β-hydroxybutyrate (48, 49). GPR109A is expressed by adipocytes and immune cells such as neutrophils, dendritic cells, monocytes and macrophages, however there is no expression by lymphocytes. Various epithelial cells i.e. intestinal cells, retinal pigment cells and keratinocytes show GPR109A surface expression. Expression by other tissues is not fully elucidated yet (49, 48, 50, 14, 51, 52).

NA is a selective agonist of GPR109A by which it mediates its lipid modifying effects. (53) In adipocytes, NA activates GPR109A via the heterotrimeric G protein, G_i, which inhibits the adenylyl cyclase and leads to a reduction of cAMP levels and protein kinase A (PKA) levels. Furthermore, NA induces a temporary increase of intracellular Ca^{2+}. This leads to a downregulation of hormone sensitive lipase (HSL) and adipocyte triglyceride lipase (ATGL) arresting lipolysis. In turn, FFA flux is decreased which leads to a diminished TG synthesis in the liver. Accordingly, VLDL-C and LDL-C are less abundant in the blood **(Fig. 3 A)** (49, 54, 13).

Neutrophils are part of the innate immune system and reflect the most abundant leukocytes in circulation. They are the first cell type of defence and also play a key role in inflammation. Under normal homeostatic conditions, a low number of neutrophils are present in organs like liver and adipose tissue (55). Regulation of granulopoiesis in the bone marrow and systemic apoptotic processes physiologically maintain balance of neutrophils (56). This balance is diminished under conditions of inflammatory diseases like obesity in which the amount of neutrophils rises quickly (55). Conglomerations of immune cells can lead to an enhanced release of toxic intracellular products that reinforce the state of chronic inflammation including tissue injury as well as organ failure. It was shown that NA can induce apoptosis in neutrophils. Via GPR109A activation, NA induces a block of adenylyl cyclase activity with downregulation of cAMP and PKA levels. In the following, dephosphorylation of Bcl-2 associated agonist of cell death (BAD) increases which induces apoptosis of neutrophils **(Fig. 3 B)** (56).

NA also reveals anti-inflammatory capacities in monocytes and macrophages (56). Via activation of GPR109A, NA is able to decrease the NF-κB signalling pathway in human monocytes (14, 51). The NF-κB transcription factors (TF) include NF-κB2 (p52/p100), RelB, c-Rel and the most common forms NF-κB1 (p50/p105) and p65 (RelA). They are of great importance since they play a crucial role in cell adaption and response to external stimuli (57–59). Phosphorylation of NF-κB`s inhibitor IκBα leads to the activation and nuclear translocation of NF-κB which initiates transcription of target genes involved in cell migration, inflammation and apoptosis. Therefore, NF-κB is a central regulator in development of metabolic diseases such as obesity and T2D (58, 14, 60, 61). In monocytes and macrophages, NA`s anti-inflammatory effects are characterized by the inhibition of NF-κB phosphorylation. This is facilitated by β-Arrestins, binding to IκBα, which leads to diminished NF-κB levels with decreased synthesis of IL-6, TNF-α and monocyte chemoattractant protein-1 (MCP-1) **(Fig. 3 C)** (51, 58, 62). Furthermore, it was reported that via GPR109A, NA mediates a reduction of cAMP levels in basal macrophages in an anti-inflammatory manner (63).

As already mentioned, pharmacological doses of NA can elicit side effects in the skin. In epidermal macrophages (Langerhans cells), GPR109A activation by NA mobilizes intracellular Ca^{2+} which induces elevated levels of phospholipase A_2 (PLA_2) and arachidonic acid (AA). The cyclooxygenase-1 (COX-1) converts AA into PGD_2 and prostaglandin E_2 (PGE_2). They consequently initiate vasodilation in the epidermal vasculature which generates the characteristic symptoms of flushing **(Fig. 3 D)** (64, 18).

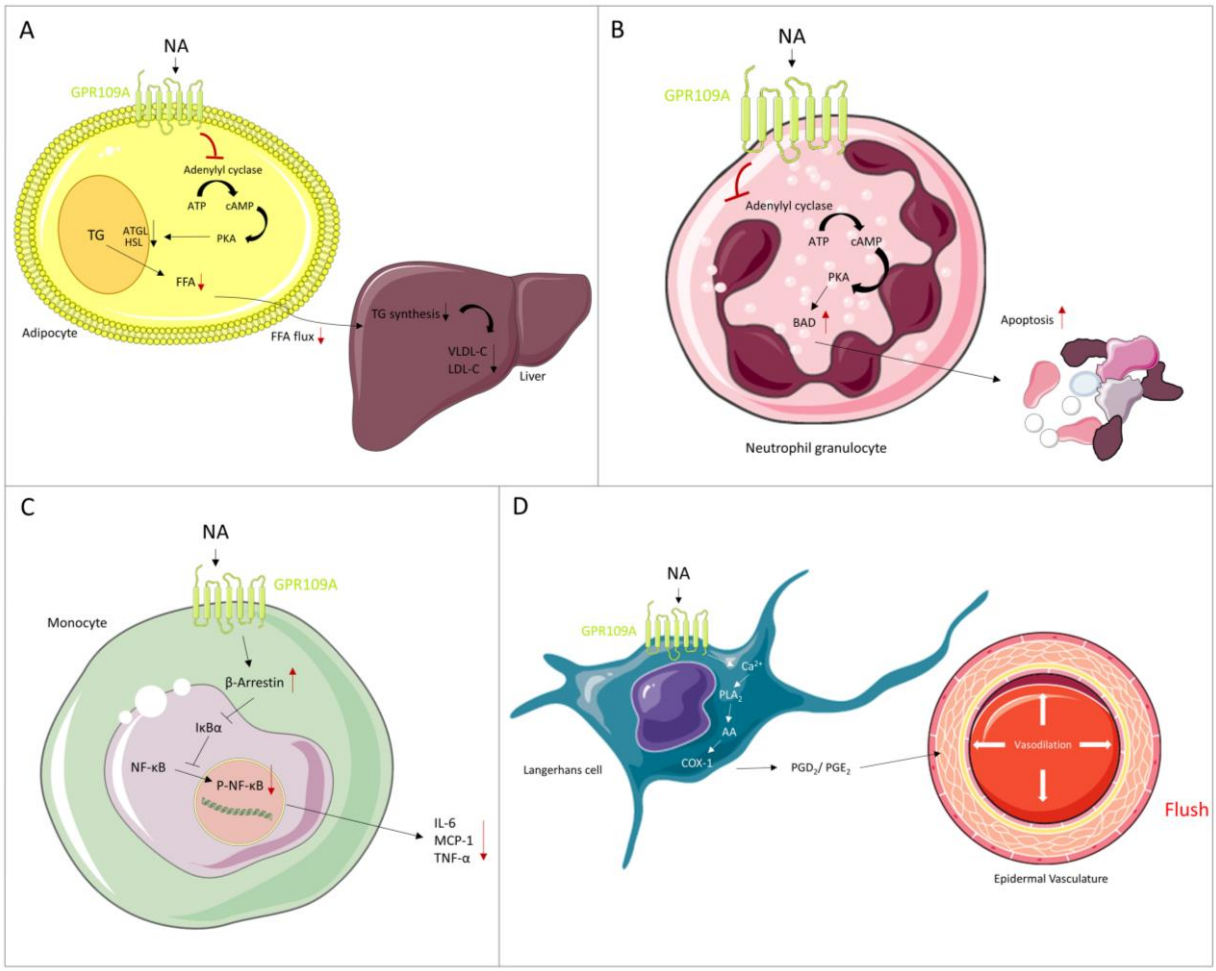

Figure 3: GPR109A dependent effects of NA on different cell types: (A) In adipocytes, NA reduces adenylyl cyclase activity which leads to reduced cAMP levels and improves levels of TG, VLDL-C, LDL-C in the liver **(B)** In neutrophils, NA also reduces adenylyl cyclase activity which induces regulatory apoptosis **(C)** In monocytes, NA induces β-Arrestin activity which inhibits phosphorylation of NF-κB. Consequently, pro-inflammatory cytokines (IL-6, MCP-1, TNF-α) are down-regulated **(D)** In Langerhans cells, NA initiates increased PGD_2/PGE_2 levels which induce vasodilation in epidermal vasculature. Symptoms of a flush generate. The figure was generated by using items of Servier Medical Art, provided by Servier, licensed under a Creative Commons Attribution 3.0 unported license (Own illustration).

2.7 The role of NA in MAPK signalling

Cells are continuously urged to be attentive to numerous stimuli from the extracellular space and therefore to coordinate their intracellular responses (65). MAPKs are components of the most ancient cell signalling pathways from the cell membrane to the nucleus and are present in all eukaryotes. Therefore, they exhibit a major role in many physiological processes. Their activation is enabled by multistep protein kinase cascades in which they are phosphorylated on a tyrosine and threonine residue (66, 67). These signalling pathways coordinate the response to various stimuli such as hormones, growth factors and inflammatory mediators acting through GPCRs. Hence, MAPKs pathways reflect a complex interplay according to cell differentiation, protein biosynthesis, gene transcription, cell cycle control and apoptosis. Together with the NF-κB pathway, the MAPKs are activated by stress and inflammatory stimuli. Therefore, they are of great concern for drug research in inflammatory diseases (68).

Extracellular signal-regulated kinases 1 and 2 (ERK1/2), JNK and p38 belong to the most investigated MAPKs in mammalians and NA is known to affect these MAPKs in different ways (69, 67, 70).

The MAPK p38 is also present in many cell types such as immune and endothelial cells and is involved in immune response, cell survival and differentiation (71, 72, 65). p38 is activated by the MAPK kinase 3 (MAPKK3) and MAPK kinase 6 (MAPKK6) (73). After activation via GPCRs, p-p38 acts downstream by phosphorylation of its substrates and TFs such as Elk-1 which in turn induces synthesis of pro-inflammatory cytokines like TNF-α, IL-1β and cyclooxygenase-2 **(Fig. 4)** (74, 71). Previous studies described the beneficial effects of NA in brain injury after cardiac arrest by downregulation of the p38 signalling pathway (69). Furthermore, inhibition of p38 phosphorylation by NA decreased pro-inflammatory myeloperoxidase which is known to reinforce chronic diseases including cancer, atherosclerosis and Parkinson`s disease (75).

ERK 1/2 plays a major role in cell differentiation, proliferation and cell signal transduction network (76). For activation, ERK1/2 is phosphorylated by the MAPK kinase 1 (MAPKK1) und MAPK kinase 2 (MAPKK2). Subsequently, p-ERK1/2 phosphorylates TFs such as c-Fos **(Fig. 4)** (73). In monocytes and macrophages, ERK1/2 activation via toll-like receptors leads to elevation of pro-inflammatory IL-6 levels which makes it an important agent in pathological conditions like chronic inflammation and obesity (77–79). ERK1/2 is also known to be a beneficial mediator in the inhibition of chemoattractant-induced migration of macrophages. Shi

et al. showed that NA induced phosphorylation of ERK 1/2 via GPR109A and inhibited chemoattractant-induced migration of macrophages (80). However, the knowledge of NA`s effects on ERK signalling is still marginal.

JNK is the third of the main MAPKs and is involved in cell differentiation, morphogenesis, cellular stress and apoptosis and displays a major factor in inflammatory responses. Activation of JNK signalling pathways via GPCRs leads to the phosphorylation of JNK at its threonine and tyrosine residues by the MAPK kinase 4 (MAPKK4) and MAPK kinase 7 (MAPKK7). p-JNK translocates into the nucleus to phosphorylate TFs such as c-Jun leading to increased synthesis of IL-6 and TNF-α **(Fig. 4)** (81–83, 73). Hereby it is to be mentioned that the two JNK members JNK1 (46kDa) and JNK2 (54kDa) especially have a high affinity for c-Jun phosphorylation (84). Previous studies showed an augmented activation of JNK signalling in obese patients (85) JNK1/2 activation in macrophages leads to increased levels of pro-inflammatory cytokines that reinforce IR (86). On the other side, it is described that phosphorylation of JNK inhibits immune cell migration (80). Studies of NA`s effects in JNK signalling in obesity and T2D barely exist (85). An *in vivo* study showed reduced JNK levels in brain homogenates of rats by different doses of NA which led to amelioration of brain damage after cardiac arrest (69).

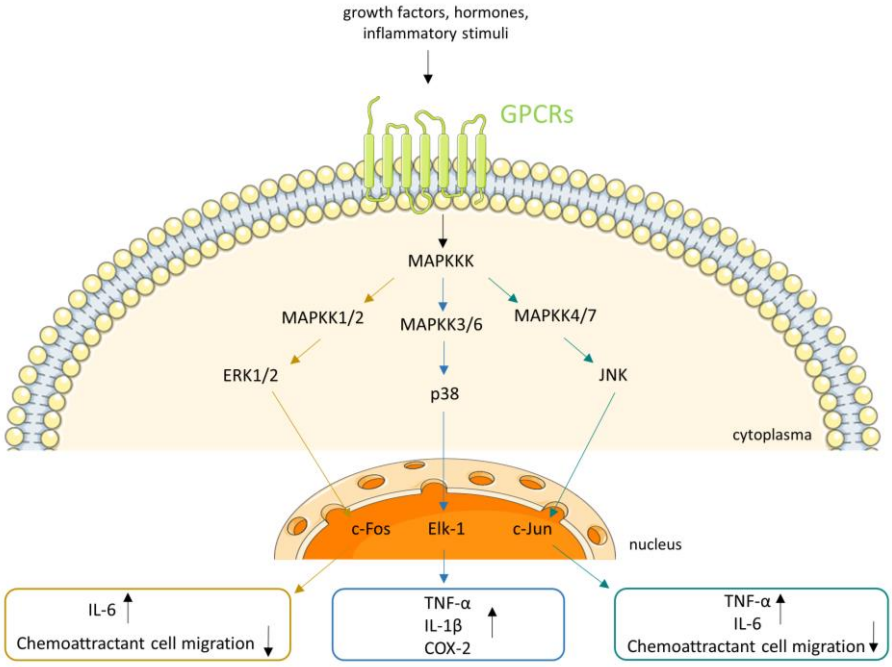

Figure 4: Signalling pathways of the MAPK ERK1/2, p38 and JNK: Via GPCRs extracellular stimuli induce phosphorylation of the MAPK kinase kinases (MAPKKK) which phosphorylate MAPKK. MAPKK 1 and 2 phosphorylate ERK1/2 which activates the TF c-Fos in the nucleus which leads to elevated levels of IL-6 or reduced immune cell migration. MAPKK 3 and 6 phosphorylate p38 which phosphorylates Elk-1 and induces increased levels of pro-inflammatory cytokines. MAPKK 4 and 7 phosphorylate JNK which activates c-Jun and promotes synthesis of pro-inflammatory cytokines or reduces immune cell migration. The figure was generated by using items of Servier Medical Art, provided by Servier, licensed under a Creative Commons Attribution 3.0 unported license (Own illustration).

2.8 The role of NA in PI3K/Akt signalling

The Akt signalling pathway is activated by the phosphoinositide-3 kinases (PI3Ks) via receptor tyrosine kinases or GPCRs. Akt is involved in a wide range of cellular processes like growth, metabolism, proliferation and apoptosis. The PI3K/Akt pathway is not only present in cells of the adaptive immune system but also in neutrophils, monocytes and macrophages and plays a crucial role in the regulation of inflammatory diseases such as rheumatoid arthritis, multiple sclerosis and T2D (54, 87, 88). NA is able to activate PI3K/Akt signalling via GPR109A in macrophages although the mechanisms are still unknown. Furthermore, it was shown that NA exhibits anti-apoptotic effects via the PI3K/Akt pathway in stroke patients and subjects suffering from UV-induced skin damage (54).

2.9 The role of NA in AMPKα signalling

5`AMP-activated protein kinase (AMPK) is a serine/threonine kinase and consists of a catalytic subunit (α) and two regulatory subunits (β, γ). It displays a pivotal role in cell metabolism by being a sensor for intracellular energy state. With increase of the AMP/ATP ratio, AMP and ADP bind to the γ-subunit. The AMPKs threonine 172 residue of the α subunit is additionally phosphorylated, resulting in the activation of AMPK. p-AMPK then downregulates anabolic pathways while catabolic pathways are enhanced to produce ATP. Therefore, AMPKα plays an important role in the adaption of metabolism, differentiation and growth (89). Activation of AMPKα leads to a downregulation of fatty acid and cholesterol synthesis in the liver as well as decreased fatty acid oxidation and glycolysis in heart and muscle tissue (90). An imbalance of intracellular AMPK signalling can reinforce progression of obesity and T2D (91). It was reported that NA mediates inhibition of lipogenesis by increased phosphorylation of AMPK in hepatocytes initiated by GPR109A activation (92). Furthermore, AMPKα phosphorylation is induced by anti-inflammatory agents and inactivated by pro-inflammatory mediators. However, the exact mechanisms are hardly investigated (90, 92).

2.10 The metabolite NUA

NUA, also called Nicotinoylglycine, was first determined in 1912 in the urine of a dog fed with NA. Further investigations also detected amounts of NUA in the urine of humans and rodents (93). NUA is the major catabolic product of NA and is also assumed to be involved in fatty acid β-oxidation (15, 94). Dietary ingested NA is rapidly converted to NAM and NAD in the intestine and in the liver. NAM is then transferred into blood system. Once the NAM pathway is saturated, NA is quickly converted into nicotinyl-CoA by binding Coenzyme A and consecutively conjugated with glycine to form NUA. Afterwards, NUA is excreted via the urine. Therefore, NUA displays a specific indicator for biotransformation of NA in the liver and they are mostly measured together by mass spectrometry (16, 95, 96, 17, 15, 97, 98). High plasma doses of NA and NUA can only be measured when administering pharmacological doses as i.v. injection or rapid release supplements. Oral application requests high doses of NUA because of its low absorption in the intestine (16, 19).

There is little knowledge about NUA`s functionality in the human body. A receptor or transporter is not known yet. Also controversial opinions about NUA being involved in flush response exist (97). A clinical study from 1989 observed that co-administration of

acetylsalicylate reduced flushing response as well as decreased NUA serum levels. It is assumed that NA and acetylsalicylate compete in glycine conjugation which reduces NUA formation (99).

First clinical investigations assumed cholesterol lowering effects by NUA, however data have not been validated yet (19). Furthermore, a positive association between urinary NUA levels and symptoms of metabolic syndrome has been postulated (15, 19). An *in vitro* study investigated polarisation behaviour in human primary macrophages after incubation with NA and its metabolites. NA and NAM increased the expression of specific phenotypic markers for M_2- macrophages (CD200R, MRC1) while NUA was observed to induce M_1-macrophages (CD80, CD64) polarization (20). These are the first *in vitro* results which showed that NUA affects cellular responses.

With regard to this, it is assumed that NUA might be more than a catabolic product.

3 Materials

Table 1: Buffer compositions

Buffer	Reagents
Blocking buffer	50 g Milk-Powder 950 g dH_2O
Extraction buffer	50% Ethanol 49% dH_2O 1% Acetic Acid
MACS buffer	PBS 2mM EDTA 0.5% BSA
RIPA cell lysis buffer	Tris/HCL (pH 7.4) 50mM NaCl 150mM Na-Deoxycholat 0.5% SDS 0.1% Nonidet P-40 1% EDTA 2mM dH_2O
1 x SDS-PAGE-Running buffer	100 mL 10 x SDS dH_2O ad 1000 mL
10 x SDS-PAGE-Running Buffer	60.4 g Tris base 288 g glycine 20 g SDS dH_2O ad 2000 mL
10 x TBS buffer	140 g NaCl 4 g KCl 60 g Tris Base pH=7.4 with HCL (25%) dH_2O ad 2000 mL
1 x TBS/T buffer	100 mL 10 x TBS 1 mL Tween-20 dH_2O ad 1000 mL
Transfer buffer A	36.34 g Tris Base 200 mL Methanol dH_2O ad 1000 mL
Transfer buffer B	3.03 g Tris Base 200 mL Methanol dH_2O ad 1000 mL
Transfer buffer C	36.34 g Tris Base 200 mL Methanol 5 g Aminocapronic acid dH_2O ad 1000 mL
Tris HCl 0.658 M	7.57g Tris HCL 70 mL dH_2O pH=6.8 with HCL (25%) dH_2O ad 100 mL

Tris HCl 1.88 M	22.71 g Tris HCL 70 mL dH_2O pH=8.8 with HCL (25%) dH_2O ad 100 mL

Table 2: Chemicals and reagents

Product	Manufacturer	Product number
ABC-HRP Kit, Peroxidase	Vector	PK-4000
Acetic Acid (glacial) 100%	Merck	1.00063.2500
Albumin Bovine Serum	Merck	126575
6-Aminocampronic acid	Sigma-Aldrich	A2504
Ammonium persulfate (APS)	Carl Roth	9592.3
Annexin V FITC	BioLegend	640905
Antibody diluent solution	Invitrogen	003218
Citrate buffer (10mM)	Roth	6490.3
DAB Substrate Kit	Vector	SK-4100
DMEM (Dulbecco's Modified Eagle Medium) Gibco	Life technologies	A4192101
Dimethyl fumarate	Sigma	242926
Dulbecco`s Phosphate Buffered Saline (DPBS) (1x)	Life technologies	14190-144
Ethanol Absolut Endotoxinfree	TH.Geyer	2273.1000
EDTA	Merck	607-429-008
Fetal Bovine Serum (FCS)	Sigma	F7524
Fluo-4, AM, cell permeant	Life technologies	F14201
Forskolin - Adenylyl Cyclase Activator	Abcam	ab120058
Fura Red™, AM, cell permeant	Life technologies	F3021
Glycine	Carl Roth	3908.2
Goat normal serum	Dako	X0907
Hanks' Balanced Salt Solution	PAN Biotech GmbH	P04-32505
HCL (25%)	Merck	1.00316.1000
HCL 0.1M	ENZO	80-0082
Hemalum solution acid acc. to Mayer	Roth	T865
Hydrogen Peroxide (30%)	Roth	8070.2
Ionomycin	Sigma	I3909
Ketamine (10%)	Pharmanovo	4635
L-Glutamine 100x (200mM)	Bio West	X0550-100
4x Laemmli Sample Buffer	BIO-RAD	161-0747
2-Mercaptoethanol	Sigma	M3148
Methanol	Roth	4627.2
Natriumchlorid (NaCl)	Roth	3957.1
Natriumhydroxid (NaOH)	Roth	P031.1
Neutral Red Solution	Santa Cruz Biotechnology	sc-281691
Nicotinic Acid	Sigma	N4126
Nicotinuric acid	Sigma	N4751

Nonidet P-40 Substitute	Roche	14060500
Penicillin/Streptomycin Solution 100x	Bio West	L0022-100
Phorbol 12-myristate 13-Acetate (PMA)	Sigma	P1585
PhosStop	Roche	04906845001
Polysucrose 400 Based Separating Solution	Bioclot	PS400-1000
Ponceau S Staining Solution	Cell Signaling	59803S
Potassium Chloride	Merck	1.04936.0500
2-Propanol	Roth	9866.1
Protease Inhibitor Cocktail	Sigma-Aldrich	P8340
Protein Assay Dye Reagent Concentrate	Bio-Rad	500-0006
Restore Western Blot stripping buffer	Life technologies	21059
RPMI-1640 Medium (1x)	Life technologies	31870-025
ROTI Histofix 4.5 %, prefilled containers	Roth	8244.1
Roti-Mount medium	Roth	HP68.1
Rotiphorese Gel 30 A (Acrylamide) (37.5:1)	Roth	3029.2
SDS Pellets	Roth	8029.1
Sodium deoxycholate	Sigma-Aldrich	D6750
Sodium dodecyl sulphate (SDS)	Biomol	04051.1
Super Signal West Dura Luminol/Enhancer Solution	Thermo Scientific	1856145
Super Signal West Dura Stable Peroxide Buffer	Thermo Scientific	1856146
TEMED (99%)	Carl Roth	2367.3
Tris Puffer	Carl Roth	4855.2
Trizma hydrochloride	Sigma	T3253
Trypan Blue Stain (0.4%)	Life technologies	15250-061
TWEEN 20	Sigma	P2287
WesternSure Pre-Stained Chemiluminescent Protein Ladder	LI-COR	926-98000
ROTI Histol (Xylene substitute)	Roth	6640
Xylazine	WDT	794-765
Zombie NIR dye (750nm)	Biolegend	423105

4 Methods

4.1 Metabolomics-based approach

4.1.1 Study population

The network of competence FoCus was funded by the German Ministry of Education and Research (BMBF) and was established from 2011 until 2015 in Kiel (Germany). This cohort includes a total of 2000 subjects. 500 subjects were recruited from the obesity outpatient clinic of the Department of Internal medicine I (University Medical Center Schleswig-Holstein, Kiel, Germany). Additionally, 1500 subjects were recruited from regional registration offices as cross-sectional controls. Only adults were recruited (18-75 years). There were no exclusion criteria. The study was permitted by the local ethics committee (Christian-Albrechts-Universität zu Kiel) and all patients provided informed written consent. All experiments were performed in accordance with relevant guidelines and regulations.

4.1.2 Anthropometric measurement

Patients were physically examined. Height and weight were measured and body mass index (BMI=weight (kg)/(height(m))^2) was calculated. Height was measured to the nearest 1 cm using a stadiometer. Weight measurement was performed without shoes and light clothes using digital scales. The weight was determined to the nearest 0.1 kg. Waist circumference was measured at the approximate midpoint between the lower margin of the last palpable rib and the top of the iliac crest according to the World Health Organisation (WHO) (100). The blood pressure was measured with a blood pressure cuff and stethoscope.

4.1.3 Biochemical measurement

For determination of metabolic and inflammatory markers, blood samples from FoCus subjects were obtained by venepuncture after an overnight fast. The Central Laboratory (University Medical Center Schleswig-Holstein, Kiel, Germany) analysed the following parameters: CRP was measured by immunoturbidimetry (Hitachi Modular, Roche), fasting glucose with a glucose-hexokinase-UV-test (Hitachi Modular, Roche). IL-6 and fasting insulin were determined by an electrochemiluminescence immunoassay (Elecsys System 2010, Roche) and TG by enzymatic test (Hitachi Modular, Roche) (101). Homeostatic Model Assessment for Insulin Resistance (HOMA-IR) was calculated as fasting glucose (mg/dL) x fasting insulin

(μU/mL)/405 to determine insulin resistance. An immunonephelometric assay was used to measure Lp(a) (Dade Behring).

Protein concentrations of wnt5a and sFRP5 were measured by using the following ELISA kits: wnt5a (analytic-sensitivity < 0.057 ng/mL) (SEP549Hu from Cloud-Clone Corp, Hölzel Diagnostika, Cologne, Germany) and sFRP5 (analytic-sensitivity < 2.53 ng/mL) (SEC842Hu from Cloud-Clone Corp., Hölzel Diagnostika, Cologne, Germany). Metabolites and bile acids in serum were measured by liquid chromatography and mass spectrometry (LC-MS/MS; Agilent 1100 HPLC/CTC-PAL Autosampler/Sciex API 4000 Triple Quadrupole) in an external specialized laboratory (Medizinisches Labor Bremen, Germany).

4.1.4 Anamnesis by a questionnaire

Pregnancy, menopause and diseases like myocardial infarction, liver disease and inflammatory bowel disease were determined by a questionnaire (Yes; No; n/a). To detect nutritional patterns, all participants completed a 12-month nutritional retrospective food frequency questionnaire (FFQ) (EPIC protocol, Prof. Boeing, DIfE Potsdam). For calculation of nutritional intake the EPICsoft database was used (102).

4.1.5 Gut microbiome analysis

Gut microbiome analysis was performed by the Institute of Clinical Molecular Biology (IKMB) (University Medical Center Schleswig-Holstein, Kiel, Germany) and our working group as previously described (101): stool samples of FoCus subjects were directly aliquoted and frozen at -80°C. DNA was extracted from stool samples using the QIAamp DNA stool mini kit (Qiagen, Hilden, Germany). Variable regions V1 and V2 of the 16S rRNA gene were amplified by polymerase chain reaction (PCR). The amplified and normalized rRNA was sequenced on the Illumina MiSeq (Illumina Inc., San Diego, CA, USA). Afterwards, quality control and microbiome bioinformatics analysis for taxonomical classification were performed.

4.1.6 Metabolome assessment

Serum samples were processed in the Department of Food Technology (Institute of Human Nutrition and Food Science Department, CAU Kiel). Separation of proteins, lipids and metabolites was conducted by the Simplex-method (modified by J. Jensen-Kroll and T.

Demetrowitsch). Metabolites were measured via Fourier-transform ion cyclotron resonance mass spectrometry (FT-ICR-MS) (Bruker, Billerica, MA, USA)).

Serum TRP-NA metabolites were determined by using the mass spectrometry software MetaboScape 2.0 (Bruker, Billerica, MA, USA). Molecular formulas of the metabolites and intermediates of the TRP-NA metabolisms were determined using the databases of Kyoto Encyclopedia of Genes and Genomes (KEGG) and the Human metabolome database (HMDB). For metabolite detection, specific software settings were selected **(Table 3)**. The level of detection (LOD) was set at 749999 counts**.**

Table 3: Settings in metabolomics software MetaboScape (Bruker) for investigation of TRP- NA metabolites in the FoCus cohort

Primary Ion	$[M+Na]^+$
Ionization & method	Positive & ultra-small molecule method (65-300 Dalton)
Polarity	Hydrophilic compounds
Max charge	1
Threshold (min. intensity of each metabolite)	>749999 counts
Calibration tolerance	0.5 ppm
m/z delta	1
Minimum numbers of features for results	6/600

4.1.7 Statistical analysis of TRP- NA metabolites in the FoCus cohort

Statistical analysis and graphical set up were performed with R Studio Version 1.2.1335 (R Studio, Boston, MA, USA). The significance level was set to $p<0.05$. To correct for multiple testing bias, the false discovery rate (FDR) was determined.

4.1.8 Association between TRP-NA metabolites and metabolic inflammation in the FoCus sub-cohort

The association between serum intensities of TRP-NA metabolites and markers of metabolic inflammation was investigated. Therefore, a sub-cohort of 597 male (42%) and female (58%) subjects (ages 23-89y) out of the FoCus cohort was selected. For investigation of the association

between metabolite intensities and BMI, the sub-cohort was divided into five BMI groups: normal (BMI<24.9), overweight (BMI: 25-29.9), obesity grade I (BMI: 30-34.9), obesity grade II (BMI: 35-39.9) and obesity grade III (BMI>40). Moreover, the subjects were stratified into 199 healthy, 200 with PreD and 198 patients with T2D defined by their fasting glucose levels (healthy: 0-100 mg/dl; PreD: 101-125 mg/dl; T2D: >126 mg/dl). As metabolite intensities reveal a high skewness, subjects could not be matched by age.

Due to the extreme skewness of metabolite intensities, the statistical evaluation was performed in three ways: (1) with the total sub-cohort and (2) with subjects who exhibited metabolite intensities over LOD (>749999 counts). To analyse the distribution of metabolites intensities, a Shapiro-Wilk test was used. Due to non-normal distribution, differences in metabolite intensities between the groups were tested by Kruskal-Wallis tests and post-hoc Wilcoxon rank-sum tests. (3) Metabolites were additionally dichotomised (0 = below LOD; 1 = above LOD) and Chi^2 tests were done to determine differences in dichotomized data between groups. To analyse correlations between the metabolites, the spearman coefficient was used. Nominally significant results are described in the text but not shown in the figures.

4.1.9 Association between NUA and clinical parameters, nutritional data and the gut microbiome in the total FoCus cohort

For statistical analysis, NUA was dichotomized using the LOD of 749999 (0 = below LOD; 1 = over LOD) and two groups were set up: subjects with NUA intensities over the LOD (NUA>LOD) and subjects with NUA intensities below the LOD (NUA<LOD). Normal distribution was evaluated by Shapiro-Wilk test. Differences for consistent variables in NUA groups were analysed using Wilcoxon rank-sum test. For investigation of categorical variables, Fisher tests or Chi^2 tests were used. To analyse correlations between significant parameters and NUA intensities, the spearman coefficient was used.

Furthermore, the association between serum NUA intensities and the gut microbiome in FoCus subjects was evaluated. Therefore, the Bray Curtis Dissimilarity was calculated to quantify differences in species populations between NUA intensities over and below LOD. Furthermore, a constrained analysis was done to adjust for BMI. Permutational multivariate analysis (PERMANOVA test) was performed to determine statistical significance in β-diversity. α-diversity of the gut microbiome was characterized by the Shannon, Chao and Species Richness indices respectively. Wilcoxon rank sum test with continuity correction was performed to

calculate differences of α- diversity between both groups. Moreover, relative phyla abundance of gut bacteria in groups of high and low NUA intensities were determined and compared.

4.2 Cell culture experiments

4.2.1 THP-1 Cultivation

Acute monocytic leukemia Cells, ACC16 (THP-1) cells (Leibniz Institute DSMZ- German Collection of Microorganisms and Cell Cultures GmbH, Braunschweig, Germany) were cultivated in RPMI 1640 medium with 10% fetal calf serum (FCS), 2mM L-Glutamine, 1% penicillin/streptomycin at 37°C and 5% CO_2. Cells were counted using trypan blue exclusion dye. Cells were seeded at $1.5x10^6$ cells/ well in a 6-well plate. To differentiate monocytes to macrophages, cells were incubated with 162nM phorbol 12-myristate 13-acetate (PMA) for 24 h. Subsequently, differentiated cells were washed with PBS. After 24 h, cells were washed and resuspended in medium.

Furthermore, pH-value in medium provided with indicated concentrations of NUA was tested and showed no change in pH-value (7-8).

4.2.2 Cytotoxicity Assay (Neutral Red Uptake)

To determine the effects of NUA on THP-1 cell viability, a neutral red uptake assay was performed. Cells were stimulated with indicated concentrations of NUA. 10% endotoxin free ethanol was used as positive control for cell death. One well was only incubated with PBS. After 24 h incubation, medium got withdrawn from wells and a neutral red solution (1/66 dilution in medium) was added for 2 h. Subsequently, cells were washed and an extraction buffer was added. Cells were incubated for 15 min on an orbital shaker at room temperature (RT). Afterwards, samples were transferred into a 96-well plate as triple determination and absorbance was measured at 540 nm on a microplate reader (Berthold Technologies, Bad Wildbach, Germany).

4.2.3 NF-κB p50 signalling in THP-1 cells

For investigation of NF-κB p50 signalling in THP-1 cells, cells were stimulated with indicated concentrations of NUA or PBS as solvent control. After indicated time points, cells were

washed, lysed with radioimmunoprecipitation assay (RIPA) buffer containing phosphatase inhibitors „PhosStop“ (1:10 dilution) and protease inhibitor cocktail (1:100 dilution). Subsequently, samples were frozen at -80°C until analysis.

4.2.4 Total protein measurement - Bradford assay

Cell lysates were centrifuged at 4°C for 30 min at maximum velocity to remove cell debris. Afterwards, supernatant was transferred into a new tube. Samples were diluted with dH_2O (1:10) for measurement. Bovine serum albumin (BSA) standards (0.5; 0.25; 0.13; 0.06 µg/µl) were used to determine concentration of total protein mix. Samples, standards and blanks were transferred into a 96-well plate as duplicates. Bio-Rad protein assay dye reagent (1:5 dilution) was added to each well and incubated for 10 min in the dark at RT. Subsequently, absorbance was measured at 630nm on a microplate reader (Berthold Technologies, Bad Wildbach, Germany).

4.2.5 SDS-PAGE

Proteins were separated according to their molecular size by sodium dodecyl sulphate polyacrylamide gel electrophoresis (SDS-PAGE). Ingredients for a denaturing 30% acrylamide gel are described in **Table 4**. 4x Lämmli sample buffer and 10% β-mercaptoethanol were mixed and added to the samples as ¼ of sample volume. Samples were denatured at 95°C for 5 min. 30µg of protein samples and WesternSure pre-stained Chemiluminescent Protein Ladder were loaded on the gel and separated at 80 volt for 10 min followed by 1.5 h at 120 volt.

Table 4: Ingredients for gels used in SDS-PAGE

Separation Gel	Stacking gel
2mL dH_2O	1.1 mL dH_2O
0.7mL SDS (1%)	0.2mL SDS (1%)
1.4mL Tris HCL (1.88M)	0.4mL Tris HCL (0.658M)
2.9mL Acrylamide (30%)	0.3mL Acrylamide (30%)
30µl APS	10µl APS
6µl TEMED	2µl TEMED

4.2.6 Western Blot

To detect NF-κB p50 protein expression, a semi-dry western blot was performed. The proteins were transferred from the SDS gel to a methanol activated PVDF membrane on a blotting device (Analytik-Jena, Jena, Germany) (1 gel: 70mA; 2 gels 140mA for 45 min). To test successful protein-transfer, the membrane was stained with Ponceau-S solution for 2 min. After removal of Ponceau-S staining, the membrane was used for western analysis.

The membrane was blocked in 5% milk-powder in TBS/T on an orbital shaker at RT for 2 h. After removal of the blocking solution, the membrane was incubated with anti-NFκB p105/p50 antibody (Abcam, Cambridge, UK) (1:10000 in 5% blocking solution) on an orbital shaker at 4°C overnight. After washing with TBS/T, the membrane was incubated with anti-rabbit antibody (Biolabs, Ipswich, MA, USA) (1:2000 in 5% blocking solution) for 45 min. Subsequently, the membrane was washed and incubated with enhanced chemiluminescence (ECL) kit (Thermo Scientific, Waltham, MA, USA) (1:1 Luminol and Peroxide Buffer) at RT for 5 min. Signals were detected on a Molecular Imager ChemiDoc XRS+ (Bio Rad, Hercules, CA, USA) and density of the detected bands was analysed using the software Image Lab (Bio Rad, Hercules, CA, USA). Membranes were stripped with a stripping buffer and glyceraldehyde 3-phosphate dehydrogenase (GAPDH) (Cell Signaling, Danvers, MA, USA) (1:5000 in 5% blocking solution) was used as a housekeeper to allow normalization of protein content.

4.3 Experiments with primary cells

4.3.1 Isolation of primary human cells

Peripheral blood was taken by venepuncture. Donors were female and between 25 and 35 years of age.

Isolation of human neutrophils

Isolation of neutrophils was conducted with MACsxpress whole blood neutrophil isolation kit (Miltenyi Biotec, Bergisch Gladbach, Germany) according to the manufacturer`s instructions. 8ml of whole blood were mixed with the provided isolation mix and subsequently incubated on an orbital shaker for 5 min. Afterwards, neutrophils were isolated by negative magnetic isolation, resulting in untouched neutrophils for subsequent analysis. Cells were counted and diluted to specific concentrations depending on the assay.

Isolation of human monocytes

Initially, peripheral blood mononuclear cells (PBMCs) were isolated from PBS diluted whole blood by a Polysuccrose 400 gradient. After centrifugation at 800 x g for 20 min, the resulting PBMC layer was taken and washed. Cells were counted with trypan blue exclusion dye. $CD14^+$ monocytes were isolated from PBMCs by positive selection with CD14 microbeads (Miltenyi Biotec, Bergisch Gladbach, Germany) according to the manufacturer`s instructions. Monocytes were centrifuged, resuspended in magnetic-activated cell sorting (MACs) buffer and counted for following experiments. Monocytes were seeded into a 6-well plate, incubated for 1-1.5 h to allow adherence and washed.

4.3.2 Animals

C57BL6/J mice were purchased from Janvier labs. $GPR109A^{-/-}$ (Hcar2tm1Soff) and red fluorescent protein (RFP)-GPR109A mice (HCA2mRFP) were originally generated and generously donated by the working group of Stefan Offermanns (103, 104). C57BL6/J and $GPR109A^{-/-}$ mice were used to generate an inbred strain by brother sister-mating. All mice were bred at the Zentrale Tierhaltung (ZTH) (University Medical Center Schleswig-Holstein, Campus Kiel, Germany) and maintained under specific pathogen free (SPF) conditions. For experiments, mice were at least between 6 and 8 weeks of age. *In vivo* experiments were carried out within the ZTH and were performed in accordance with the German Animal Welfare Legislation. Permission was received from the Ministerium für Energiewende, Landwirtschaft, Umwelt, Natur und Digitalisierung des Landes Schleswig-Holstein (MELUND) (AZ: V 242-75980/2020(1-1/21).

Isolation of murine bone marrow derived (BMD) neutrophils

$GPR109A^{+/+}$ and $GPR109A^{-/-}$ mice were sacrificed and bone marrow cells were separated from femurs by gentle destruction of the bone material in PBS. The cell suspension was transferred into a canonical tube passing a 100 µm strainer to remove bone debris. Cells were centrifuged at 380 x g for 10 min and resuspended in PBS with 2% FCS and 0.5M EDTA. The Easy Sep Mouse neutrophil enrichment kit (Stemcell technologies, Vancouver, Canada) was used to isolate neutrophils according to the manufacturer`s instructions. For following experiments, cells were counted and resuspended for analysis.

Isolation of murine peritoneal macrophages (PEMs)

GPR109A$^{+/+}$ and GPR109A$^{-/-}$ mice were sacrificed and ice-cold PBS was injected into peritoneum with a 22-gauge needle. After belly massage, peritoneum was opened and peritoneal suspension was transferred into a new tube. Samples were centrifuged at 400 x g for 10 min (4°C) and cells were counted. Cells were seeded into a 6-well plate and incubated at 37°C for 1.5 h to obtain adherence of macrophages. Non-adherent cells were removed by washing with PBS.

4.3.3 Annexin V apoptosis assay

Murine neutrophils were seeded at 1x10^6 cells/well into a 96-well plate, centrifuged at 380 x g for 3 min and resuspended in Dulbecco's modified Eagle's medium (DMEM) with 10% FCS. Cells were incubated with indicated concentrations of NUA, PBS or dimethyl fumarate (DMF) (positive control for cell death) for 2 h at 37°C and 5% CO_2. Subsequently, cells were centrifuged at 380 x g for 5 min and resuspended in PBS. Cells were stained with Annexin V, GR-1 antibody (Biolegend, San Diego, CA; USA) and Zombie NIR live/dead dye and incubated for 15 min on ice in the dark. After incubation, samples were washed, resuspended in PBS and analysed by flow cytometry.

4.3.4 Measurement of intracellular Ca^{2+} levels

Effects of NUA on intracellular Ca^{2+} flux in human and murine (GPR109A$^{+/+}$; GPR109A$^{-/-}$) neutrophils were investigated. 1x10^7 cells/ml were used for flow cytometry analysis. 3 µM Fluo-4 and 6 µM Fura-red were added to samples and incubated for 45 min at 37°C and 5% CO_2. Afterwards, the samples were centrifuged at 380 x g for 8 min and resuspended with Hanks' Balanced Salt Solution (HBSS). Samples were allowed to rest for another 20 min in the dark. Neutrophils were then acquired on a flow cytometer for 20 s before indicated concentrations of NUA, NA, Ionomycin or PBS were added to the tubes and acquisition was continued for another of 60 s. Ionomycin was used as a positive control since it mobilizes intracellular calcium stores (105). When Fluo-4 and Fura-red get in contact with Ca^{2+}, they change their fluorescence intensity. The change in ratio of fluorescence intensity between Fluo-4 and Fura-red was calculated over time **(Fig. 5)**.

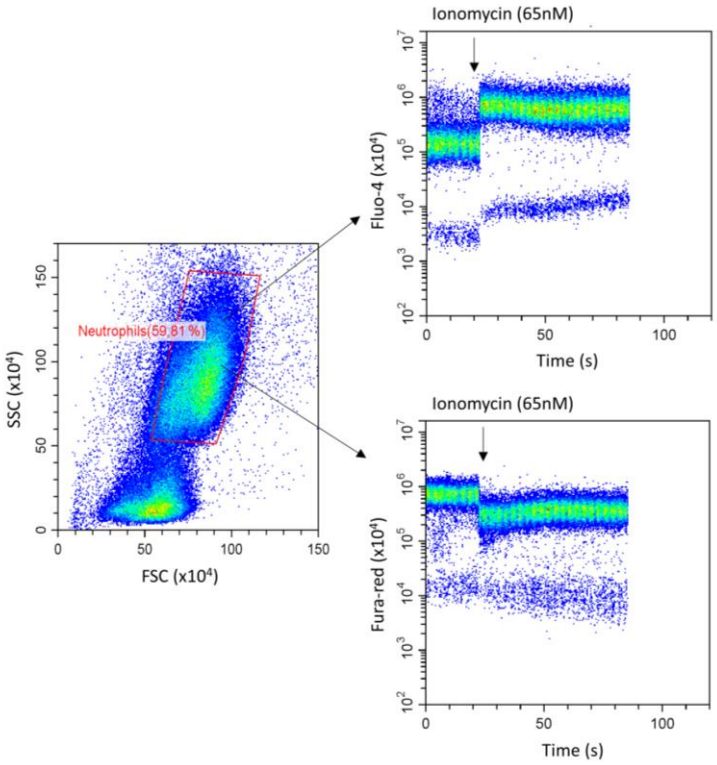

Figure 5: Flow cytometry - Ionomycin induces intracellular Ca^{2+} in human neutrophils: Samples were acquired on a flow cytometer for 20 s, stimulated with Ionomycin (65nM) and acquisition was continued for another 60s. The ratio of intensity of Fluo-4 and Fura-red changes when in contact with Ca^{2+}.

4.3.5 Flow cytometry

Flow cytometry was conducted on a CytoFLEX flow cytometer using CytExpert software (Beckmann Coulter, Krefeld, Germany). The resulting date were analysed using FlowJo v10 software (Becton, Dickinson & Company)

4.3.6 Determination of intracellular cAMP levels

The effects of NUA on intracellular cAMP levels were determined in forskolin treated samples. Forskolin activates the adenylyl cyclase which produces cAMP (106). Human neutrophils/monocytes and GPR109A$^{+/+}$ and GPR109A$^{-/-}$ neutrophils/PEMs were used. Cell amount ranged between 0.5x10^6 and 1x10^6 per sample. Neutrophils were seeded into a 96-well plate and incubated for 5 min at 37°C. Indicated concentrations of NUA, NA, forskolin and PBS were given to samples and incubated for 5 min at 37°C. Neutrophils were centrifuged at 380 x g for 5 min and lysed with 0.1M HCL. Monocytes and PEMs were washed with PBS and

lysed with 0.1M HCL. After 10 min at 4°C, cells were frozen at -20°C. To analyse cAMP concentration, the Direct cAMP ELISA Kit (ENZO, New York, NY, USA) was used according to manufacturer`s instructions. All samples were acetylated before the assay was performed.

4.3.7 Phosphorylation of MAPKs, NF-κB p65, β-Arrestin1, AMPKα and Akt

Effects of NUA and NA on intracellular phosphorylation status of MAPKs, NF-κB p65, β-Arrestin1, AMPKα and Akt were investigated. Human monocytes were used ($0.5x10^6$-$1x10^6$ cells/well) and stimulated with indicated concentrations of NUA and NA for 5 min and 15 min at 37°C. Afterwards, cells were lysed with RIPA buffer and stored at -80°C until analysis.

Before measurement of protein concentrations, cell debris was removed from samples by centrifugation at 13000 x g for 10 min. Afterwards, supernatant was transferred into new tubes. A Pierce Bicinchoninic Acid Protein Assay (Thermo Scientific, Waltham, MA, USA) was performed according to manufacturer`s instructions. Sample volumes were adjusted to the concentration of the samples with the lowest protein concentration and stored at -20°C until analysis.

Protein phosphorylation was determined by capillary-based Western analysis using 12-230kDA separation modules (ProteinSimple, San Jose, CA, USA) according to the manufacturer's instructions. Antibodies **(Table 5)** were diluted 1:50 in antibody diluent. The housekeeping protein β-Actin was used for normalization. The anti-Rabbit detection module (ProteinSimple, San Jose, CA, USA) was used as a secondary antibody. Samples were measured with the WES analyser (ProteinSimple, San Jose, CA, USA) and results were evaluated by using the Compass SW software (ProteinSimple, San Jose, CA, USA).

Table 5: Antibodies (Cell Signaling, Danvers, MA, USA) used for WES analysis

Selection of antibodies
β-Actin (13E5)
p-p38 MAPK (T180/Y182)
p-β-Arrestin1 (S412)
NF-κB p65 (D14E12)
p- NF-κB p65 (Ser 536) (93H1)
p-p44/42 (T202/Y204)
p-Akt (S473) (D9E)
p-SAPK/JNK (T183/Y185)
p-AMPKα (Thr172) (40H9)

4.4 Statistical analysis for *in vitro* experiments

Statistical analysis and graphical set up were performed with GraphPad Prism Version 9 (GraphPad, San Diego, CA, USA). Group differences were evaluated by Kruskal-Wallis test and the post hoc Dunns test. Due to limitation of the replication amount (n=4-5), tests were performed without correction for multiple comparisons. Values of $p<0.05$ were considered significant.

4.5 Immunohistochemistry

For investigation of GPR109A expression in various tissues, RFP mice were used since there is no validated antibody for GPR109A yet. RFP mice carry a construction of the RFP gene which is located behind the human GPR109A promotor. As control, GPR109A$^{-/-}$ mice were used. After animals were sacrificed, liver and brain were taken and fixed in 4.5% formaldehyde solution. Immunohistochemistry was performed by the IKMB (University Medical Center Schleswig-Holstein, Kiel, Germany) and the Department of Anatomy (University Medical Center Schleswig-Holstein, Kiel, Germany). Paraffin embedded liver and brain tissues were cut into 3.5 µm (liver) and 5 µm (brain) thick tissue sections. Brain was cut by frontal section to obtain the hypothalamic region.

Paraffin embedded liver and brain samples were deparaffinised with a xylene substitute (1x10 min) and decreasing EtOH series: 100% EtOH (3 x 60s), 96% EtOH (2 x 60 s), 70% EtOH (1 x 60 s). Afterwards, slides were washed under running dH_2O and with PBS (3 x 4 min). For

demasking antigens and epitopes, slides were cooked with 10mM citrate buffer in a pressure cooker for 3 min. After cooling, slides were blocked with 3% hydrogen peroxide for 10 min. Subsequently, slides were washed with PBS (3 x 4 min) and blocked (liver: BSA; hypothalamus: goat normal serum) for 20 min. After another wash with PBS, liver slides were incubated over night with RFP polyclonal antibody (Invitrogen, Waltham, MA, USA) (1:500 antibody diluent solution), while hypothalamic slides were incubated with RFP polyclonal antibody (1:2000 antibody diluent solution) and Iba-1 polyclonal antibody (Dako, Santa Clara, CA, USA) (1:500 antibody diluent solution) as marker for microglia. After washing, slides were incubated with goat anti-rabbit antibody biotinylated (Dako, Santa Clara, CA, USA) (1:400 antibody diluent solution) for 45 min at RT. After PBS washing (3 x 4min), slides were treated with ABC reagents (Vector Laboratories, Burlingame, CA, USA) for 45 min and incubated with peroxidase-substrate-solution for 10 min until colour change. Subsequently, slides were washed with dH_2O for 5 min. For an efficient evaluation of staining, slides were counterstained. Slides were treated with hemalum solution for 2 min and washed with H_2O (5 min) for blueing. Afterwards, slides were treated with increasing EtOH series: 70% (1x wash), 96% (3x wash), 100% (2x wash; 3 x 2 min) and xylene substitute (2 x 2 min). A mounting medium was used to fix cover slip on the slides. Slides were scanned with Nano Zoomer (Hamamatsu, Japan) and evaluated with NDP.view2 software (Hamamatsu, Japan).

4.6 In vivo experiment - gastrointestinal absorption of NUA

$GPR109A^{+/+}$ and $GPR109A^{-/-}$ mice were housed under a constant temperature of 23-25°C, a 12h light/dark cycle and with ad libitum access to water and food. One week before and during experiment, animals received a high-fat diet (60% kcal from fat (lard)) (D12492; ssniff Spezialdiäten GmbH, Soest, Germany) which was modified by exclusion of TRP and NA (S8728-E714; ssniff Spezialdiäten GmbH, Soest, Germany) (list of ingredients is attached in supplemental information **(Table S1)**. 300mM NUA was administered by drinking water or one-time oral gavage with 800 mg NUA/kg body weight (BW). Water was given as control. Blood was drawn from mice after 24 h, 48 h, 72 h or 7 days when dosed by drinking water or after 30 min, 1 h, 2 h or 5 h when dosed by oral gavage **(Fig 6)**. 3 mice were analysed per time point.

Animals were put under deep anaesthesia with ketamine (100µg/g BW) and xylazine (16µg/g BW) intraperitoneally. Blood was taken via cardiocentesis on closed thorax. Serum was obtained by centrifugation (800 x g 20 min RT). Serum samples were proceeded in the

Department of Food Technology (Institute of Human Nutrition and Food Science Department, CAU Kiel). Separation of proteins, lipids and metabolites was conducted by the Simplex-method (modified by J. Jensen-Kroll and T. Demetrowitsch). NUA was measured by FT-ICR-MS (Bruker, Billerica, MA, USA). Intensities (counts) of NUA were analysed by using MetaboScape 2.0 software (Bruker, Billerica, MA, USA). The LOD was set at $1x10^6$ million counts.

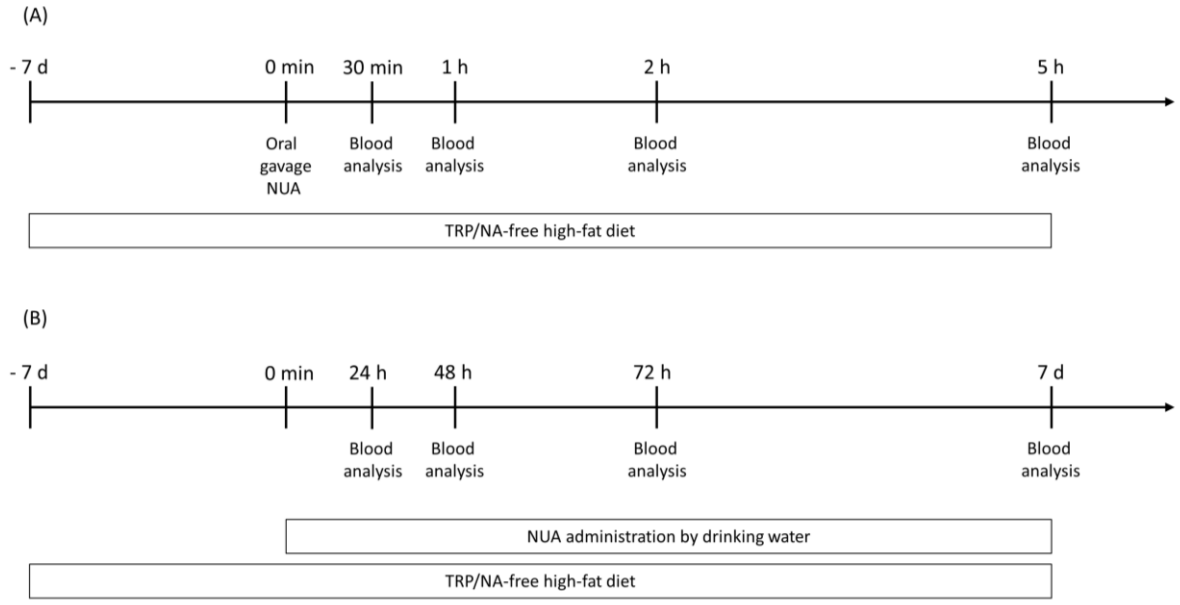

Figure 6: Investigation of NUA`s gastrointestinal uptake in GPR109A$^{+/+}$ and GPR109A$^{-/-}$ mice - experimental set up: (A) Administration of NUA via oral gavage and blood analysis after 30 min, 1 h, 2 h and 5 h **(B)** Administration of NUA via drinking water and blood analysis after 24 h, 48 h, 72 h and 7 d.

5 Results

5.1 TRP-NA metabolism in subjects of the FoCus sub-cohort

5.1.1 Detected serum TRP-NA metabolites

A metabolomics-based approach was performed to investigate which TRP-NA metabolites show differences in their serum intensities between healthy and obese or diabetic subjects. Serum TRP metabolites like anthranilic acid, TRP itself, L-kynurenine and xanthurenic acid could be detected. Determined NA metabolites included NUA and several intermediates, but not NA or NAM. Except for TRP and NUA, the other detected metabolites revealed no evaluable intensities due to the extreme skewness of values. Therefore, it was investigated if serum intensities of TRP and NUA from FoCus subjects are linked to obesity and T2D.

5.1.2 Basic characteristics of the FoCus sub-cohort

Differences in serum intensities of TRP and NUA between lean and obese subjects were examined Therefore, the sub-cohort was divided into 5 groups defined by their BMI. There were significant group differences in age ($p<0.001$) weight ($p<0.001$), glucose ($p<0.001$), HOMA-IR ($p<0.001$), TG ($p<0.001$), IL-6 ($p<0.001$) and CRP ($p<0.001$) with highest levels in subjects with obesity grade III. No significant differences in the number of women and men and Lp(a) levels were recorded **(Table 6)**.

Table 6: Basic characteristics of the FoCus sub-cohort divided into BMI groups with normal weight, overweight and obesity grade I-III; Results are shown as Median (25th;75th percentile); Kruskal-Wallis test (*p<0.05; **p<0.01; ***p<0.001)

Basic characteristics of FoCus sub-cohort stratified by BMI						
Variable	**Normal** (n=161)	**Overweight** (n=125)	**Obesity I** (n=81)	**Obesity II** (n=56)	**Obesity III** (n=174)	***p*-value**
Age (y)	60.6 (52/74)	66.6 (58/76)	66 (57/75)	63.3 (56/72)	56.5 (48/64)	***
Sex (%) F/M	64/36	42/58	47/53	55/45	71/29	
Weight (kg)	67 (59/74)	83 (75/88)	96 (87/103)	107 (99/117)	138 (123/156)	***
Glucose (mg/dl)	94 (88/102)	101 (92/112)	107 (101/118)	108 (102/138)	109 (103/134)	***
HOMA-IR Index	1.61 (1.17/2.13)	2.47 (1.75/3.92)	4.02 (2.52/5.89)	5.69 (4.22/11.20)	7.36 (4.76/13.25)	***
TG (mg/dl)	81 (61/107)	119 (76/164)	139 (110/189)	135 (105/204)	150 (119/216)	***
Lp (a) (mg/l)	286 (140/517)	440 (182/609)	237 (144/457)	325 (189/445)	256 (149/493)	
IL-6 (pg/ml)	3.1 (2.3/4.9)	3.4 (2.5/5.0)	4.3 (3.1/5.8)	4.6 (3.5/6.2)	5.4 (4.0/7.9)	***
CRP (mg/l)	1.7 (1.1/3.6)	2.3 (1.3/4.1)	2.6 (1.8/4.4)	4.0 (2.0/7.8)	8.6 (4.9/13.5)	***

Furthermore, the sub-cohort was stratified into three groups defined by their fasting glucose levels. There were no significant differences in the number of men and women between the groups. Age ($p<0.001$), weight ($p<0.001$), BMI ($p<0.001$), HOMA-IR ($p<0.001$), TG ($p<0.001$), IL-6 ($p<0.001$) and CRP ($p<0.001$) differed significantly between groups and were highest in diabetic subjects. Groups showed no differences in Lp(a) levels **(Table 7)**.

Table 7: Basic characteristics of the FoCus sub-cohort divided into healthy, pre-diabetic and diabetic subjects; Results are shown as Median (25th;75th percentile); Kruskal-Wallis test (*p<0.05; **p<0.01; ***p<0.001)

Basic characteristics of FoCus sub-cohort stratified by fasting glucose levels				
Variable	**Healthy** (n=199)	**PreD** (n=200)	**T2D** (n=198)	***p*-Value**
Age (y)	53 ± 14	60 ± 13	63 ± 11	***
Sex (%) F/M	67/43	52/48	56/44	
Weight (kg)	75 (65; 92)	93 (78; 120)	112 (90; 140)	***
BMI (kg/m^2)	24.6 (22.2; 30.1)	30.4 (25.3; 41.2)	39.0 (30.8; 46.3)	***
HOMA-IR Index	1.71 (1.26; 2.83)	3.65 (2.18; 6.16)	7.09 (3.86; 16.31)	***
TG (mg/dl)	83.0 (65.0; 119.3)	124.0 (87.5; 166.3)	154.5 (118.8; 238.5)	***
Lp (a) (mg/l)	273 (149; 497)	311 (170.5; 474.5)	310 (142; 585)	
IL-6 (pg/ml)	3.30 (2.30; 5.43)	4.30 (2.93; 5.78)	5.05 (3.50; 7.30)	***
CRP (mg/l)	2.80 (1.40; 6.90)	3.80 (1.88; 8.63)	5.15 (2.55; 10.30)	***

5.1.3 Obese subjects showed increased TRP intensities

It was investigated if there are alterations in serum TRP intensities between lean and obese subjects. Results showed a significant difference between the BMI groups (p<0.001). Subjects with normal weight showed significant lower TRP intensities compared to subjects with obesity grade I (p<0.01), obesity grade II (p<0.001) and obesity grade III (p<0.001). Subjects with overweight revealed nominally significant lower TRP intensities compared to subjects with obesity grade II (p<0.01) and significant lower TRP intensities compared to subjects with obesity grade III (p<0.01). The group of obesity grade I showed nominally significant lower TRP intensities compared to group of obesity grade III (p<0.05) **(Fig. 7 A)**. Evaluation with dichotomised TRP values confirmed significant differences between BMI groups (p<0.001).

BMI group analysis with TRP intensities over LOD showed significant differences (p<0.001) with significant higher TRP intensities in subjects with obesity grade II (p<0.01) and obesity grade III (p<0.001) compared to individuals with normal weight **(Fig. 7 B)**.

Taken together, these results demonstrate that FoCus subjects, suffering from obesity, had elevated serum TRP intensities compared to lean subjects.

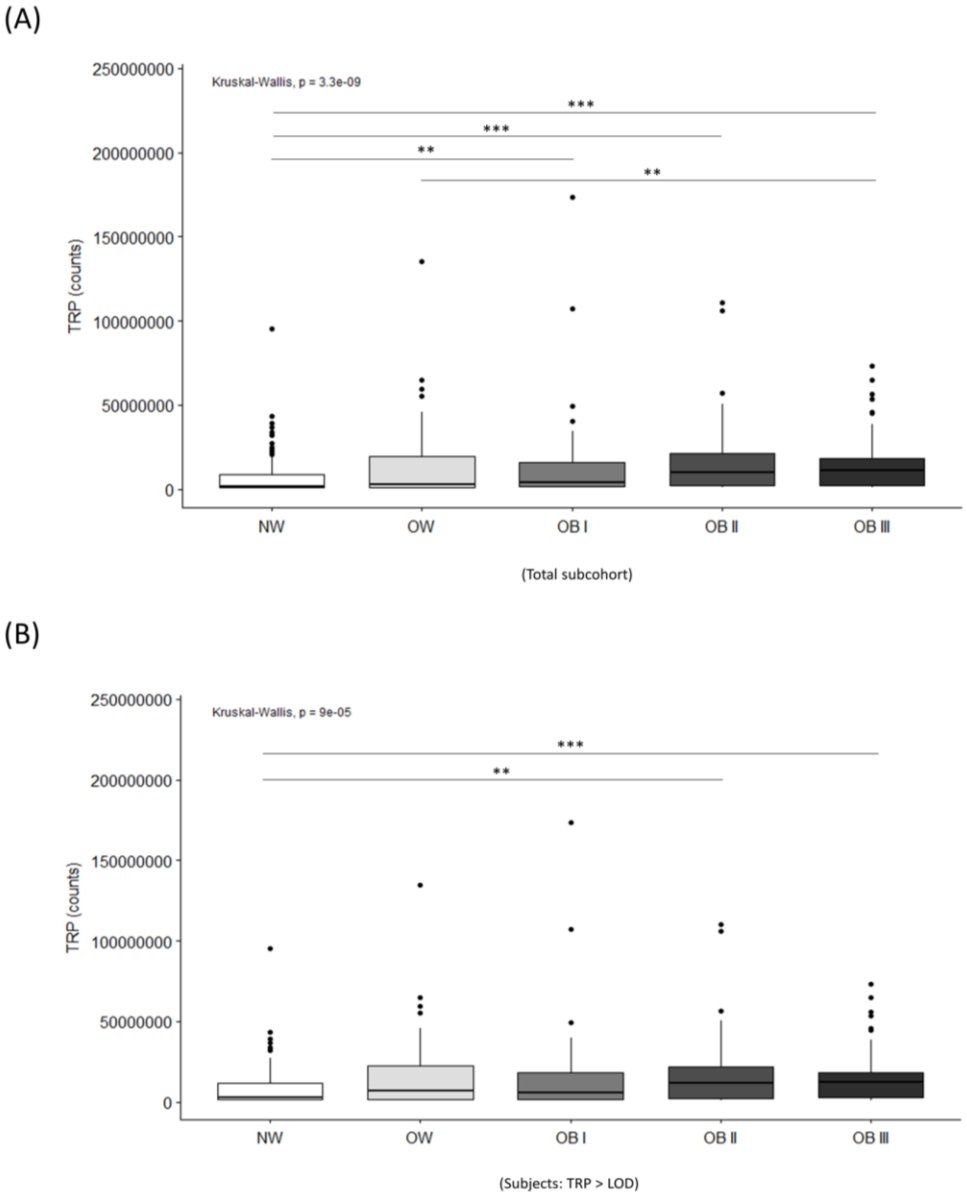

Figure 7: Alterations in serum TRP intensities (counts) between subjects with normal weight, overweight and different grades of obesity in the FoCus sub-cohort: **(A)** Total sub-cohort: Subjects with normal weight showed lower TRP intensities compared to groups with obesity grad I,II, III. Subjects with overweight showed lower TRP intensities than subjects with obesity grade III **(B)** Subjects with TRP intensities over LOD: subjects with normal weight had lower TRP intensities compared to groups with obesity grade II and III; Kruskal-Wallis test/ Wilcoxon test (*p<0.05; **p<0.01; ***p<0.001).

5.1.4 TRP intensities were increased in diabetic subjects

Moreover, it was examined if healthy, pre-diabetic and diabetic subjects show differences in serum TRP intensities. Results showed significant differences between the three groups (p<0.001). While healthy subjects revealed significant lower TRP intensities compared to the PreD group (p<0.001) and T2D group (p<0.001), subjects of PreD and T2D groups showed no significant differences **(Fig. 8 A)**. A Chi^2 test confirmed the significant difference between the 3 groups (p<0.001).

Group comparisons with TRP intensities over LOD also showed significant differences (p<0.001) with increased TRP levels in subjects of PreD (p<0.001) and T2D (p<0.001) compared to healthy subjects **(Fig. 8 B)**.

These results demonstrate that TRP serum intensities are enhanced in diabetic subjects.

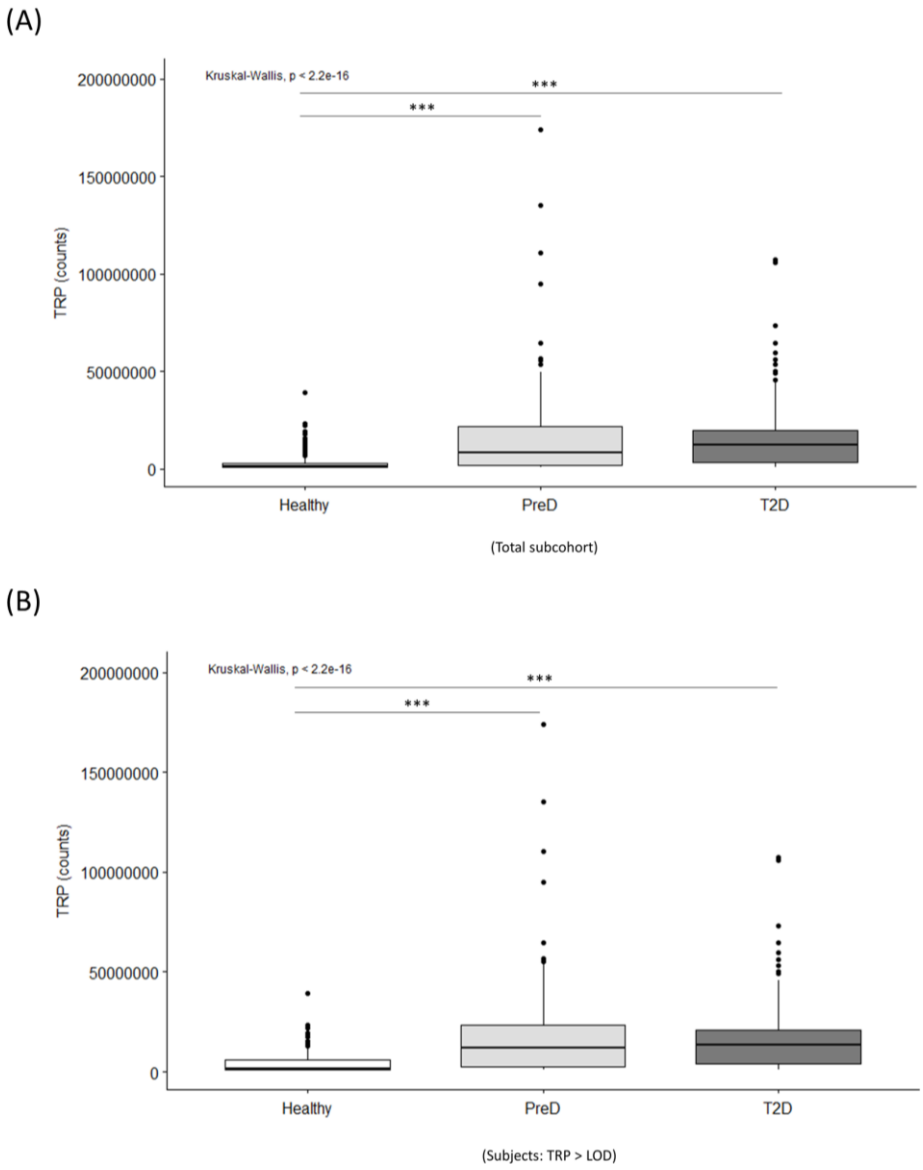

Figure 8: Comparison of serum TRP intensities (counts) between healthy, pre-diabetic and diabetic subjects of the FoCus sub-cohort: (A) Total sub-cohort: Healthy subjects showed lower TRP intensities compared to PreD and T2D subjects **(B)** Subjects with TRP intensities over LOD: Healthy subjects showed lower TRP intensities compared to PreD and T2D subjects; Kruskal-Wallis test/ Wilcoxon test (*p<0.05; **p<0.01; ***p<0.001).

5.1.5 Obese subjects showed elevated serum NUA intensities

Furthermore, the association between NUA intensities and BMI were analysed. Kruskal-Wallis test showed significant differences between lean, overweight and obese subjects (p<0.001). Subjects with normal weight revealed significant lower NUA intensities compared to subjects with obesity grade III (p<0.001). Subjects with overweight exhibited nominally significant lower NUA intensities compared to subjects with obesity grade III (p<0.01). Subjects with obesity grade I showed significant lower NUA intensities compared to subjects with obesity grade III (p<0.05) **(Fig. 9 A)**. Additional BMI group comparisons with dichotomised NUA values were performed and also showed significant group differences (p<0.001).

Moreover, BMI group comparisons of subjects with NUA intensities over LOD were evaluated. There was no significant difference between the groups. Subjects with obesity grade III showed nominally significant higher intensities compared to subjects with obesity grade I (p<0.05) **(Fig. 9 B)**. In summary, subjects with increased BMI showed increased serum NUA intensities.

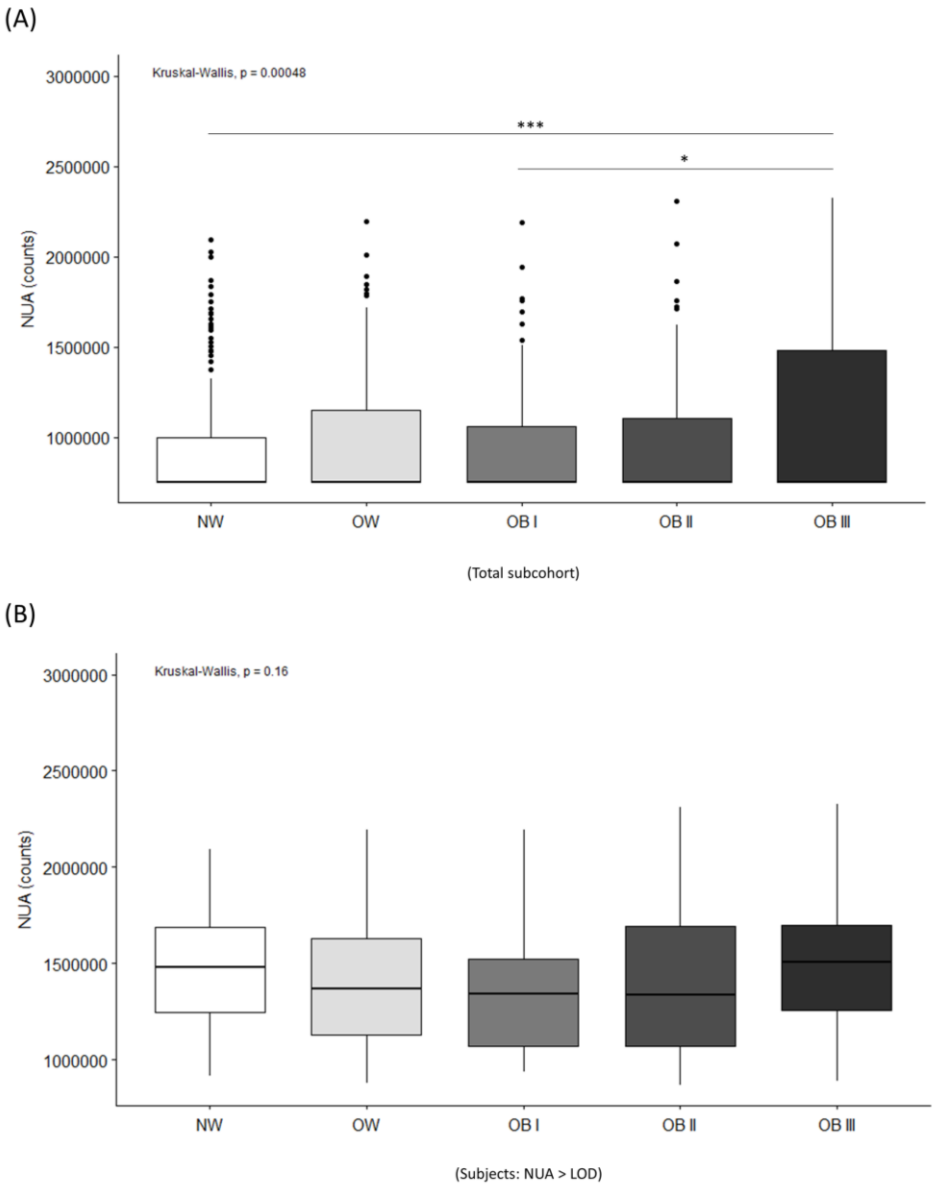

Figure 9: Alterations of serum NUA intensities (counts) between subjects with normal weight, overweight and different grades of obesity in the FoCus sub-cohort: (A) Total sub-cohort: Subjects with normal weight showed lower NUA intensities compared to subjects with obesity grade III. Subjects with obesity grad I showed lower NUA intensities compared to subjects with obesity grade III **(B)** Subjects with NUA intensities over LOD: no group differences in NUA intensities; Kruskal-Wallis test/ Wilcoxon test (*p<0.05; **p<0.01; ***p<0.001).

5.1.6 Diabetic subjects revealed increased serum NUA intensities

Moreover, it was examined if diabetic subjects show alterations in serum NUA intensities. Analysis showed significant differences between healthy, pre-diabetic and diabetic subjects (p<0.001). NUA intensities were lower in healthy subjects compared to the PreD group (p<0.001) and T2D group (p<0.001). There was no significant difference in NUA intensities

between subjects with PreD and T2D **(Fig. 10 A)**. Results of Chi^2 test confirmed significant group differences (p<0.001).

Additionally, group comparisons of subjects with NUA intensities over LOD were performed, however this did not result in any significant differences **(Fig. 10 B)**.

Taken together, serum NUA intensities were increased in diabetic FoCus subjects.

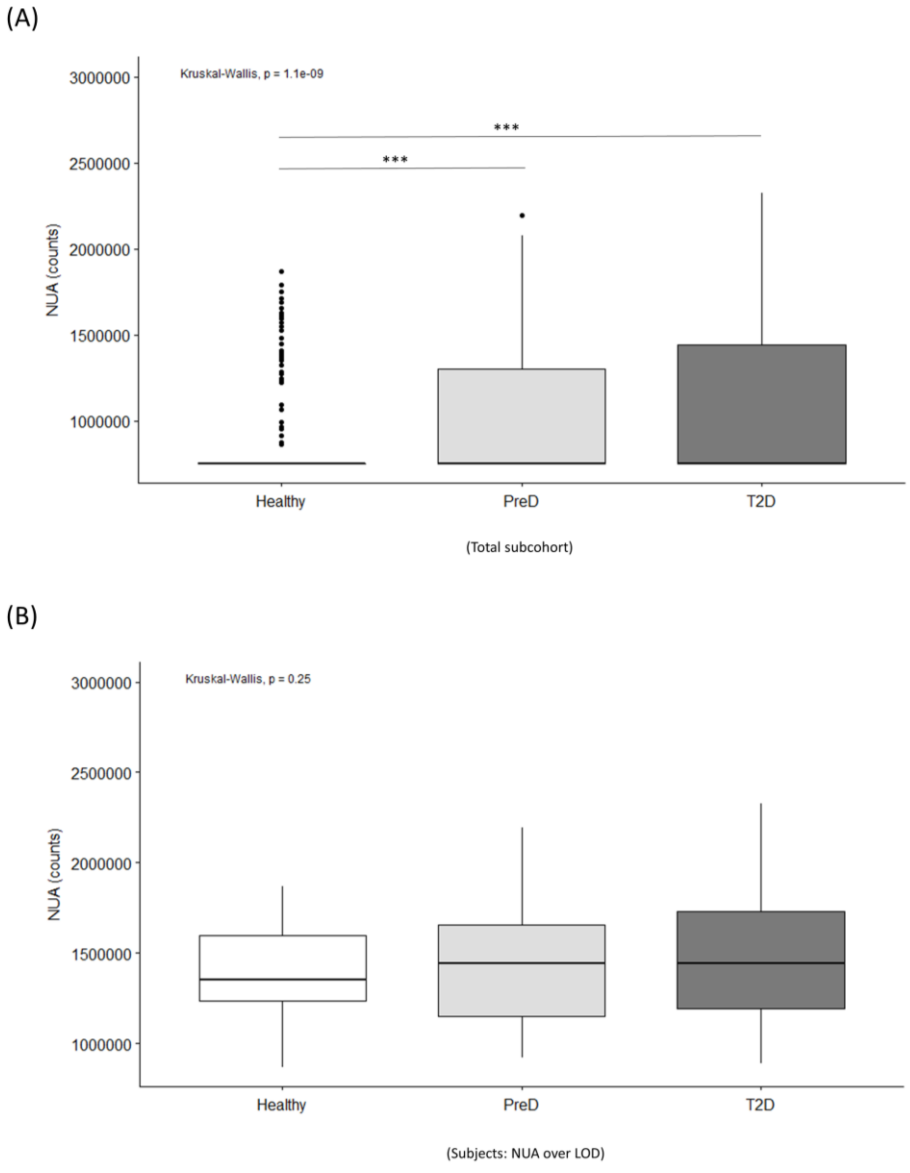

Figure 10: Analysis of serum NUA intensities (counts) between healthy, pre-diabetic and diabetic subjects of the FoCus sub-cohort: (A) Total sub-cohort: Healthy subjects showed lower NUA intensities compared to PreD and T2D subjects **(B)** Subjects with NUA intensities over LOD: no group differences in NUA intensities; Kruskal-Wallis test/ Wilcoxon test (*p<0.05; **p<0.01; ***p<0.001)

5.1.7 NUA and TRP were positively associated

Since the metabolisms of TRP and NA are closely related (34), the association between NUA und TRP intensities was analysed.

Results showed a significant positive correlation between serum NUA intensities and serum TRP intensities in the total sub-cohort (p<0.001; R=0.53) (data not shown). Furthermore, subjects with NUA and TRP intensities over LOD also showed a positive correlation (p<0.001; R= 0.61) **(Fig. 11)**.

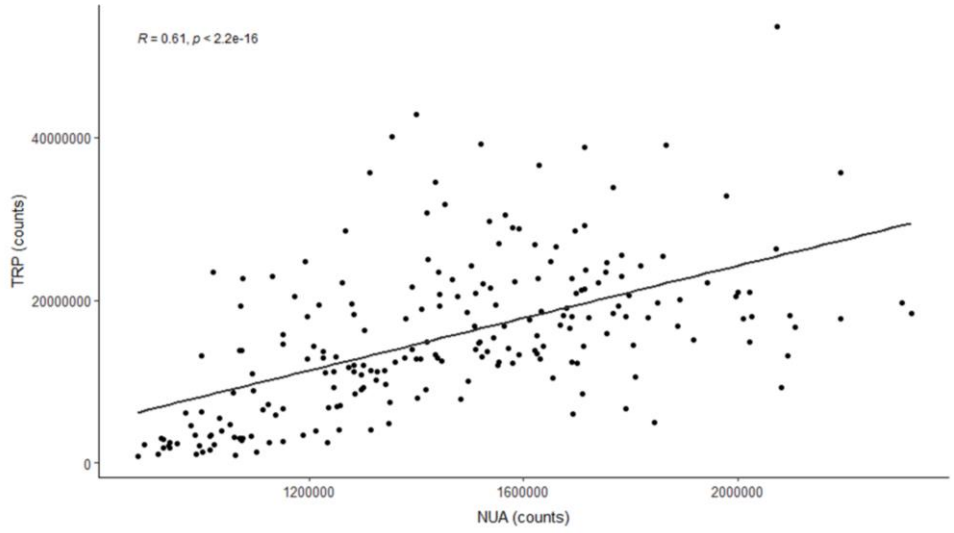

Figure 11: Association of NUA and TRP intensities over LOD in subjects of FoCus sub-cohort: Subjects showed a significant positive correlation between NUA and TRP serum intensities; Spearman correlation test (statistical significance p<0.05).

5.2 Association between serum NUA levels and clinical markers

In the previous chapters, it was shown that diabetic and obese subjects had increased serum NUA intensities compared to healthy controls. Therefore, an analysis with subjects from the total FoCus cohort (n=1775) was performed to investigate the association between serum NUA intensities and clinical markers such as inflammatory parameters, lipid markers and other diseases. Furthermore, it was examined if NUA is associated with hormonal state such as menopause and pregnancy. Because of a small amount of values, the anthropometric markers visceral fat and body fat percentage were excluded from evaluation. Since the amount of NA values was too small, it was excluded from evaluation.

The cohort was stratified into subjects with NUA intensities over the LOD (n=603) and below the LOD (n=1137) **(Table 8)**. Both groups did not show significant differences in age and gender.

Table 8: Basic characteristics of the FoCus cohort divided into subjects with NUA intensities below and over LOD; Results are shown as Median (25th;75th percentile) for continuous variables and as N (%) for categorical variables

	N	**NUA<LOD** (n=1137)	**NUA>LOD** (n=603)
Continuous Variables			
Age (y)	1767	52 (42, 63)	53 (43, 63)
Anthropometry			
BMI	1740	27 (23, 34)	29 (24, 39)
Waist measure (cm)	1732	96 (84, 113)	101 (88, 122)
Weight (kg)	1740	82 (69, 100)	88 (70, 115)
Glucose state			
Insulin (mIU/l)	1734	10 (6, 16)	11 (7, 21)
Glucose (mg/dl)	1738	94 (88, 103)	97 (90, 108)
HOMA-IR Index	1734	2.3 (1.5, 4.0)	2.6 (1.6, 5.5)
Inflammatory markers			
CRP (mg/l)	1739	1.5 (0.9, 4.1)	1.9 (0.9, 5.2)
TNF-α (pg/ml)	106	6 (0, 8)	0 (0, 6)
IL-6 (pg/ml)	1738	3.10 (1.80, 4.70)	3.40 (2.10, 5.50)
Wnt5a (ng/ml)	850	0.34 (0.21, 0.51)	0.36 (0.24, 0.53)
sFRP5 (ng/ml)	803	5 (3, 13)	7 (3, 16)

Lipid profile			
Lp (a) (mg/l)	1262	95 (95, 237)	120 (95, 330)
TG (mg/dl)	1739	103 (73, 148)	116 (79, 164)
Metabolites			
NAM (µg/l)	489	17 (14, 23)	17 (14, 22)
TRP (mg/dl)	489	1.65 (1.45, 1.83)	1.65 (1.46, 1.84)
Bile acids			
Chenodeoxycholic acid (µmol/L)	489	0.02 (0.02, 0.32)	0.02 (0.02, 0.27)
Cholic acid (µmol/L)	489	0.06 (0.03, 0.17)	0.08 (0.03, 0.25)
Desoxycholic acid (µmol/L)	489	0.26 (0.12, 0.50)	0.32 (0.18, 0.56)
Glycochenodeoxycholic acid (µmol/L)	489	0.57 (0.29, 0.96)	0.60 (0.31, 1.09)
Glycocholic acid (µmol/L)	489	0.11 (0.06, 0.23)	0.12 (0.06, 0.27)
Glycodeoxycholic acid (µmol/L)	480	0.26 (0.14, 0.45)	0.27 (0.14, 0.51)
Taurochenodeoxycholic acid (µmol/L)	489	0.07 (0.03, 0.13)	0.08 (0.03, 0.14)
Ursodeoxycholic acid (µmol/L)	489	0.020 (0.02, 0.02)	0.020 (0.02, 0.02)

Categorical Variables			
Gender	1736		
Male		419 (37%)	227 (38%)
Female		715 (63%)	375 (62%)
Apoplexy	1727		
Yes		21 (1.9%)	11 (1.8%)
No		1104 (98%)	591 (98%)
Atrial fibrillation	1717		
Yes		39 (3.5%)	25 (4.2%)
No		1084 (97%)	569 (96%)
Cardiac insufficiency	1707		
Yes		36 (3.2%)	22 (3.7%)
No		1079 (97%)	570 (96%)
Heart attack	1726		
Yes		32 (2.8%)	22 (3.7%)
No		1095 (97%)	577 (96%)
Hypertension	1721		
Yes		433 (38%)	287 (48%)
No		692 (62%)	309 (52%)

Body fat scale	1727		
Yes		33 (2.9%)	14 (2.3%)
No		1097 (97%)	583 (98%)
High blood lipids	1701		
Yes		315 (28%)	190 (32%)
No		797 (72%)	399 (68%)
Food allergy	1705		
Yes		100 (9.0%)	65 (11%)
No		1010 (91%)	530 (89%)
Inflammatory bowel disease	1719		
Yes		69 (6.1%)	30 (5.0%)
No		1054 (94%)	566 (95%)
Rheumatoid arthritis	1682		
Yes		79 (7.2%)	56 (9.6%)
No		1018 (93%)	529 (90%)
Liver disease	1718		
Yes		65 (5.8%)	39 (6.6%)
No		1058 (94%)	556 (93%)
Periodontitis	1713		
Yes		262 (23%)	145 (25%)
No		861 (77%)	445 (75%)
Menopause	1025		
Yes		286 (42%)	159 (45%)
No		389 (58%)	191 (55%)
Pregnancy	1083		
Yes		1 (0.1%)	0 (0%)
No		706 (99%)	373 (100%)

5.2.1 Subjects with increased levels of glucose profile markers showed elevated NUA intensities

The association between serum NUA intensities and parameters of the glucose profile was investigated. Glucose (p<0.001) and insulin (p<0.01) revealed significant higher serum levels in subjects with NUA intensities over LOD compared to subjects with NUA intensities below LOD **(Fig.12 A, B)**. Furthermore, increased HOMA indices were observed in subjects with NUA intensities over LOD compared to subjects with NUA intensities below LOD (p<0.001) **(Fig. 12 C)**.

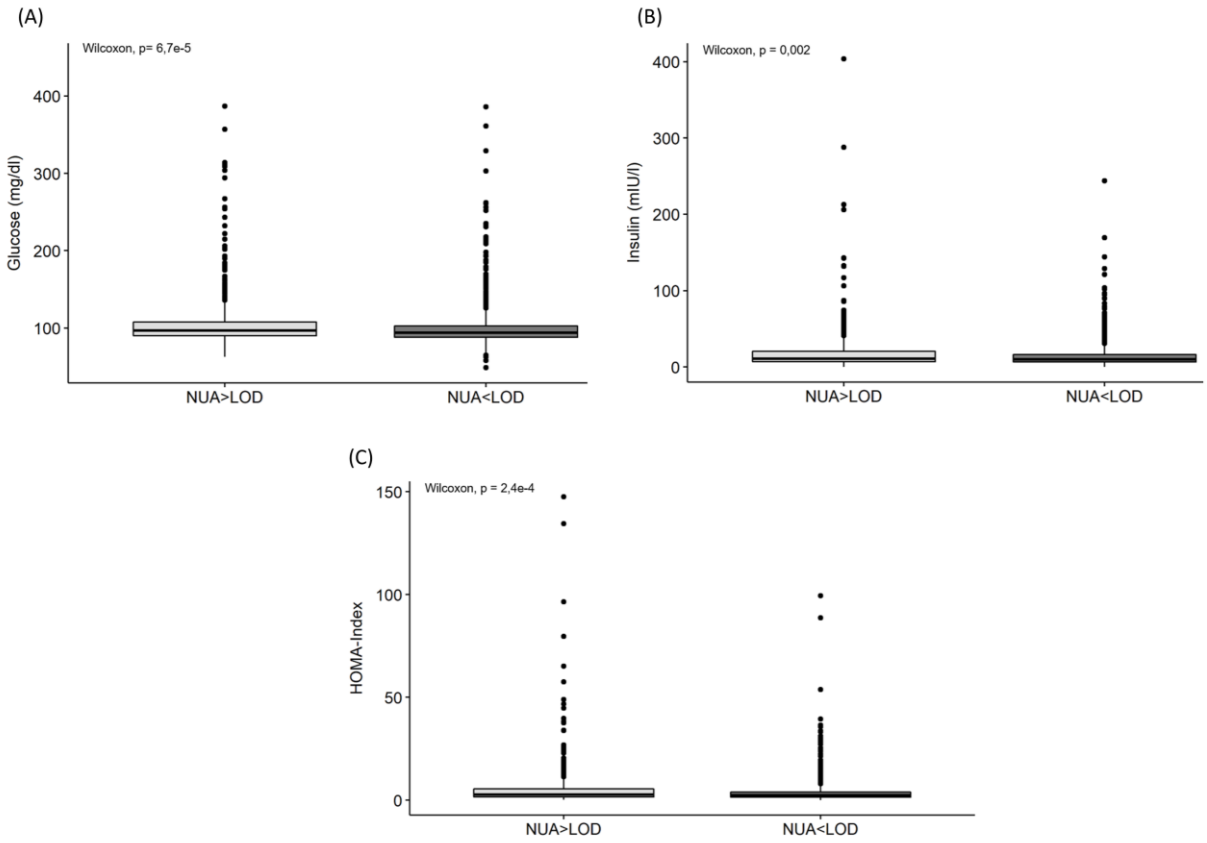

Figure 12: Differences in glucose markers between subjects with NUA intensities over/ below LOD: Subjects with NUA intensities over LOD showed significant higher **(A)** glucose levels **(B)** insulin levels **(C)** HOMA indices compared to subjects with NUA intensities below LOD; Wilcoxon test (statistical significance p<0.05).

5.2.2 Subjects with increased values of anthropometric markers had elevated serum NUA levels

Differences of anthropometric markers between groups with serum NUA intensities over and below LOD were examined. Subjects with NUA intensities over LOD showed higher values in BMI (p<0.001), weight (p<0.001) and waist circumference (p<0.001) compared to subjects with NUA intensities below LOD **(Fig. 13)**. No significant differences in body fat scale between the two groups were observed.

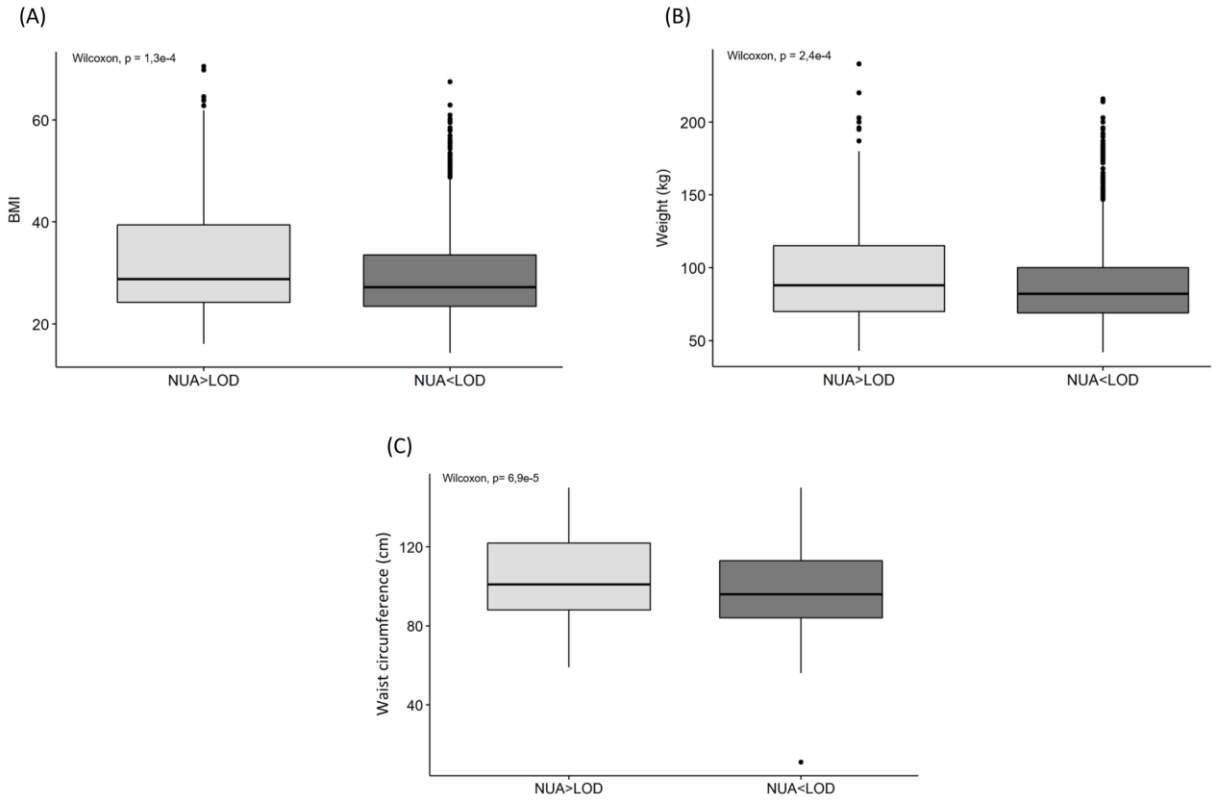

Figure 13: Differences in anthropometric parameters between subjects with NUA levels over/ below LOD: Subjects with NUA intensities over LOD showed a significant a higher **(A)** BMI **(B)** Weight **(C)** waist circumference compared to subjects with NUA intensities below LOD; Wilcoxon test (statistical significance p<0.05).

5.2.3 Subjects with high levels of inflammatory markers showed increased serum NUA intensities

Moreover, it was investigated if serum NUA intensities and inflammatory markers are associated. Results showed significant higher levels of CRP (p<0.01) and IL-6 (p<0.01) in subjects with NUA intensities over LOD compared to subjects with NUA intensities below LOD **(Fig. 14)**. TNF-α, Wnt5a and sFRP5 did not show significant group differences.

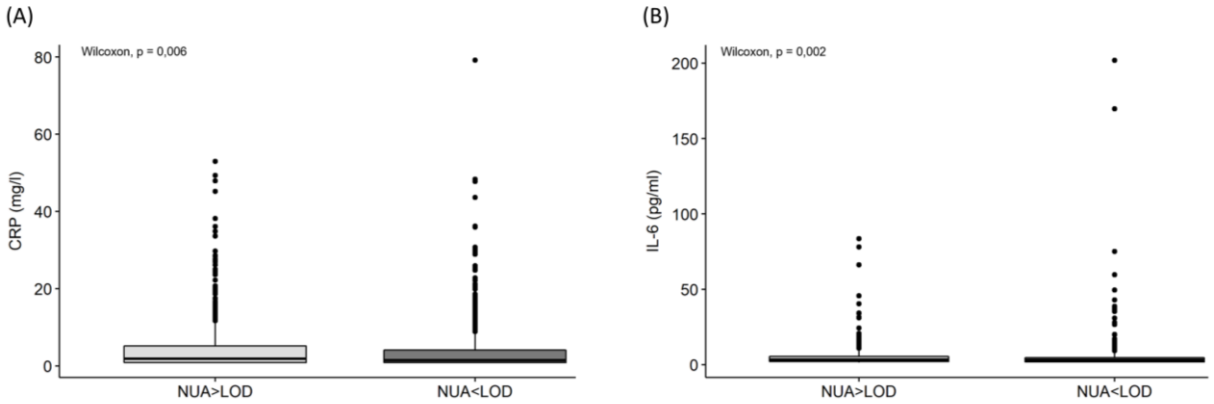

Figure 14: Differences in inflammatory parameters between subjects with NUA intensities over/ below LOD: Subjects with NUA intensities over LOD showed significant higher **(A)** CRP levels **(B**) IL-6 levels compared to subjects with NUA intensities below LOD; Wilcoxon test (statistical significance p<0.05).

5.2.4 Subjects with increased levels of lipid markers revealed elevated serum NUA intensities

Differences in lipid profile parameters between subjects with NUA intensities over and below LOD were investigated. Subjects with NUA intensities over LOD showed significant higher levels of TG (p<0.01) and Lp(a) (p<0.001) compared to subjects with NUA intensities below LOD **(Fig. 15).**

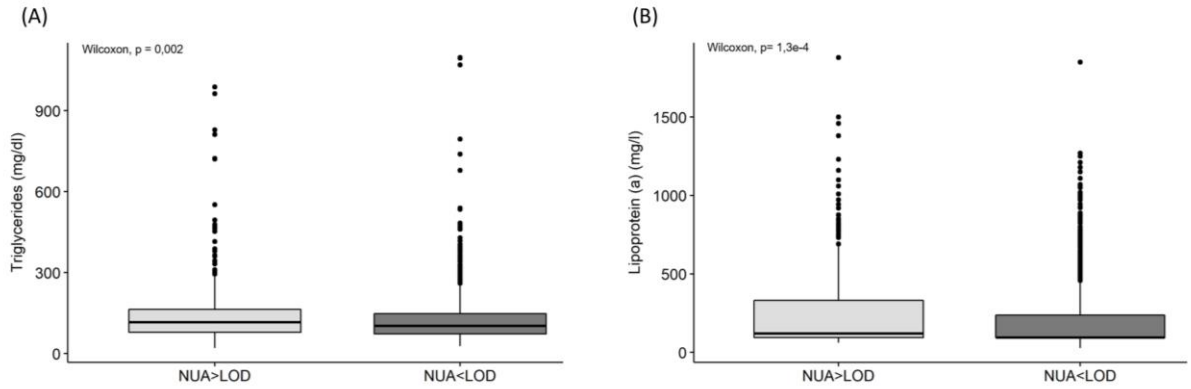

Figure 15: **Differences in lipid profile parameters between subjects with NUA intensities over/ below LOD:** Subjects with NUA intensities over LOD showed significant higher **(A)** triglyceride levels **(B)** Lp(a) levels compared to subjects with NUA intensities below LOD; Wilcoxon test (statistical significance $p<0.05$).

5.2.5 Serum NUA levels were positively associated with clinical markers

Furthermore, a correlation analysis with the significant parameters of the group analysis was performed and showed a significant positive association between NUA intensity and serum glucose levels (p<0.001; R=0.12), insulin levels (p<0.001; R=0.12) and HOMA-index (p<0.001; R=0.13). Anthropometric markers also revealed a positive correlation with NUA intensity (BMI: p<0.001; R=0.11; Weight: p<0.001; R=0.10; Waist circumference: p<0.001; R=0.12). IL-6 and CRP serum levels showed a positive association with NUA intensity, (CRP: p<0.001; R=0.08; IL-6: p<0.001; R=0.09). Additionally, NUA intensities revealed a significantly positive correlation with TG and Lp(a) levels (TG: p<0.001; R=0.09; Lp(a): p<0.001; R=0.13). However, the effect size for all analysed parameters was low **(Fig. 16)**.

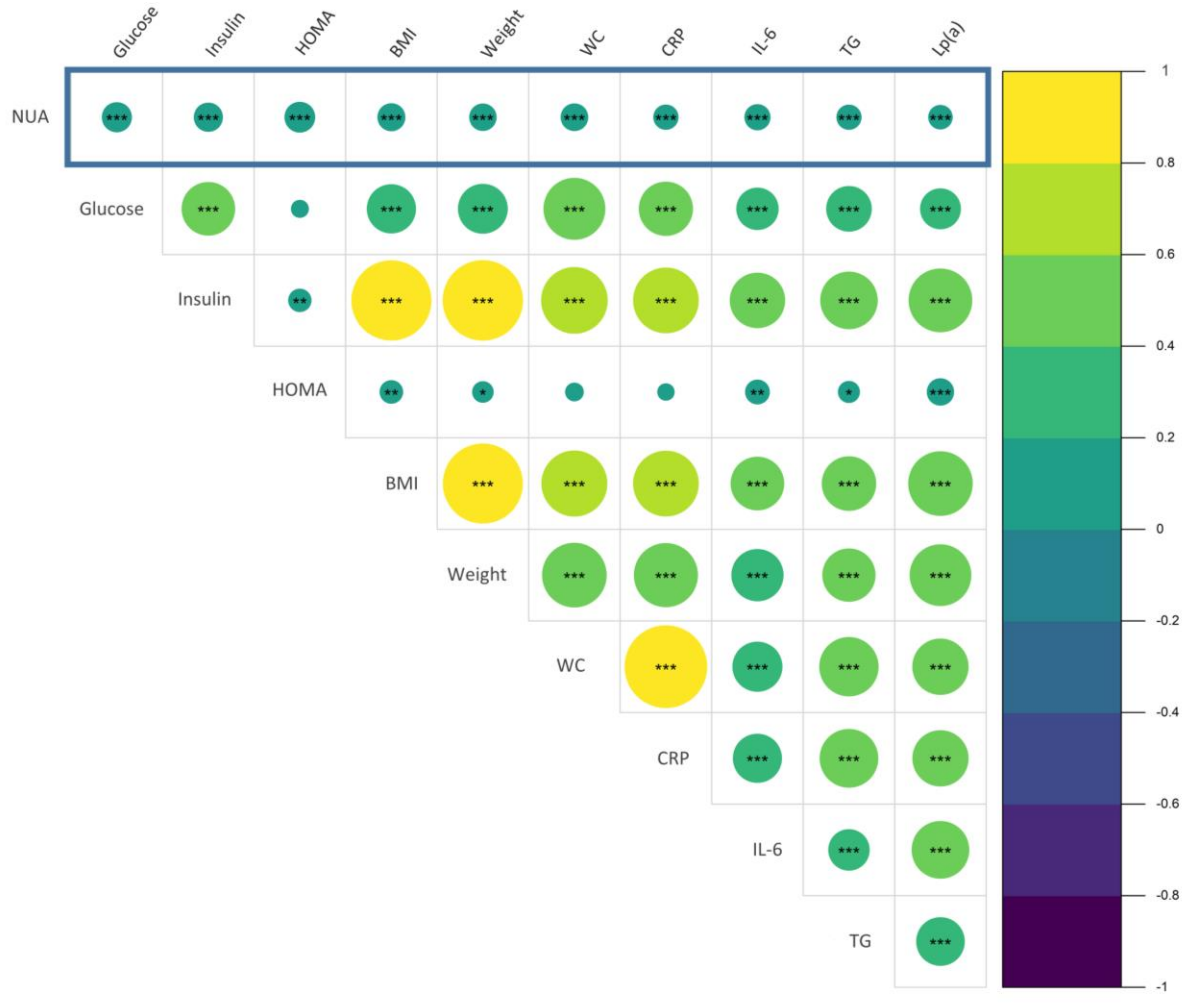

Figure 16: Correlation matrix for serum NUA intensities and clinical parameters: NUA intensities showed a significant positive correlation with markers of glucose state (glucose, insulin, HOMA-index), anthropometric parameters (BMI, weight, waist circumference (WC), inflammatory markers (CRP, IL-6) and parameters of lipid profile (TG, Lp(a)) with low effect size for all; Spearman-correlation test (*p<0,05; **p<0,01; ***p<0,001).

5.2.6 Association between NUA intensity and other clinical markers

Since NUA was shown to be associated with obesity and T2D, it was investigated if serum NUA levels are also linked to other diseases. It was observed that subjects with hypertension also showed elevated NUA intensities compared subjects with no hypertension ($p<0.01$) (data not shown). There was no association with other diseases. Furthermore, subjects with NUA intensities over and below LOD showed no significant differences in bile acids, metabolites and hormonal state.

Taken together, results show that markers of metabolic inflammation show a positive association with serum NUA intensities.

5.3 NUA was nominally associated with nutritional intake

Following, it was examined if the nutritional intake of FoCus subjects is associated with serum NUA intensities. Nutritional data from FoCus subjects (n=1623) included subtypes of carbohydrates, proteins, fat, dietary fibres, minerals, organic acids, water and alcohol. The cohort was stratified into subjects with NUA intensities over LOD (n=557) and below LOD (n=1066).

With regard to carbohydrates, subjects with NUA levels over LOD showed a nominally lower intake of lactose compared to subjects with NUA levels below LOD ($p<0.05$). Maltose ($p<0.05$) and absorbable oligosaccharides ($p<0.05$) intake was nominally higher in subjects with NUA levels over LOD compared to subjects with NUA levels below LOD ($p<0.05$) **(Fig. 17)**.

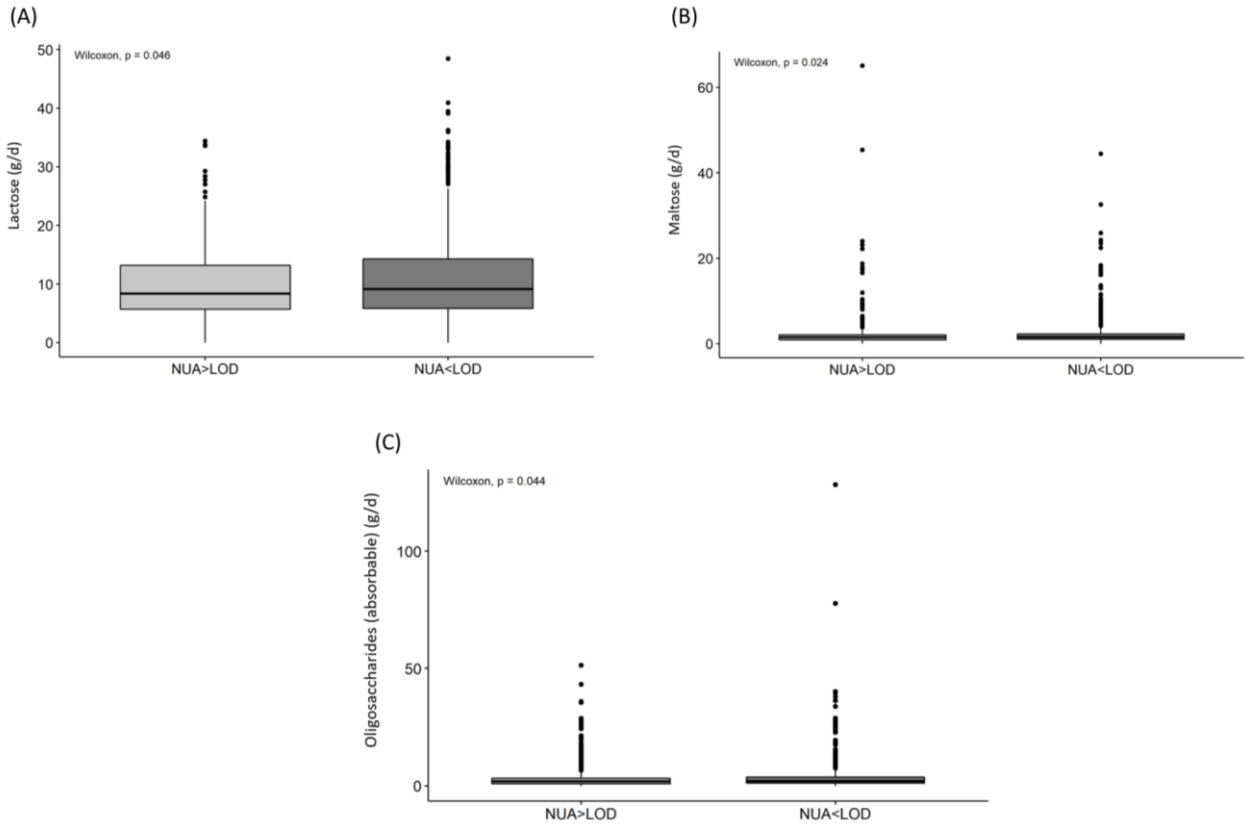

Figure 17: Differences of carbohydrates (maltose, lactose, absorbable oligosaccharides) between subjects with NUA levels over/ below LOD: (A) Subjects with NUA intensities below LOD showed a nominally significant higher lactose intake compared to subjects with NUA intensities over LOD. Subjects with NUA intensities over LOD had a nominally significant higher **(B)** maltose intake and **(C)** oligosaccharides intake compared to subjects with NUA intensities below LOD; Wilcoxon test (statistical significance $p<0.05$).

Furthermore, differences in amino acids intake between both groups were analysed. Cysteine ($p<0,05$) and arginine ($p<0,05$) intake was nominally higher in subjects with NUA intensities over LOD compared to subjects with NUA intensities below LOD **(Fig. 18)**.

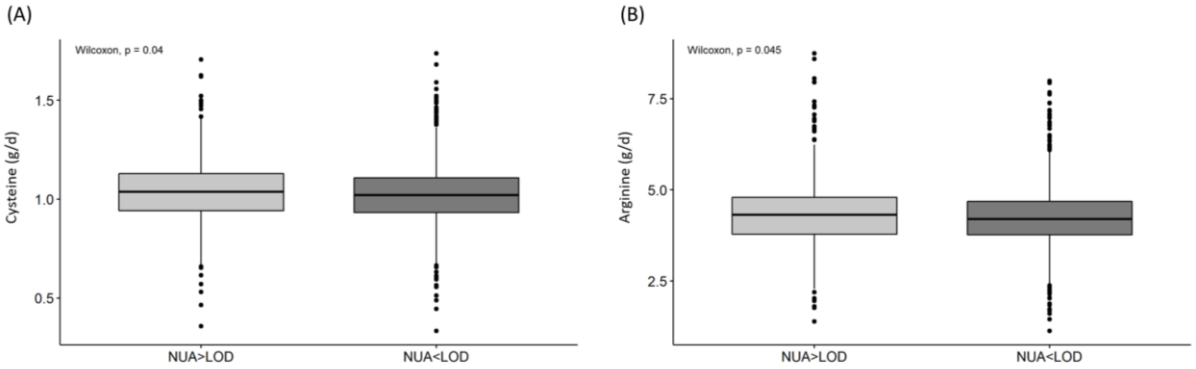

Figure 18: Differences in amino acid intake (cysteine and arginine) between subjects with NUA levels over/ below LOD: Subjects with NUA intensities over LOD showed a nominally significant higher: **(A)** cysteine intake **(B)** arginine intake compared to subjects with NUA intensities below LOD; Wilcoxon test (statistical significance $p<0.05$).

With respect to vitamins, a nominally higher intake of vitamin A (retinol equivalent) ($p<0,05$) and retinol ($p<0,05$) was observed in subjects with NUA intensities over LOD compared to subjects with NUA intensities below LOD **(Fig. 19)**.

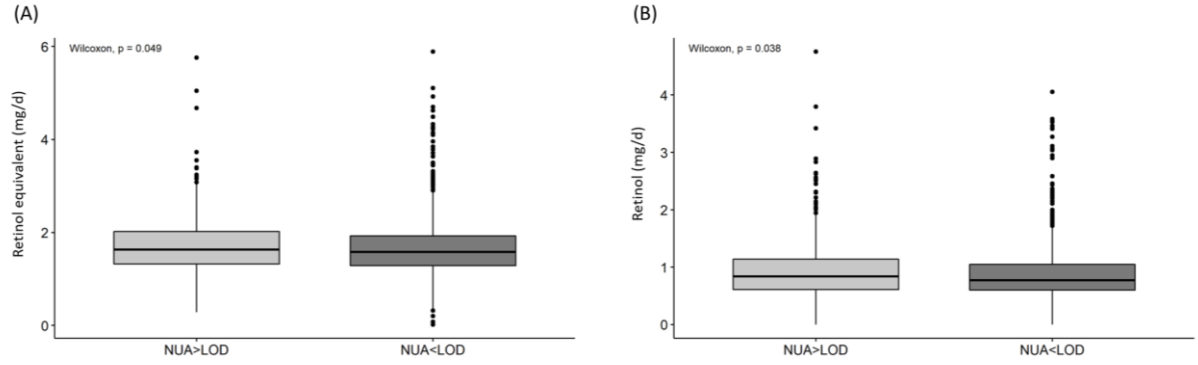

Figure 19: Differences in vitamin intake (retinol equivalent and retinol) between subjects with NUA levels over/ below LOD: Subjects with NUA intensities over LOD showed a nominally significant higher: **(A)** retinol equivalent intake **(B)** retinol intake compared to subjects with NUA intensities below LOD; Wilcoxon test (statistical significance $p<0.05$).

Additionally, subjects with NUA intensities over LOD showed a nominally lower alcohol intake compared to subjects with NUA levels below LOD ($p<0.01$) **(Fig. 20)**.

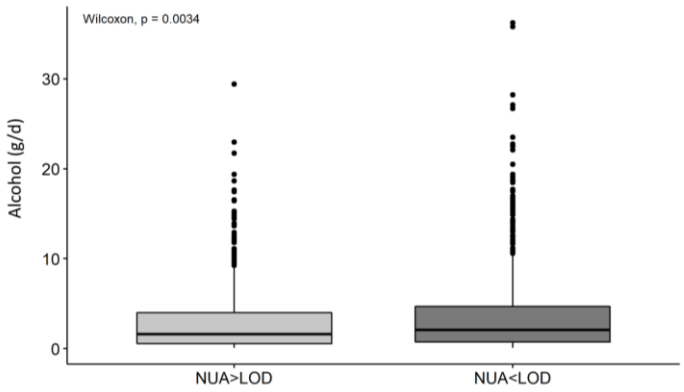

Figure 20: **Differences in alcohol intake between subjects with NUA intensities over/ below LOD:** A nominally significant lower alcohol intake was observed in subjects with NUA intensities over LOD compared to subjects with NUA intensities below LOD; Wilcoxon test (statistical significance $p<0.05$).

Furthermore, a correlation analysis was performed to examine the association between NUA intensities and nutritional parameters. Serum NUA intensities and lactose intake showed a nominally negative correlation ($p<0.01$; $R=-0.07$). Intake of maltose and oligosaccharides revealed a nominally positive correlation with NUA intensities (Maltose: n.s., $R=0.05$; Oligosaccharides: $p\leq0.05$, $R=0.05$) NUA also showed a nominally negative correlation with cysteine (n.s.; $R=-0.05$) and arginine intake ($p<0.05$; $R=-0.06$). While retinol equivalent revealed a nominally negative correlation with NUA intensities ($p\leq0.05$; $R=-0.05$), retinol intake was positively associated with NUA intensities ($p\leq0.05$; $R=0.05$). Additionally, a nominally positive correlation between alcohol intake and NUA intensities ($p\leq0.05$; $R=0.05$) was observed. The effect size for all analysed parameters was low **(Fig. 21)**.

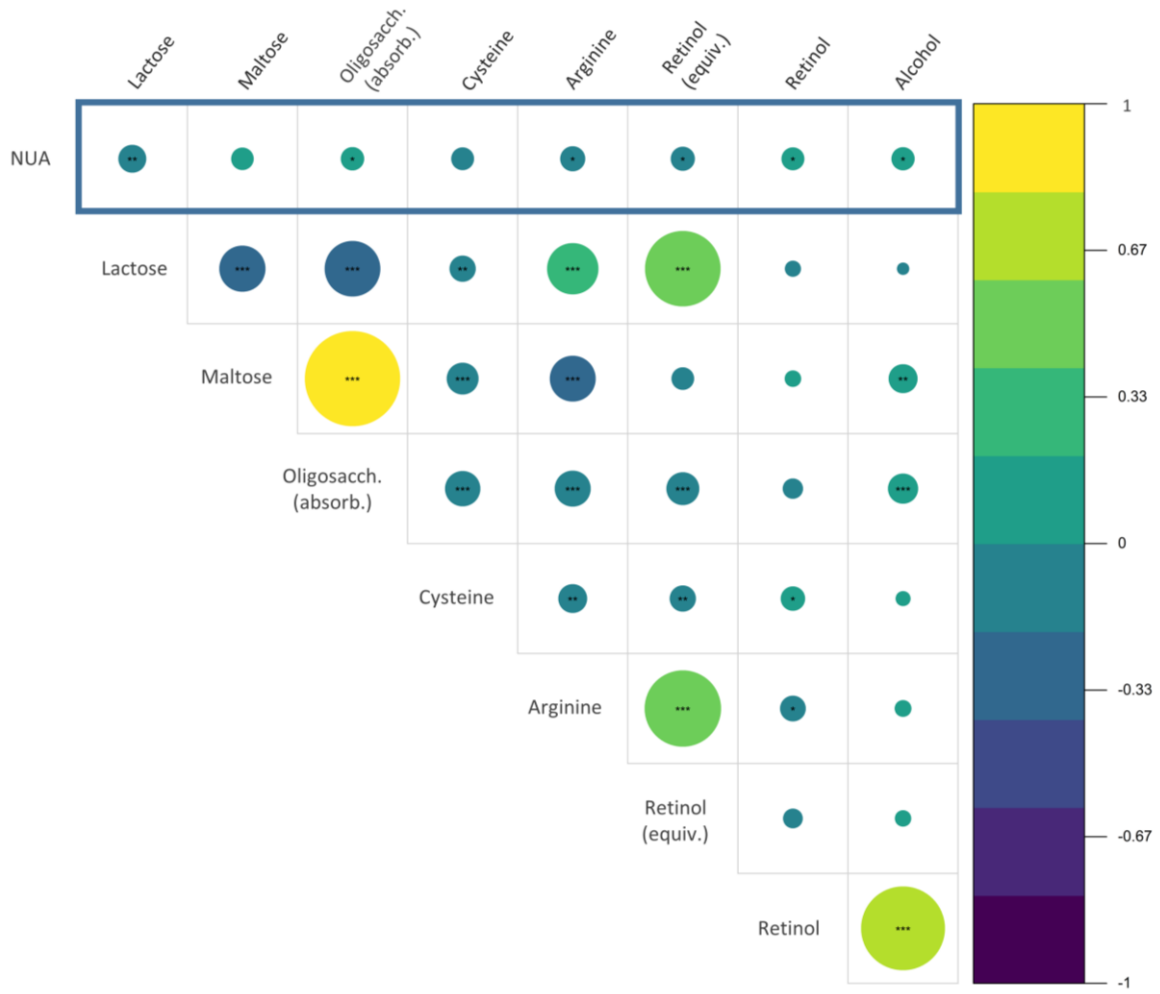

Figure 21: Correlation matrix for serum NUA intensities and nutritional intake: Serum NUA intensities showed a nominally negative correlation with lactose, cysteine, arginine and retinol equivalent intake. A nominally positive association was observed between NUA intensities and maltose, absorbable oligosaccharides, retinol and alcohol intake. All correlations showed a low effect size. Spearman-correlation test (*p<0.05; **p<0.01; ***p<0.001).

No group differences in subtypes of fat, dietary fibres, minerals and water intake between both groups were recorded.

Taken together, serum NUA intensities and nutritional intake only showed a nominal association.

5.4 NUA showed no association with the human gut microbiome

NA levels are linked to alterations in human gut microbiome (7). Therefore, it was examined if serum NUA intensities also show an association with the composition of the gut microbiome in FoCus subjects (n=1488). For evaluation, the cohort was stratified into subjects with NUA intensities over LOD (n=516) and below LOD (n=972).

A Bray-Curtis dissimilarity model was performed to investigate quantitative differences in operational taxonomic units (OTUs) between the two groups. Evaluation of β-diversity showed that both groups revealed a high congruence of OTUs, with no significant group differences in β-diversity **(Fig. 22)**. However, the adjustment for BMI revealed to have a significant impact on β-diversity between both groups (p<0.001) (data not shown).

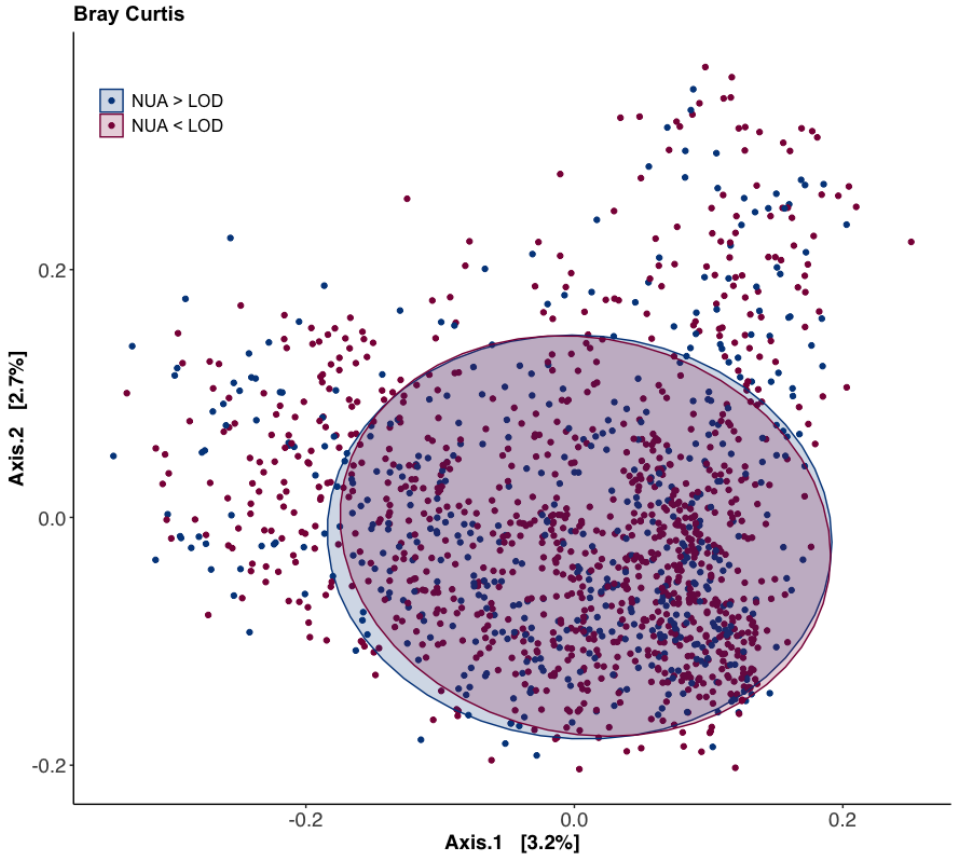

Figure 22: Differences in β-diversity in FoCus subjects with NUA intensities over/ below LOD: Both groups showed no significant differences in β-diversity. PERMANOVA test (statistical significance p<0.05).

Furthermore, differences in α-diversity between both groups were investigated. Results showed no significant differences of Shannon, Chao and Species Richness indices between both groups **(Fig. 23)**.

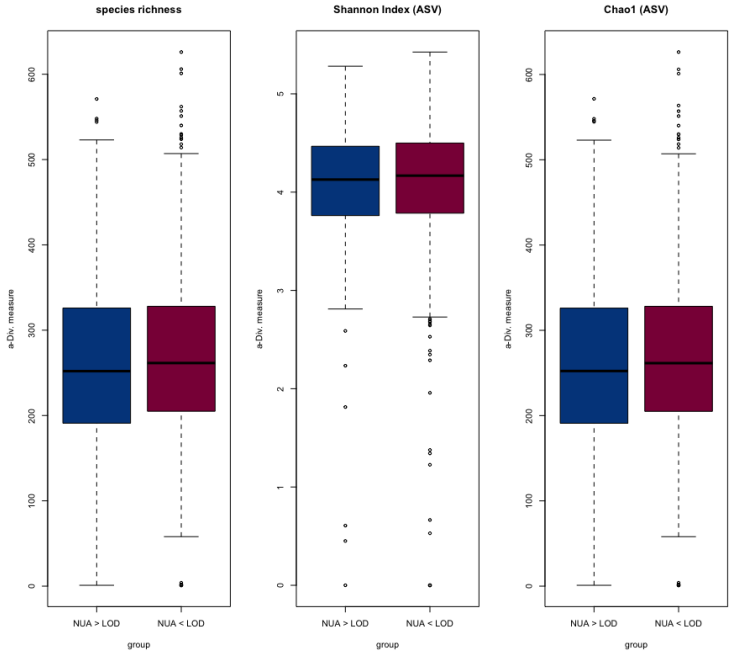

Figure 23: Alterations in α-diversity between subjects with NUA levels over/ below LOD: There were no differences between the two groups. Wilcoxon test (statistical significance $p<0.05$).

Moreover, the relative abundances of gut bacteria families in subjects with NUA intensities over LOD and below LOD were investigated. Results showed no significant differences between both groups **(Fig. 24)**.

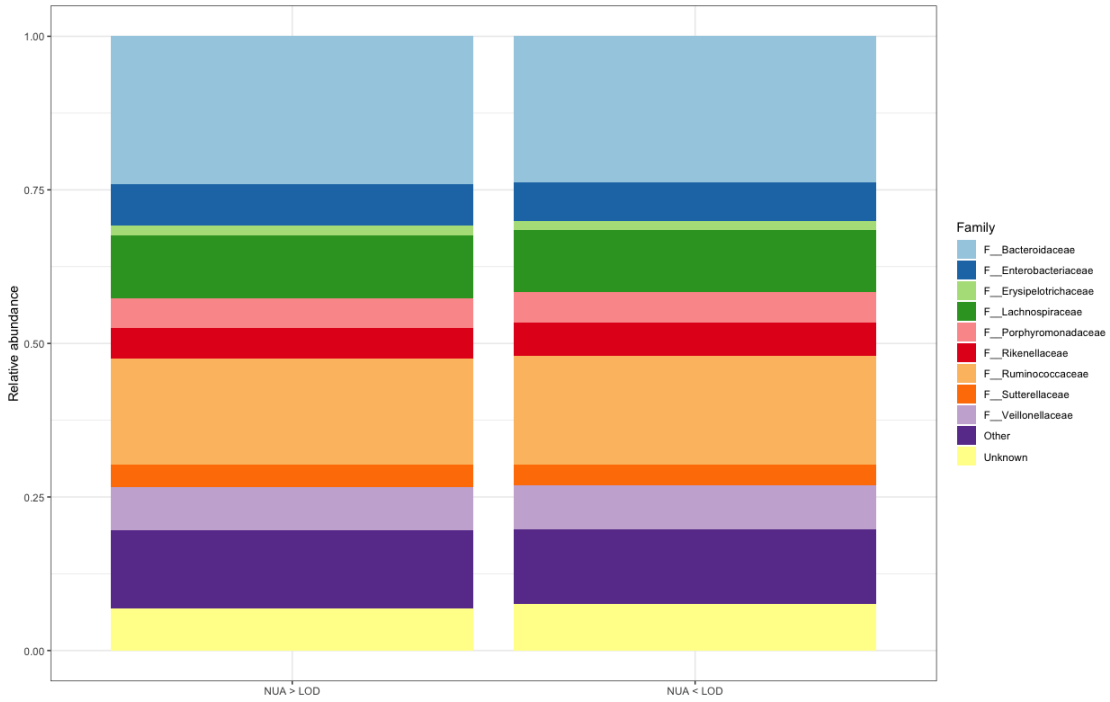

Figure 24: Differences in the relative abundances (%) of gut bacteria families between subjects with NUA intensities over/ below LOD: There were no differences between the two groups.

Taken together, serum NUA levels showed no association with the composition of the human gut microbiome.

5.5 *In vitro* studies

Results from the metabolomics-based approach showed a positive association between serum NUA intensities and markers of metabolic inflammation. If NUA induces an upregulation of clinical markers or elevated serum NUA level exhibit a reactive compensatory mechanism is still elusive. Therefore, *in vitro* experiments were performed to examine the effects of NUA on intracellular signalling in human and murine immune cells.

5.5.1 Effects of NUA on cultured THP-1 cells

Immortalized cell lines represent a useful model to examine cellular mechanisms in health and disease (107). Therefore, first *in vitro* experiments were performed with cultured THP-1 macrophages to investigate the effects of NUA on immune cell signalling.

5.5.2 NUA had no detrimental effects on THP-1 viability

To exclude detrimental effects of NUA on macrophages, a neutral red uptake assay was performed. Cells were stimulated with 100µM, 500µM, 1mM, 5mM or 10mM NUA, 10% ethanol and PBS as solvent control for 24 h. Results showed no group differences with no significant reduction in cell viability compared to control. Only non-physiological concentrations of 10mM NUA reduced cell viability ($p<0.05$). 10% Ethanol, as positive control for cell death, showed a significant reduction in cell viability ($p<0.01$) compared to control **(Fig. 25)**.

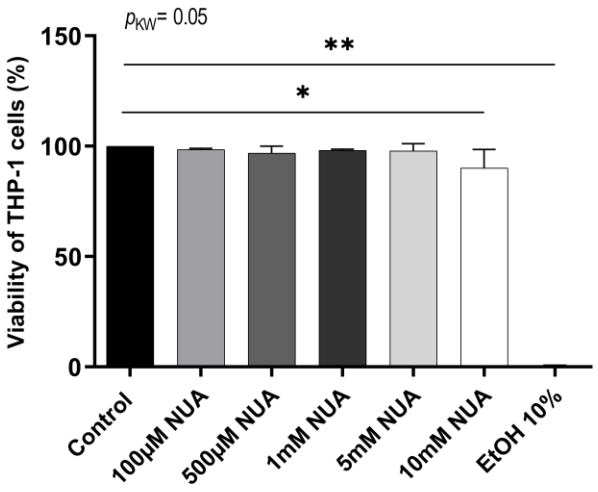

Figure 25: Neutral red uptake assay – Investigation of cytotoxic effects by NUA on THP-1 cells: NUA showed no detrimental effects on cells. 10% ethanol (EtOH) as positive control, PBS as negative control. n=3. Bars are shown as median with 95% CI. p_{KW} demonstrates p-value of Kruskal-Wallis test. Post-hoc Dunn`s test without correction for multiple comparisons (*p<0,05; **p<0,01; ***p<0,001).

5.5.3 NUA showed no effects on Nf-κB p50 protein expression in THP-1 cells

As already described, NF-κB plays a crucial role in metabolic diseases since it mediates the synthesis of pro-inflammatory cytokines. As it is known, that NA is able to reduce NF-κB expression, it was investigated if NUA also affects NF-κB expression in macrophages.

A pre-experiment was performed to analyse which stimulation time of NUA affects NF-κB p50 expression in THP-1 macrophages. Cells were stimulated with 100µM NUA and PBS as control for 30 min, 2 h, 4 h, 8 h and 24 h and NF-κB p50 protein expression was determined by Western blot analysis. Results showed a decrease in NF-κB p50 expression during all incubation times compared to controls. Stimulation with NUA for 2 h revealed the lowest levels of NF-κB p50 **(Fig. 26)**.

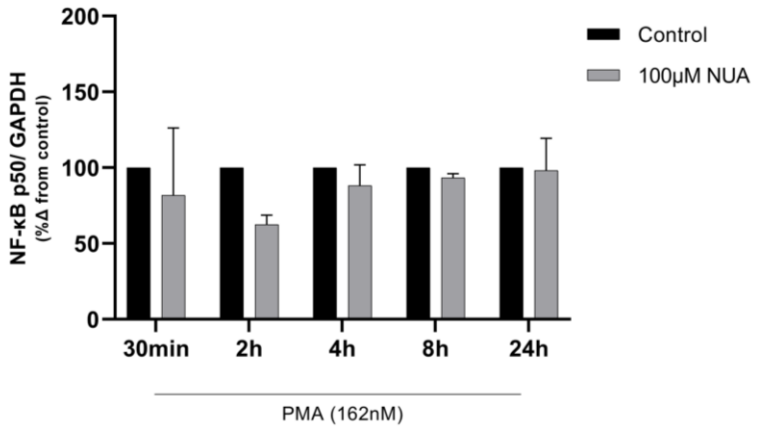

Figure 26: Pre-experiment: Effects of 100µM NUA on NF-κB p50 protein expression in THP-1 cells after 30 min, 2 h, 4 h, 8 h or 24 h: NF-κB p50 levels were mainly reduced after 2h treatment with NUA. 162nM PMA was used for cell differentiation, PBS as solvent control. GAPDH as housekeeping protein. n=2. Raw data of densitometry are listed in supplemental information (Table S2). Bars are shown as median with 95% CI.

In the following, a dose-response experiment was performed to investigate the effects of different NUA concentrations on NF-κB p50 protein expression in THP-1 cells. Cells were stimulated with 100µM, 500µM, 1mM, 5mM and 10mM NUA for 2 h and a Western blot was performed. Although no significant differences were observed, results showed slightly increased NF-κB p50 expression levels in a dose dependent manner (up to 5mM) compared to control (Fig. 27).

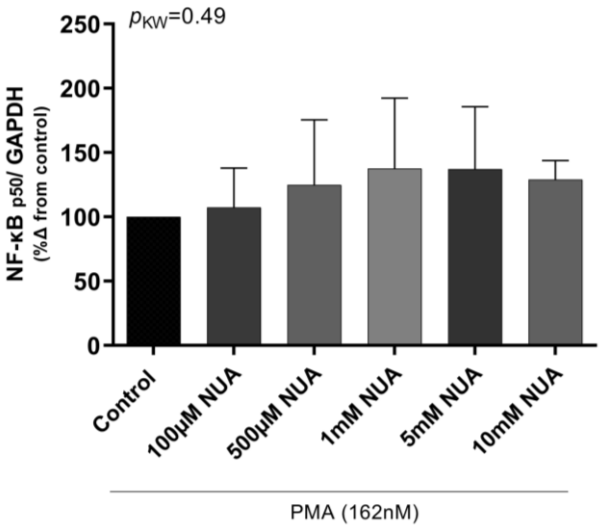

Figure 27: NF-κB p50 protein expression in THP-1 cells dependent on different doses of NUA (100µM, 500µM, 1mM, 5mM, 10mM) for 2h: Increasing doses showed no significant effects on NF-κB p50 protein expression. 162nM PMA was used for cell differentiation. GAPDH as housekeeping protein. n=4. Associated raw data of densitometry are noted in supplemental information (Table S3). Bars are shown as median with 95% CI; Kruskal-Wallis test, Dunn`s test without correction for multiple comparisons (statistical significance: $p<0.05$).

5.5.4 Effects of NUA on human primary immune cells

As NUA showed no remarkable effects on NF-κB p50 protein expression in THP-1 cells, primary neutrophils and monocytes were used for further investigations of NUA`s role in intracellular signalling.

5.5.5 NUA induced intracellular Ca^{2+} flux in human neutrophils

It was investigated if NUA is able to activate intracellular Ca^{2+} mobilisation in human neutrophils. Cells were incubated with Fluo-4 and Fura-red. Fluorescence intensity of these dyes was measured when neutrophils were acquired on a flow cytometer for 20 s. Afterwards, 100µM NUA, 500µM NUA, 100µM NA, 65nM ionomycin or PBS as solvent control were added to the tubes and acquisition was continued for another 60 s.

Results showed a change in fluorescence ratio after application of both NUA concentrations as observed in samples with NA and ionomycin. PBS did not show alterations in Ca^{2+} levels **(Fig. 28)**.

These results demonstrate that NUA is able to initiate intracellular Ca^{2+} flux in human neutrophils.

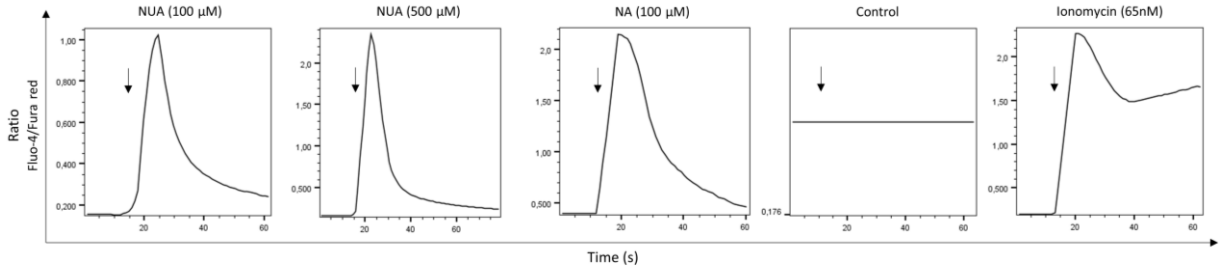

Figure 28: Effects of NUA on Ca^{2+} signalling in human neutrophils: Via flow cytometry, an intracellular Ca^{2+} flux over time (s) was detected as a change in fluorescence ratio of the dyes Fluo-4 and Fura-red elicited by NUA. NA and ionomycin were used as positive controls. PBS as negative control. Data show one representative out of 4 experiments.

5.5.6 NUA decreased cAMP levels in human neutrophils and monocytes

Furthermore, the effects of NUA on the forskolin-activated adenylyl cyclase in human neutrophils and monocytes was examined.

To induce synthesis of cAMP by adenylyl cyclase, cells were treated with 250µM forskolin and 100µM, 125µM, 500µM NUA or 100µM NA were simultaneously added for 5 min. cAMP levels were analysed by ELISA.

Results for neutrophils showed significant group differences ($p \leq 0.001$) with a significant decrease of adenylyl cyclase activity in cells stimulated with 125µM NUA ($p < 0.01$) and 500µM NUA ($p < 0.01$) compared to control. NA did not show differences in adenylyl cyclase activity compared to control **(Fig. 29 A)**.

For human monocytes, a significant reduction in adenylyl cyclase activity by 500µM NUA ($p < 0.05$) compared to control was observed. NA and 100µM NUA did not show differences in adenylyl cyclase activity compared to control **(Fig. 29 B)**.

Taken together, NUA led to an inhibition of forskolin-activated adenylyl cyclase and therefore a reduction of intracellular cAMP levels in human neutrophils and monocytes.

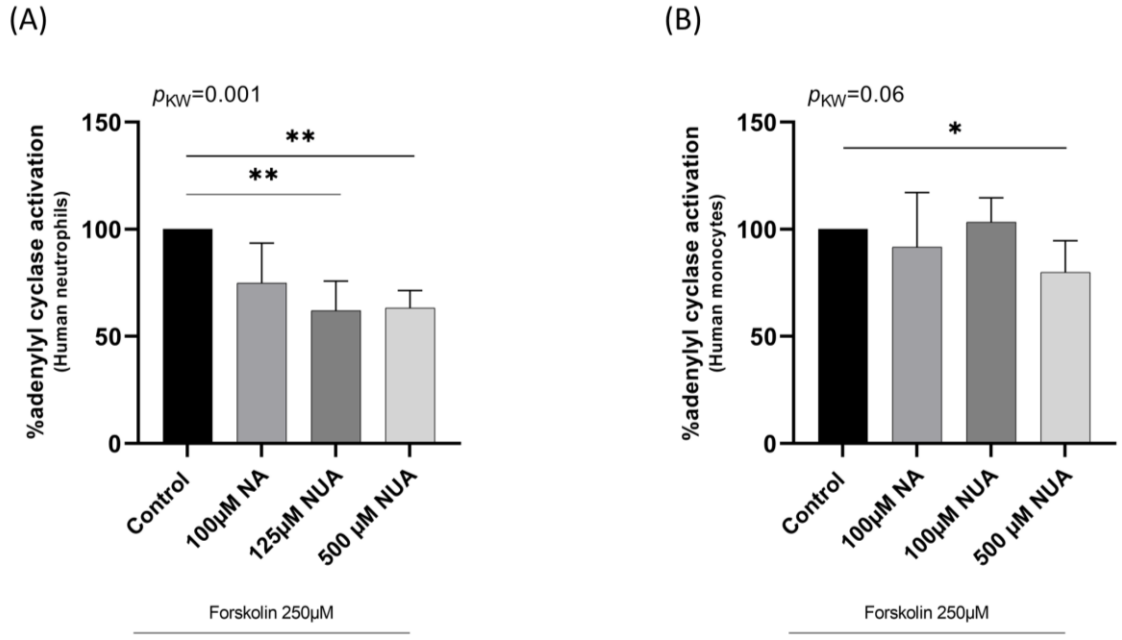

Figure 29: Inhibition of forskolin-activated adenylyl cyclase (reflecting cAMP synthesis) by NUA in human immune cells: NUA reduced cAMP levels in **(A)** neutrophils (n=4) **(B)** monocytes (n=5). Bars are shown as median with 95% CI. p_{KW} demonstrates p-value of Kruskal-Wallis test. Post hoc Dunn`s test without correction for multiple comparisons (* p<0.05, ** p<0.01, *** p<0.001).

5.5.7 NUA showed no alterations in β-Arrestin1 phosphorylation, but affected NF-κB p65 expression and phosphorylation in a time and dose dependent manner

THP-1 cells did not show alterations in NF-κB protein expression when treated with NUA. Therefore, it was investigated if NUA affects the NF-κB signalling pathway in human primary monocytes. β-Arrestin1 was included into investigation as it represents one of the first constituents in NF-κB signalling pathway and inhibits activation of NF-κB (108, 60).

Monocytes were treated with 100µM, 500µM NUA, 100µM NA or PBS as solvent for 5 min and 15 min. A capillary-based Western analysis was performed to determine phosphorylation of β-Arrestin 1, expression levels of NF-κB p65 and phosphorylation of NF-κB p65 (p-NF-κB p65).

Results showed no significant differences in p-β-Arrestin1 levels when stimulated with 100µM, 500µM NUA or 100 µM NA for 5 min and 15 min compared to control **(Fig. 30)**.

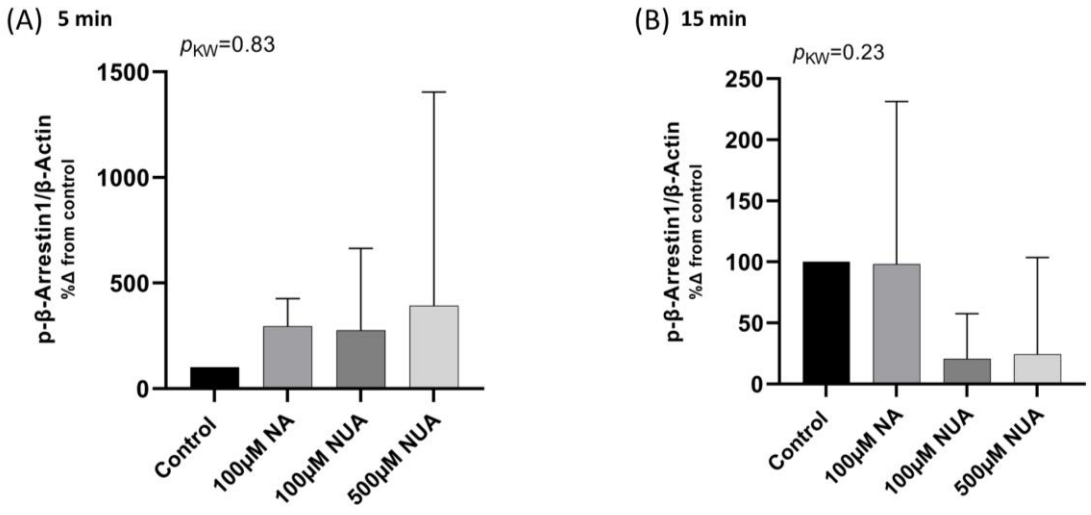

Figure 30: β-Arrestin1 phosphorylation in human primary monocytes after NUA treatment: No differences in p-β-Arrestin1 levels after **(A)** 5 min stimulation with NUA **(B)** 15 min stimulation with NUA. β-Actin as housekeeping protein. n=4. Raw data of densitometry are shown in supplemental information (Table S4). Bars are shown as median with 95% CI. p_{KW} demonstrates p-value of Kruskal-Wallis test. Post hoc Dunn`s test without correction for multiple comparisons (statistical significance: $p<0.05$).

5 min stimulation of monocytes with NUA and NA did not show differences in expression levels of NF-κB p65 compared to control **(Fig. 31 A)**. However, cells stimulated for 15 min showed significant group differences ($p<0.01$) with significant lower expression levels of NF-κB p65 when treated with 100µM NUA compared to control ($p<0.01$). No group differences were detected when cells were treated with 500µM NUA or 100µM NA **(Fig. 31 B)**.

With regard to activation of NF-κB p65 in monocytes, it was observed that 5 min stimulation with 100µM, 500µM NUA induced phosphorylation of NF-κB p65 significantly (100µM NUA: $p\leq0.05$; 500µM NUA: $p\leq0.05$) compared to control. NA did not induce significant differences in p-NF-κB p65 levels **(Fig. 31 C)**. Monocytes stimulated with 100µM, 500µM NUA and 100 µM NA for 15 min did not exhibit significant differences in p-NF-κB p65 levels **(Fig. 31 D)**.

Taken together, NUA and NA had no effect on β-Arrestin1 phosphorylation while NUA showed alterations in NF-κB p65 expression and phosphorylation dependent on dose and stimulation time.

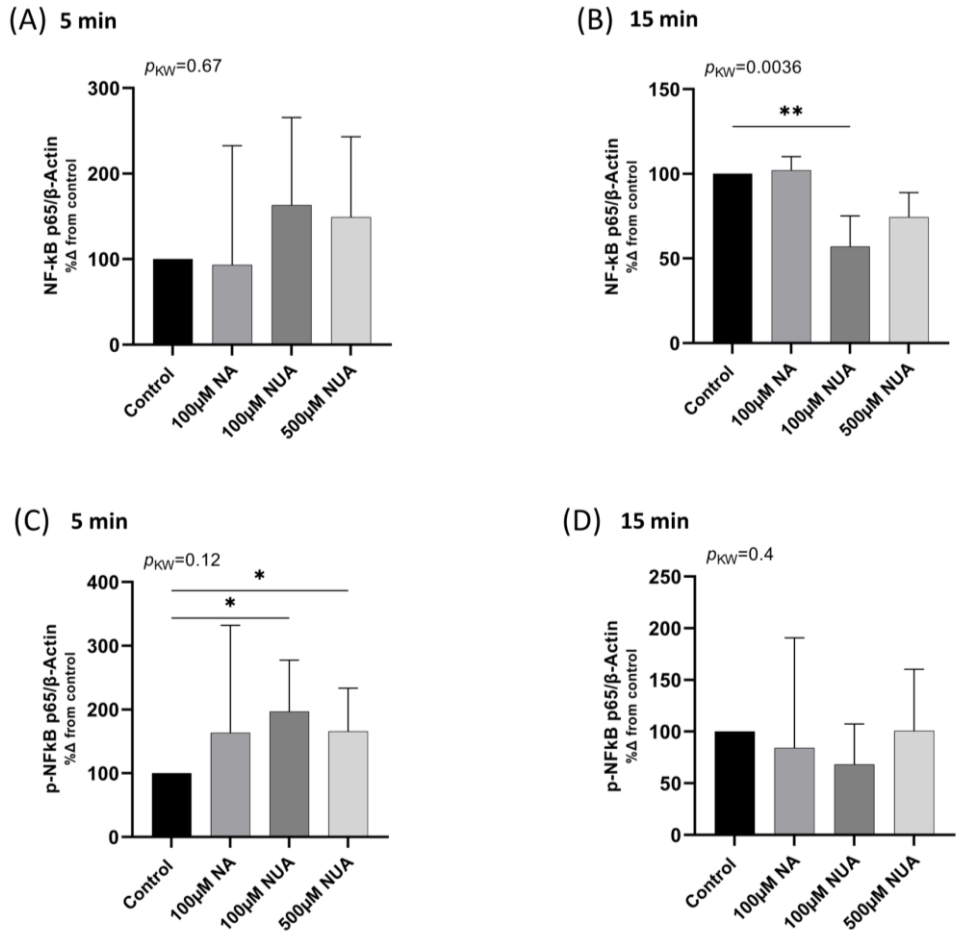

Figure 31: Effects of NUA on NF-κB p65 protein expression and phosphorylation in human primary monocytes: Measurement of NF-κB p65 protein expression after NUA treatment for **(A)** 5 min: n.s. differences compared to control **(B)** 15 min: significant reduction in NF-κB p65 expression by 100µM NUA. Detection of NF-κB p65 phosphorylation after NUA treatment for **(C)** 5 min: significant increase in NF-κB p65 phosphorylation with 100µM, 500µM NUA **(D)** 15 min: n.s. differences compared to control. β-Actin as housekeeping protein. n=5. Raw data of densitometry are demonstrated in supplemental information (Table S4). Bars are shown as median with 95% CI. p_{KW} demonstrates p-value of Kruskal-Wallis test. Post hoc Dunn`s test without correction for multiple comparisons (* p<0.05, ** p<0.01, *** p<0.001).

5.5.8 NUA reduced activation of MAPKs

Besides NF-κB, the MAPKs p38, ERK1/2 and JNK are crucial players in metabolic inflammation as already described in a previous chapter. Therefore, it was investigated if NUA affects the activation of these MAPKs in monocytes.

A capillary-based Western analysis was performed to detect alterations in phosphorylation of p38, ERK1/2, JNK^{46} and JNK^{54} in human primary monocytes after stimulation with 100µM, 500µM NUA, 100µM NA or PBS as solvent control for 5 min and 15 min.

It was observed that monocytes stimulated with NUA and NA for 5 min showed no differences in phosphorylation of all MAPKs compared to controls **(Fig. 32 A, C, E, G)**.

After 15 min of stimulation, monocytes treated with 100µM NUA induced a significant lower phosphorylation of p38 compared to control ($p<0.05$). Phosphorylation of p38 in cells stimulated with 500µM NUA and 100µM NA did not show alterations **(Fig. 32 B)**.

Monocytes stimulated for 15 min revealed significant group differences in p-ERK1/2 levels ($p<0.05$). Cell treatment with 100µM NUA led to a significant lower ERK 1/2 phosphorylation compared to control ($p<0.01$), while there were no differences in groups with 500µM NUA or 100µM NA treatment **(Fig. 32 D)**.

Phosphorylation of JNK^{46} showed significant group differences ($p<0.01$) after 15 min stimulation, with remarkably reduced JNK^{46} phosphorylation by 100µM NUA compared to control ($p<0.05$). Cells stimulated with 500µM NUA and 100µM NA showed no differences in JNK^{46} phosphorylation **(Fig. 32 F)**. JNK^{54} phosphorylation was no significantly altered by NUA or NA **(Fig. 32 H)**.

In conclusion, NUA treatment for 5 min showed no effect on MAPK activation while after 15 min, 100µM NUA reduced MAPK phosphorylation significantly. For NA, no alterations in MAPK phosphorylation were observed.

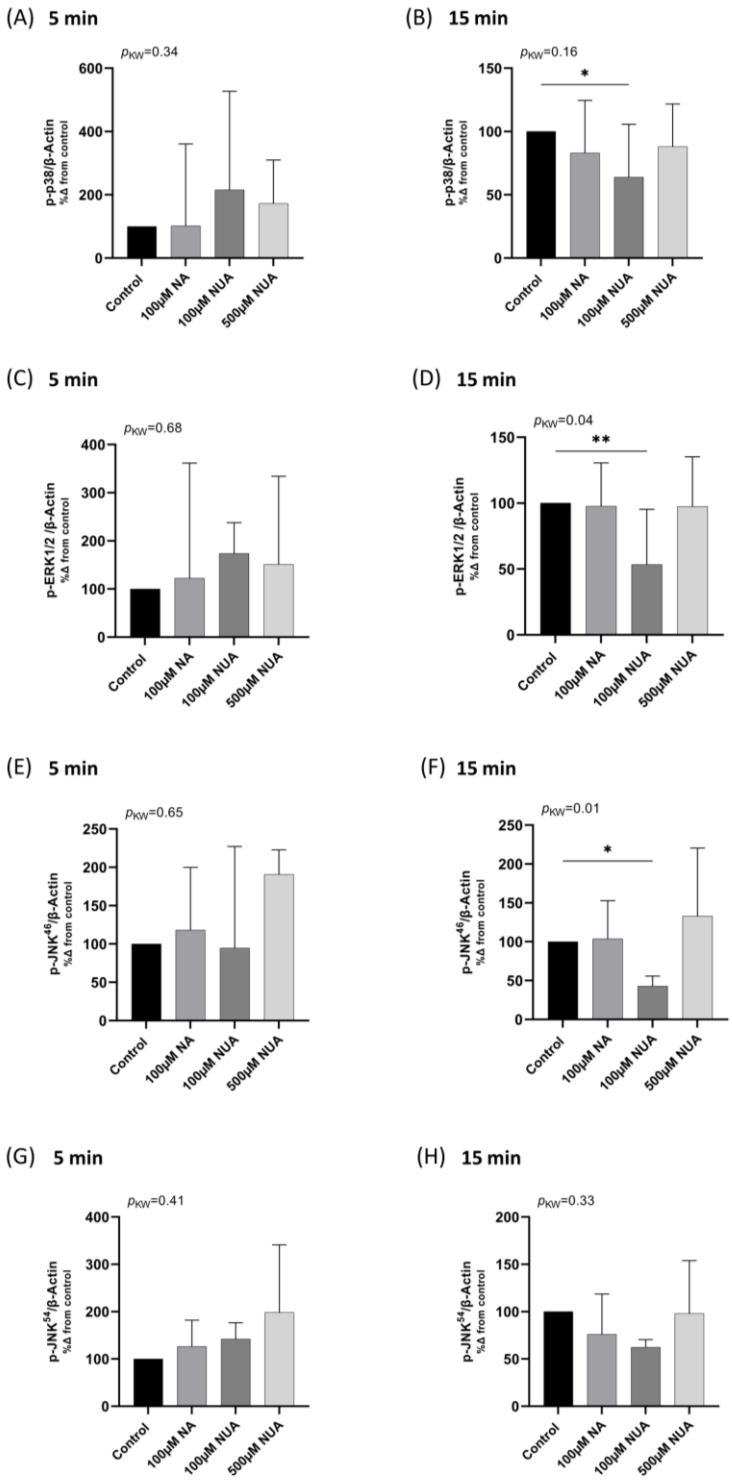

Figure 32: Investigation of MAPK activation by NUA in human primary monocytes by capillary-based Western analysis: Phosphorylation of: **(A)** p38 **(C)** pERK1/2 **(E)** p-JNK^{46} **(G)** p-JNK^{54} after 5 min NUA treatment: n.s. differences compared to control. Phosphorylation of: **(B)** p38 **(D)** pERK1/2 **(F)** p-JNK^{46} after 15 min: significant reduction in phosphorylation levels by 100µM compared to controls **(H)** p-JNK^{54} phosphorylation levels after 15 min: n.s. differences compared to controls. β-Actin as housekeeping protein. p38, ERK1/2: n=5; JNK: n=4. Associated raw data are listed in supplemental information (Table S5). Bars are shown as median with 95% CI. p_{KW} demonstrates p-value of Kruskal-Wallis test. Post hoc Dunn`s test without correction for multiple comparisons (* p<0.05, ** p<0.01, *** p<0.001).

5.5.9 NUA decreased phosphorylation of Akt

Moreover, it was investigated if NUA is able to elicit alterations in the phosphorylation of Akt.

Human monocytes were stimulated with 100µM, 500µM NUA, 100µM NA or PBS as solvent for 5 min and 15 min and phosphorylation of Akt was measured by capillary-based Western analysis.

Results showed no significant differences in p-Akt levels between groups after 5 min **(Fig. 33 A)**. Monocytes treated with 100µM NUA for 15 min revealed significant lower p-Akt levels compared to control (p<0.01). Stimulation with 500µM NUA and 100µM NA did not exhibit significant differences in Akt phosphorylation compared to control **(Fig. 33 B)**.

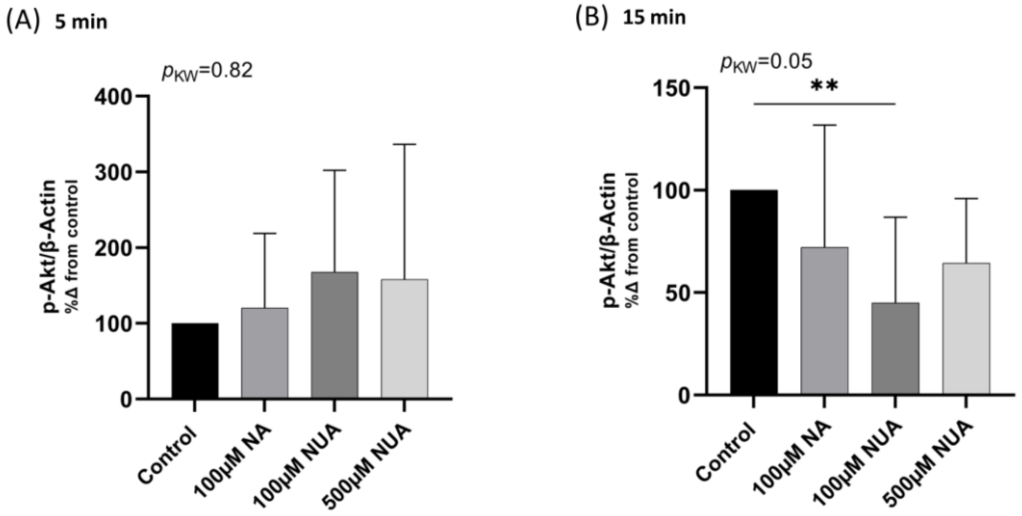

Figure 33: Effects of NUA on Akt phosphorylation in human monocytes: Phosphorylation of Akt after cell stimulation with NUA and NA **(A)** 5 min: n.s. differences compared to control **(B)** 15 min: significant reduction in Akt phosphorylation levels by 100µM NUA compared to control. β-Actin as housekeeping protein. n=5. Raw data of densitometry are demonstrated in supplemental information (Table S6). Bars are shown as median with 95% CI. p_{KW} demonstrates p-value of Kruskal-Wallis test. Post hoc Dunn`s test without correction for multiple comparisons (* p<0.05, ** p<0.01, *** p<0.001).

5.5.10 AMPKα phosphorylation was reduced by NUA

It is known that anti-inflammatory stimuli induce AMPKα phosphorylation while pro-inflammatory stimuli decrease p-AMPKα levels (90). With regard to this, human primary monocytes were treated with NUA to examine its effects on AMPKα signalling.

Cells were treated with 100µM, 500µM NUA, 100µM NA or PBS as solvent control for 5 min and 15 min. Subsequently p-AMPKα levels were measured by capillary-based Western analysis.

Results showed no differences in p-AMPKα levels between groups after 5 min treatment with NUA and NA **(Fig. 34 A)**. Stimulation with 100µM NUA for 15 min revealed significant lower p-AMPKα levels compared to control (p<0.05). 500µM NUA and 100µM NA did not show significant differences in AMPKα activation **(Fig 34 B)**.

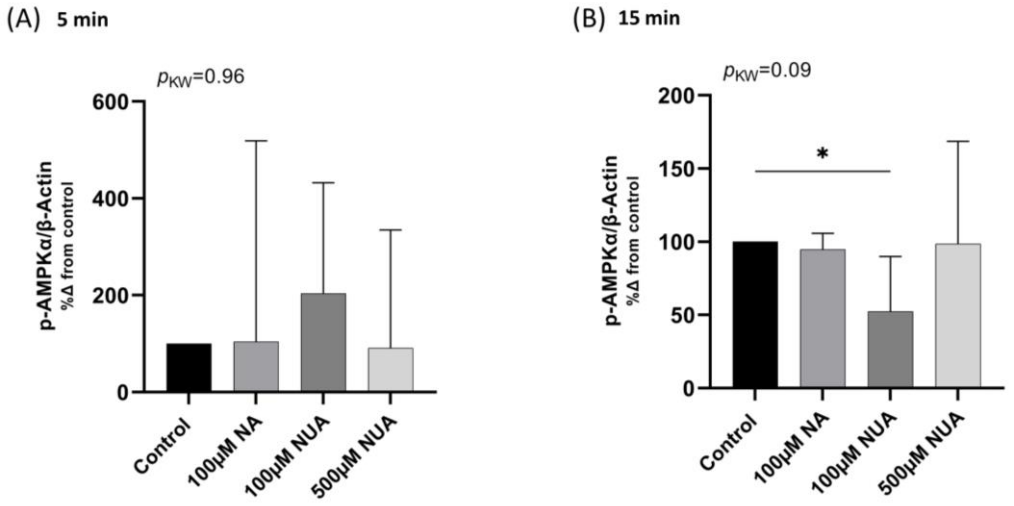

Figure 34: AMPKα phosphorylation after treatment with 100µM, 500µM NUA in human primary monocytes after: (A) 5 min: n.s. differences compared to control **(B)** 15 min: significant decrease in p-AMPKα levels by 100µM NUA compared to control. β-Actin as housekeeping protein. n=5. Associated raw data of densitometry are listed in supplemental information (Table S7). Bars are shown as median with 95% CI. P_{KW} demonstrates p-value of Kruskal-Wallis test. Post hoc Dunn`s test without correction for multiple comparisons (* p<0.05, ** p<0.01, *** p<0.001).

5.5.11 Identification of a NUA receptor

In the previous experiments, it was shown that NUA affects intracellular signalling in human immune cells. With regard to this, it was investigated if NUA acts via the NA receptor GPR109A. Therefore, murine GPR109A$^{+/+}$ and GPR109A$^{-/-}$ neutrophils and PEMs were used.

5.5.12 NUA had no detrimental effects on viability of murine neutrophils

To exclude detrimental effects of NUA on neutrophils of GPR109A$^{+/+}$ and GPR109A$^{-/-}$ mice, an Annexin apoptosis assay was performed.

Cells were treated with 250µM, 1mM, 100mM NUA, 10mM DMF or PBS as solvent control for 2 h. After staining of samples with Annexin V, GR-1 antibody and Zombie NIR live/dead dye, cell viability was determined by flow cytometry.

Results showed, that regardless of the concentration, at least 98% of GPR109A$^{+/+}$ and GPR109A$^{-/-}$ neutrophils were observed to be in viable state compared to control. Flow cytometry plots of neutrophils from GPR109A$^{+/+}$ **(Fig. 35 A)** and GPR109A$^{-/-}$ **(Fig. 35 B)** mice show that there is no significant difference between the percentage of viable, apoptotic, apoptotic dead and dead state after NUA treatment. This was confirmed by quantitative analysis of GPR109A$^{+/+}$ **(Fig. 35 C)** and GPR109A$^{-/-}$ **(Fig. 35 D)** mice.

Taken together, NUA does not have detrimental effects in murine neutrophils independent of the receptor.

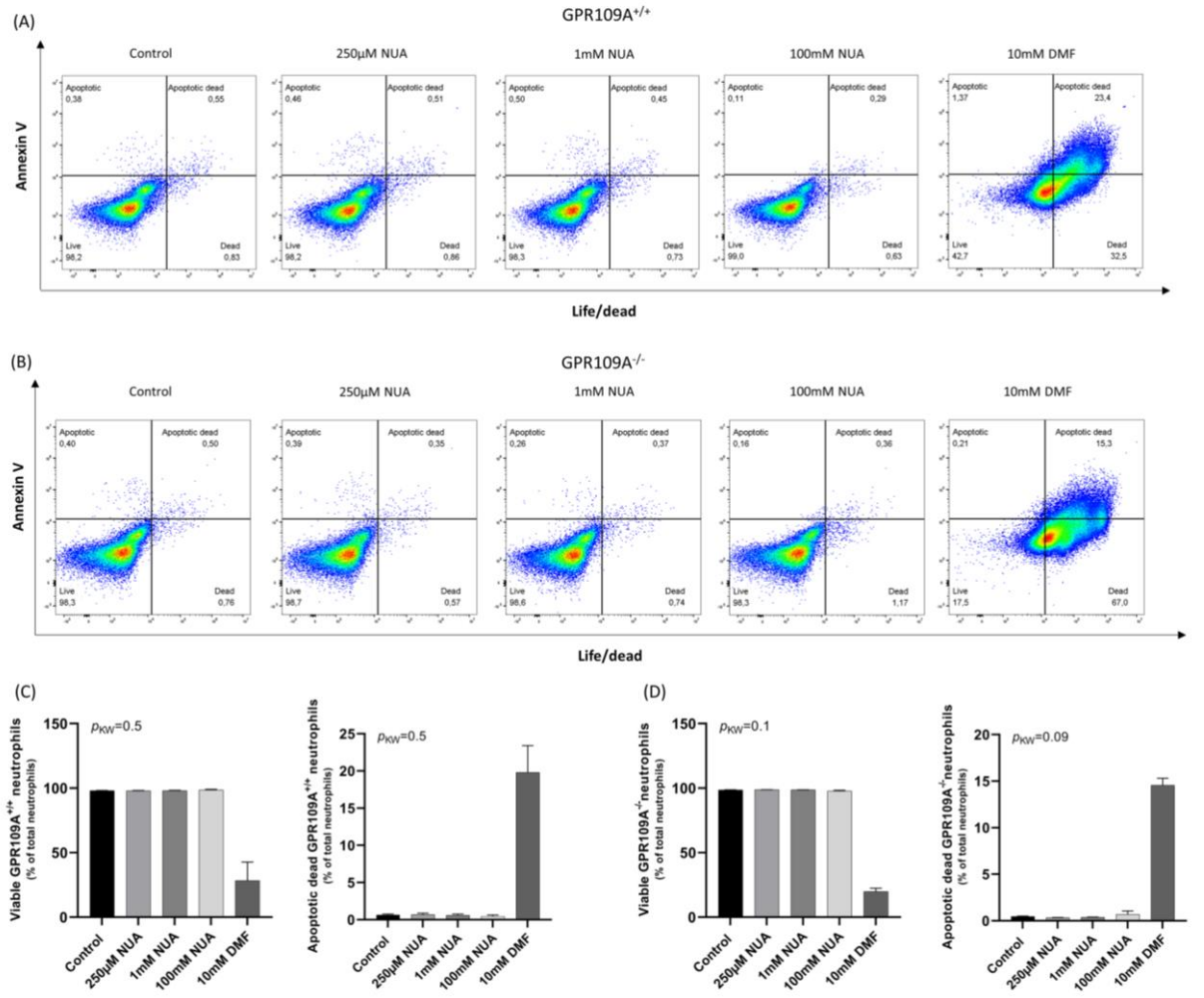

Figure 35: Annexin V apoptosis assay with murine neutrophils treated with NUA: No detrimental effects by NUA (**A,B)** Flow cytometry plots for GPR109A$^{+/+}$ and GPR109A$^{-/-}$ neutrophils **(C,D)** Quantitative analysis for GPR109A$^{+/+}$ and GPR109A$^{-/-}$ neutrophils viability. PBS and DMF as controls. Bars are shown as median with 95% CI. P_{KW} demonstrates p-value of Kruskal-Wallis test. Post hoc Dunn`s test without correction for multiple comparisons (statistical significance: $p<0.05$). This shows one representative example out of two experiments.

5.5.13 NUA induced Ca^{2+} flux in GPR109A$^{+/+}$ neutrophils, but not in GPR109A$^{-/-}$ neutrophils

Since NUA initiated an intracellular Ca^{2+} flux in human neutrophils, it was investigated if this effect is mediated via GPR109A.

Murine GPR109A$^{+/+}$ and GPR109A$^{-/-}$ neutrophils were incubated with Fluo-4 and Fura-red and fluorescence intensity of these dyes was measured when neutrophils were acquired on a flow cytometer for 20 s. Subsequently, 100µM, 500µM NUA, 100µM NA, 65nM ionomycin or PBS

as solvent control were added to the tubes and the change in Fluo-4/ Fura-red ratio was measured during acquisition for another 60 s.

GPR109A$^{+/+}$ neutrophils, treated with 100µM, 500µM NUA, showed an increase in the dye fluorescence ratio as samples treated with 100µM NA and 65nM ionomycin. However, these effects were abolished in GPR109A$^{-/-}$ neutrophils after NUA and NA stimulation **(Fig. 36)**. These results show that NUA induced intracellular Ca^{2+} flux via GPR109A in neutrophils.

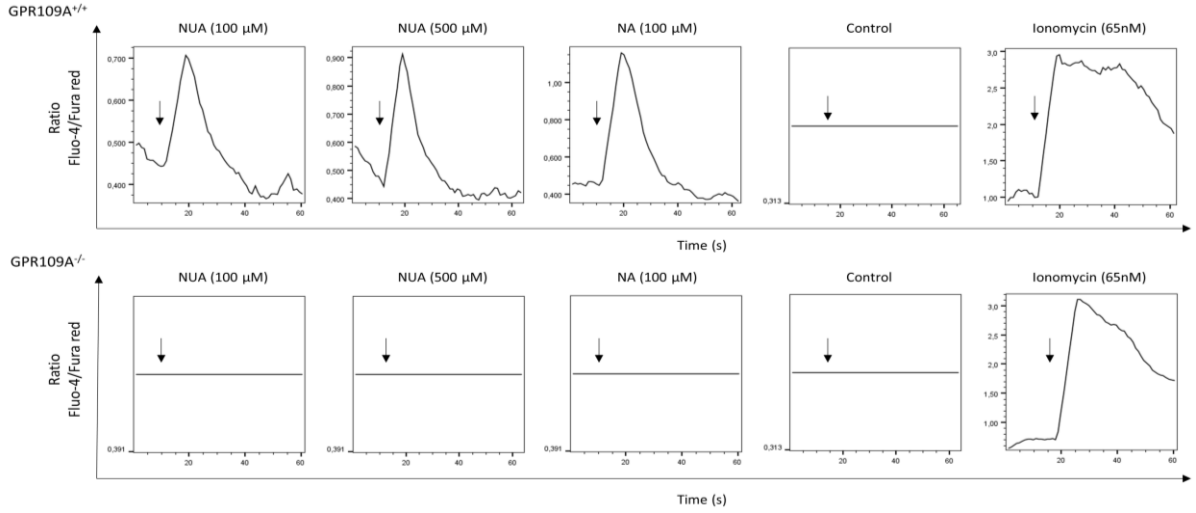

Figure 36: Effects of NUA on Ca^{2+} signalling in murine GPR109A$^{+/+}$ and GPR109$^{-/-}$ neutrophils: Via flow cytometry an intracellular Ca^{2+} flux over time (s) was detected as a change in fluorescence ratio of the dyes Fluo-4 and Fura-red elicited by NUA in GPR109A$^{+/+}$ neutrophils but not in GPR109$^{-/-}$ neutrophils. NA and ionomycin were used as positive controls, PBS as negative control. Data show one representative out of 2 experiments.

5.5.14 NUA reduced cAMP levels in neutrophils and PEMs of GPR109A$^{+/+}$ and GPR109A$^{-/-}$ mice

In human neutrophils and monocytes, reduced cAMP levels after treatment with NUA were observed. An experiment with murine GPR109A$^{+/+}$ and GPR109A$^{-/-}$ neutrophils and PEMs was performed to investigate if NUA inhibits the forskolin-activated adenylyl cyclase via GPR109A.

For synthesis of cAMP by adenylyl cyclase, cells were treated with 250µM forskolin and simultaneously 100µM, 125µM, 500µM NUA, 100µM NA or PBS as solvent control were added for 5 min. Cellular cAMP levels were determined by ELISA.

Neutrophils of GPR109A$^{+/+}$ mice stimulated with 125µM NUA showed significant lower cAMP levels compared to control (p<0.05). NA did not show alterations in cAMP levels **(Fig. 37 A)**. For GPR109A$^{-/-}$ neutrophils, significant lower cAMP levels by 125µM NUA (p<0.05) and 500µM NUA (p<0.05) compared to control were recorded. Stimulation with NA did not show significant differences **(Fig. 37 B)**.

Both, GPR109A$^{+/+}$ and GPR109A$^{-/-}$ PEMs, showed significant group differences (p<0.05, p<0.05) and 500µM NUA revealed significantly reduced cAMP levels compared to control in both genotypes (p<0.01, p<0.01). 100µM NUA and 100µM NA showed no alterations in cAMP levels **(Fig. 37 C, D)**.

In conclusion, NUA reduced cAMP levels in neutrophils and macrophages GPR109A-independently.

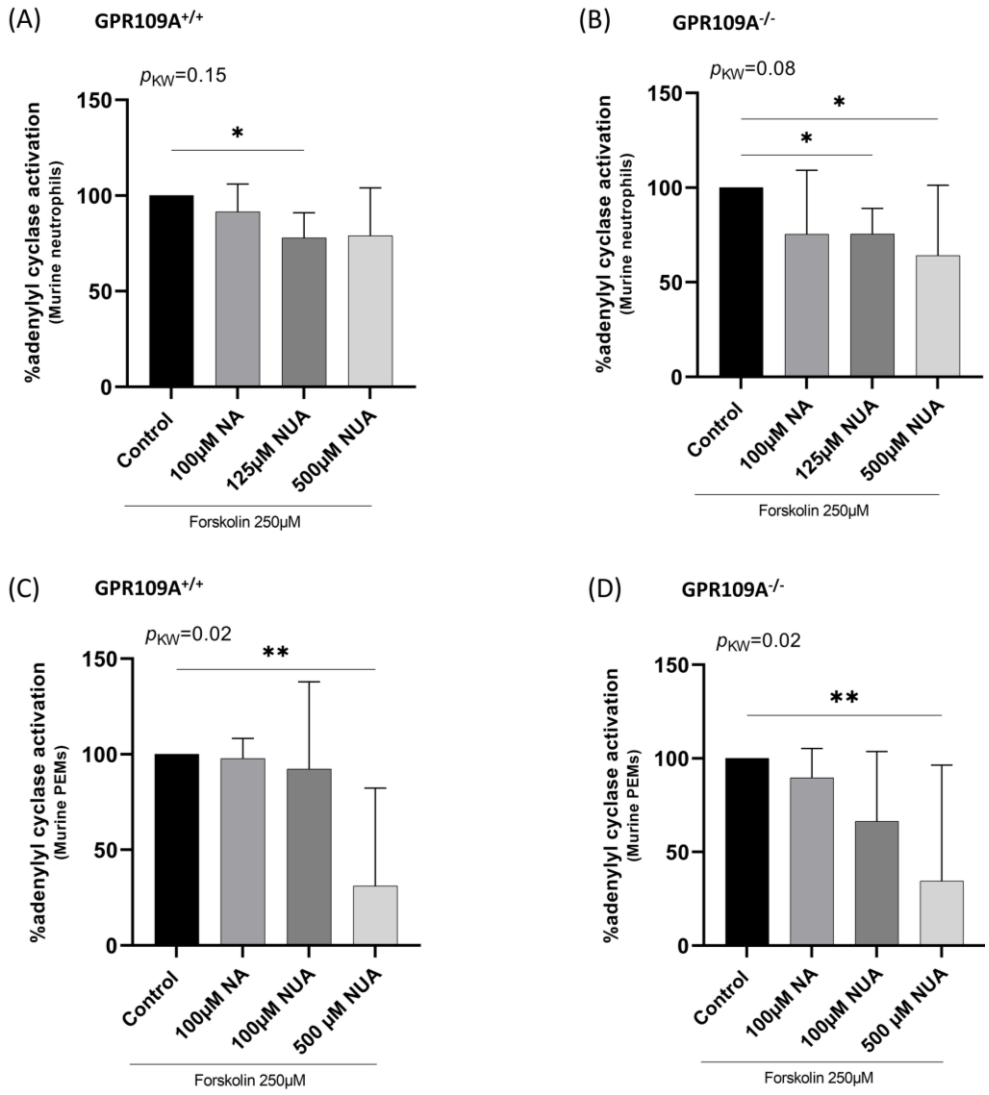

Figure 37: Inhibition of the forskolin-activated adenylyl cyclase (reflecting cAMP synthesis) by NUA in murine (GPR109A$^{+/+}$ and GPR109A$^{-/-}$) immune cells: Adenylyl cyclase activation was inhibited by NUA in: **(A, B)** GPR109A$^{+/+}$ and GPR109A$^{-/-}$ neutrophils and **(C, D)** GPR109A$^{+/+}$ and GPR109A$^{-/-}$ peritoneal macrophages (PEMs). n=5. Bars are shown as median with 95% CI. p_{KW} demonstrates the p-value of Kruskal-Wallis test. Post hoc Dunn`s test without correction for multiple comparisons (* p<0.05, ** p<0.01, *** p<0.001).

5.6 Immunohistochemistry - GPR109A was expressed in murine liver and hypothalamic tissues

Since the liver and hypothalamus also display metabolic active tissues, the expression of GPR109A in these tissues was investigated.

GPR109A expression in liver and hypothalamic tissue was examined by immunohistochemical analysis. Since there is no validated mouse anti-GPR109A antibody, a transgenic mouse line expressing RFP under the control of the GPR109A promotor was used (103). Samples of liver and hypothalamic tissue of $RFP^{+/+}$ and $GPR109A^{-/-}$ (control) mice were stained with polyclonal RFP antibody.

Results showed a positive RFP staining in $RFP^{+/+}$ liver tissue compared to $GPR109A^{-/-}$ liver tissue. Due to characteristic morphology, GPR109A expression was detected in Kupffer cells by visual evaluation **(Fig. 38 A, B)**.

Hypothalamic tissue of $RFP^{+/+}$ mice showed GPR109A expression compared to $GPR109A^{-/-}$ control **(Fig. 38 C, D)**. To verify if these RFP positive cells were glia cells, the microglia cell specific marker Iba-1 was used. Results showed a positive staining of glia cells which were identical in morphology to cell types stained with RFP antibody **(Supplemental Fig. S1)**.

Taken together, these results show that GPR109A is expressed in Kupffer cells of liver tissues and in microglia of hypothalamus.

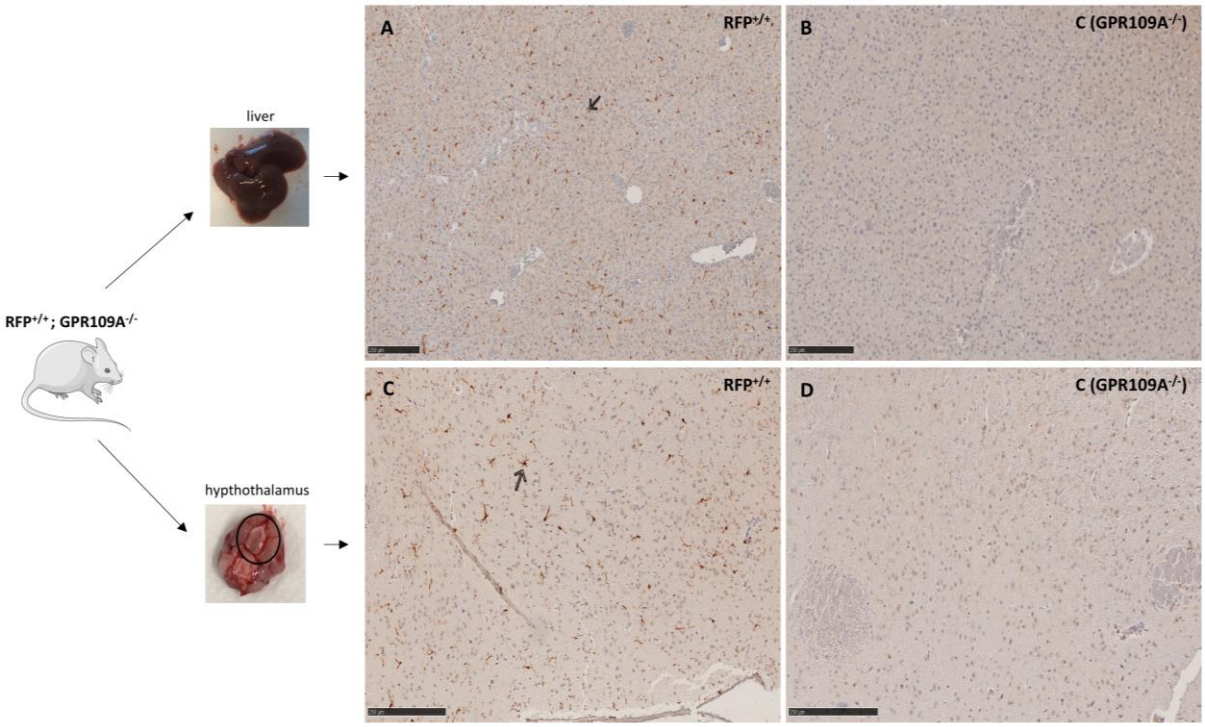

Figure 38:Immunohistochemical detection of GPR109A in liver and hypothalamic tissue of RFP$^{+/+}$ and GPR109A$^{-/-}$mice: 3.5µm liver tissue samples were stained with RFP monoclonal antibody; 5µm hypothalamic tissue samples were stained with RFP monoclonal antibody **(A)** GPR109A expression in liver tissue (Kupffer cells) of RFP$^{+/+}$ mice **(B)** GPR109A$^{-/-}$ as negative control **(C)** GPR109A expression in hypothalamic tissue (microglia) of RFP$^{+/+}$ mice **(D)** GPR109A$^{-/-}$ as negative control. Scale=250µm; This shows one representative example out of two experiments.

5.7 *In vivo* experiment - NUA was absorbed in the gastrointestinal tract

Results from metabolomics-based approach showed that NUA is linked to the metabolic diseases obesity and T2D and *in vitro* experiments demonstrated alterations in intracellular signalling of immune cells by NUA. With regard to this, it is also necessary to investigate the effects of NUA *in vivo*. Planned experiments will provide information on the effects of NUA in a diet-induced obesity model with GPR109A$^{+/+}$ and GPR109A$^{-/-}$ mice. For this study, it is of relevance to ensure that mice are able to intestinally absorb NUA and show detectable levels in the serum. Therefore, an experiment was performed to investigate the gastrointestinal absorption of NUA in GPR109A$^{+/+}$ and GPR109A$^{-/-}$ mice and the most appropriate application method.

Mice were fed with a TRP/NA free high fat diet to eliminate NUA metabolism from food. Mice received NUA as drinking water (300mM) for 24 h, 48 h, 72 h, 7 d or as one-time oral gavage (800mg NUA/kg BW). After indicated exposure times, blood was taken. The control groups were treated with water. Collected serum was measured by FT-ICR-MS to determine NUA intensities.

Serum analysis showed that NUA is detectable in the blood after oral application, while in control animals, no serum NUA levels were detected. Mice which had been administered NUA by one-time oral gavage already revealed elevated levels after 30 min. After 2 h, NUA levels were reduced. Application by drinking water showed higher NUA intensities compared to groups with oral gavage. Mice revealed high levels after 24-72 h while after 7 d, NUA levels dropped. Furthermore, it was observed that both GPR109A$^{+/+}$ and GPR109A$^{-/-}$ mice showed similar serum NUA levels **(Fig. 39)**.

In conclusion, oral application led to a GPR109A independent absorption of NUA. Administration by drinking water revealed higher serum NUA levels with maximum levels after 24 h, 48 h and 72 h.

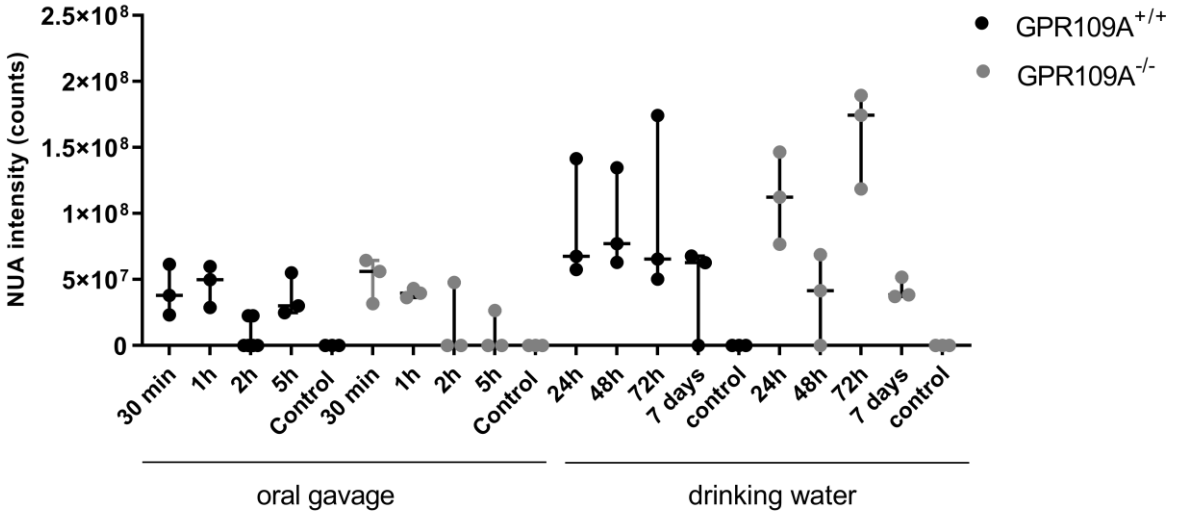

Figure 39: Detection of serum NUA intensities (counts) in GPR109A$^{+/+}$ and GPR109A$^{-/-}$ mice by FT-ICR-MS after oral application: NUA was detectable after one-time oral gavage and after drinking water administration. GPR109A$^{+/+}$ and GPR109A$^{-/-}$ mice showed NUA levels in serum. After 30min and 1h, oral gavage showed highest levels in both genotypes. 72h application by drinking water revealed the highest NUA intensities in both genotypes. In control groups no NUA levels were detected. Values are shown as median with 95% CI. Each group contained three replicates.

6 Discussion

6.1 Association between serum NUA levels and markers of metabolic inflammation

In the last decades, several studies reported an association between TRP/NA metabolism and the development of T2D. However, the exact mechanisms are still largely unknown (109). Therefore, TRP and NA metabolites in the serum of subjects from the FoCus sub-cohort were analysed to further elucidate the association between these pathways and obesity as well as T2D.

Although several TRP metabolites were identified in serum, most of the data were not evaluable due to the extreme skewness of metabolite intensities, except for TRP itself. It was observed that FoCus subjects with normal weight and overweight had lower TRP intensities compared to groups of obesity grade I-III. These results agree with the findings of another working group. They additionally showed that TRP levels were increased in obese men with Chinese or with American background, but not in obese women from China or America. This indicates, that TRP metabolism is independent of ethnical background but dependent of gender (110). In contrast, other working groups observed a negative association between obesity and TRP levels (111–113). Although these results seem contradictory, they might show potential compensatory properties of TRP. The depletion of TRP in metabolic diseases can be explained by an increased conversion rate of TRP to kynurenine (114). IDO1, which catalyses this reaction, is activated by inflammatory stimuli in immune and non-immune cells which leads to decreased local and systemic TRP levels while kynurenine levels rise intra- and extracellularly. Simultaneously, the expression of the aryl hydrocarbon receptor (AhR) is also increased by inflammatory stimuli. Kynurenine activates AhR which in the following leads to secretion of anti-inflammatory cytokines such as interleukin-10. This mechanism even indicates that in obesity the TRP-kynurenine pathway might exhibit anti-inflammatory and immunosuppressive properties (115). However, the results of Xie et al. suggest that these mechanisms might be gender dependent. Therefore, it is recommended to perform future investigations in TRP metabolism in a gender specific manner. It is necessary to mention that in this metabolomics-based approach, the groups were not age matched due to the skewness of metabolite intensities. Another working group observed age-related differences in TRP levels. While obese adults exhibited an increased IDO1 activity with an elevated kynurenine/TRP ratio, obese juveniles showed a decreased kynurenine/TRP ratio which is driven by cytokines such as interleukin-4 (IL-4)

(116). These results indicate that age influences the extend of TRP conversion which in turn has an impact on the progression of metabolic inflammation.

Furthermore, group comparisons showed that healthy subjects had lower TRP levels compared to pre-diabetic and diabetic subjects. These results are in line with observations from other working groups (117, 118). Chen et al. assumed TRP to be a potential biomarker for patients at high risk for T2D. They showed in a 10-year longitudinal study that from 213 healthy subjects, 51 participants developed T2D and were positively associated with plasma TRP levels compared to healthy controls (119).

Moreover, the association between NA metabolism and metabolic inflammation was investigated. Due to the skewness of metabolite intensities, FoCus subjects also showed no evaluable intensities of NA or its metabolites except for NA`s major catabolic product NUA. FoCus subjects suffering from obesity grade I-III showed significant higher NUA levels compared to subjects with normal weight or overweight. Furthermore, group comparisons of subjects with NUA levels over LOD showed nominally higher NUA levels in subjects with obesity grade III compared to subjects with obesity grade. Huang et al. observed a positive correlation between urinary NUA levels and BMI (15).

Group comparisons of the total sub-cohort showed that healthy subjects revealed significant lower NUA levels compared to pre-diabetic and diabetic subjects. However, group comparisons of subjects with NUA levels over LOD did not show significant differences. This might be explained by the fact that most of the healthy subjects had NUA intensities below the LOD compared to the PreD and T2D group. Huang et al. detected in a metabolomics-based approach urinary NUA levels in subjects with metabolic syndrome. They observed that diabetic subjects showed higher NUA levels than non-diabetic subjects (15). In another current case-control study, serum NUA levels were investigated in subjects with diabetic retinopathy, a concomitant disease of T2D. It was observed that subjects with diabetic retinopathy revealed higher serum NUA levels compared to diabetic and healthy controls (120). Taken together, these results indicate that serum and urine NUA levels are positively associated with obesity and the development of T2D.

As already described, the TRP and NA metabolisms are closely linked to each other. Therefore, the association of serum TRP and serum NUA intensities in FoCus subjects was investigated. They revealed a significant positive correlation which gives first insights into the role of NUA

in TRP metabolism: NA levels are known to be lowered/deficient in metabolic inflammation. On the one hand, it is caused by a shift towards xanthurenic acid in the kynurenine pathway which is additionally reinforced by coexisting pyridoxine depletion (34). On the other hand, obese patients often show NA deficiency by increased activity of NA degrading enzymes followed by rising levels of NA metabolites (121). This might be an explanation for the very small amount of NA values in this study and furthermore a reason for the increased NUA intensities in obese and diabetic subjects.

Since NUA showed an association with obesity and T2D in subjects of the FoCus sub-cohort, serum NUA intensities of subjects from the total FoCus cohort in association with other clinical markers were examined. Subjects with NUA intensities over and below the LOD showed no significant differences in age and gender which might suggest that NUA intensities are gender and age independent. However further studies evaluating group comparisons of different ages are necessary. Subjects with NUA intensities over LOD showed increased levels of glucose parameters (glucose, insulin, HOMA-indices) and anthropometric markers (BMI, weight, waist circumference) compared to subjects with NUA intensities below LOD. Furthermore, subjects with NUA intensities over LOD had increased levels of inflammatory markers (CRP, IL-6) and lipid markers (TG, Lp(a)). All these parameters showed a positive correlation with NUA intensity, however with low effect size. Moreover, subjects with hypertension showed significant higher NUA levels compared to subjects without hypertension. These results are in line with the observations from Huang et al. who investigated the association of NUA intensities in human urine with parameters of metabolic syndrome. They further reported a positive association between urinary NUA levels and the lipid markers LDL-C and total cholesterol. HDL-C levels were negatively associated with urinary NUA levels (15). Furthermore, one of the first clinical studies, investigating the functionality of NUA, was performed in 1960. Miller and colleagues investigated the effects on serum cholesterol levels by administration of different NUA doses (1,5-9g/d). It was observed that application of 9g/d remarkably reduced serum cholesterol levels. These levels were similar to levels evoked by NA (19). This might suggest that in obesity, NUA intensities are elevated in a compensatory manner to ameliorate serum lipid levels. However, this assumption requires further investigations.

This thesis is one of the first reports which showed the association between serum NUA levels and metabolic diseases. In the FoCus cohort, no association of NUA with other diseases such

as inflammatory bowel disease, rheumatoid arthritis or cardio vascular diseases was observed, which suggest that NUA might rather play a role in metabolic diseases such as obesity and T2D.

6.2 Association of serum NUA levels with nutrition and the gut microbiome

As serum NA levels are dependent on dietary intake (10), the association between serum NUA intensities and nutritional intake was investigated. Subtypes of carbohydrates, amino acids, vitamins and alcohol intake only showed nominal differences between subjects with high and low NUA intensities and very low correlation coefficients which suggests the independence of NUA levels from nutritional intake. Since this is the first study of the association between NUA and nutrition, further studies are required to validate these results. Furthermore, it needs to be considered that collected data from FFQ were biased since subjects tend to report their dietary behaviour based on expected norms which can influence results.

NA intake is positively associated with α-diversity and *Bacteriodetes* abundance in obese subjects. Administration of delayed-release NA microcapsules entered ileocolonic region to interact with microbiome resulting in ameliorated *Bacteriodetes* abundance and improved systemic insulin sensitivity (7). With regard to this, it was investigated if NUA is also associated with the gut microbiome of FoCus subjects. Results showed that subjects with high and low NUA levels did not show significant differences in α-diversity and β-diversity. Only adjustment for BMI revealed significant differences between groups which confirms previous studies that obesity impacts microbiome diversity (7). Furthermore, no differences in relative phyla abundance between subjects with high and low NUA intensities were observed. An explanation for these results might be that dietary NA is absorbed in the small intestine and subsequently converted into NAM/NAD. This reduces the possibility of NA`s conversion into NUA by the gut microbiome in the lower intestine (7, 16). To my knowledge, this is the first analysis of an association between NUA and the human gut microbiome. Further investigations should consider the administration of delayed-release NUA microcapsules in a murine model to examine if NUA might directly interact with the gut microbiome.

6.3 NUA`s effects on NF-κB signalling in THP-1 cells and human primary monocytes

Since results from metabolomics-based approach showed a positive association between NUA and markers of metabolic inflammation, *in vitro* experiments were performed to extend the knowledge of NUA`s functionality in immune cell metabolism.

First of all, effects of NUA on intracellular NF-κB signalling were investigated. THP-1 cells showed no differences in NF-κB p50 levels after stimulation with 100µM-10mM NUA. However, doses of 100µM up to 5mM NUA showed a slight increase in NF-κB p50 levels compared to control. NF-κB remains inactivated in non-stimulated cells by complex formation of IκB with the NF-κB dimers (p50/p65). External stimuli, like PMA, induce phosphorylation of IκB which leads to a release of the dimers which migrate to the nucleus and initiate target gene transcription (57, 122). With regard to these mechanisms, it might be assumed that NUA induces a short-time increase of NF-κB p50 dimers resulting in augmented NF-κB phosphorylation. Results of the neutral red uptake assay showed no detrimental effects by 100µM-5mM NUA. Only 10mM NUA showed increased apoptotic effects which might be an explanation why cells treated with 10mM NUA had a slightly decreased NF-κB p50 expression compared to the 1mM and 5mM dose groups.

Since NUA showed no effects on NF-κB expression in THP-1 cells, it was further investigated if NUA treatment leads to an altered NF-κB signalling in human primary monocytes which are closer to *in vivo* conditions (107). The effects of NUA on β-Arrestin1 phosphorylation, NF-κB p65 protein expression and NF-κB p65 phosphorylation were examined. Shorter expositions times (5 min, 15 min), compared to cell culture experiments, were selected. It was reported that primary cells reveal significant faster nuclear translocations of NF-κB with highest peaks after 5 min followed by functional degradation. A slower signalling in cell lines such as THP-1 cells might be due to the fact that they are genetically modified (123).

Monocytes treated with NUA and NA for 5 min and 15 min showed no differences in p-β-Arrestin1 levels. However, it was observed that 5 min stimulation slightly increased p-β-Arrestin1 levels by NUA and NA. After 15 min, only 100µM,500µM NUA showed mildly reduced levels of p-β-Arrestin1. It could suggest that both metabolites might be able to induce β-Arrestin1 phosphorylation within 5 min followed by functional degradation after 15 min. Since primary cells might show signalling peaks after 5 min (123) and β-Arrestins belong to

the first constituents in NF-κB signalling (108), experiments with incubation times less than 5 min should be considered.

Treatment for 5 min showed no differences in NF-κB p65 protein expression between groups, however it was observed that NUA slightly increased NF-κB p65 levels compared to control. Furthermore, NF-κB p65 phosphorylation showed a significant increase in cells treated with 100µM,500µM NUA after 5 min. As mentioned above, NUA might be able to induce a short-time intracellular release of NF-κB p65 dimers with following phosphorylation which could explain elevated p-NF-κB p65 levels. Monocytes, stimulated with NUA for 15 min showed a significant reduction in NF-κB p65 protein expression, however no group differences in phosphorylation of NF-κB p65 were observed. These results show, that NUA induces changes in NF-κB signalling in human primary monocytes within 5 min and after 15 min signalling events are down-regulated again.

Of interest, NA did not induce changes in NF-κB p65 expression and phosphorylation after 5 min and 15 min. An explanation could be that monocytes were activated by adherence on plastic 6-well plates instead of pre-treatment with lipopolysaccharide (LPS). In another study, the use of LPS led to significantly reduced NF-κB levels after NA stimulation (14). Therefore, it is recommended to repeat experiments by using LPS to examine the effects of NUA on NF-κB signalling. Moreover, it would be of interest to investigate the downstream inflammatory pathways of NF-κB such as IL-6 and TNF-α synthesis after NUA treatment to better classify NUA in its functional characteristics.

6.4 The effects of NUA on phosphorylation of the MAPKs, Akt and AMPKα

The MAPKs, Akt and AMPKα also play a major role in inflammatory diseases since they are activated by stress and inflammatory stimuli (68, 87, 91). To further examine the functional characteristics of NUA, its role in the phosphorylation of ERK1/2, p38, JNK, Akt and AMPKα in human primary monocytes was investigated.

Although 5 min treatment with NUA showed no significant changes in p38, ERK1/2 and JNK phosphorylation, a slight increase in phosphorylation levels of the MAPK were observed. These results indicate that NUA might induce MAPK phosphorylation. After 15 min, phosphorylation of p38, ERK1/2 and JNK was significantly reduced by 100µM NUA compared to control. It might suggest that NUA actively down-regulates MAPK phosphorylation levels which could

be interpreted as an anti-inflammatory effect by NUA. However, another explanation has to be considered that reduced phosphorylation of the MAPKs was initiated NUA-independently.

NA did not affect MAPK phosphorylation after 5 min and 15 min. Another *in vitro* study showed that NA was able to decrease levels of pro-inflammatory myeloperoxidase in HL-60 cells via the inhibition of the p38 signalling pathway. However, cells were incubated for 24 h (75). An *in vivo* study demonstrated that rats with cardiac arrest had decreased p-p38 and p-JNK levels after NA treatment which reduced brain injury and ameliorated neurological outcome (69). These results suggest that NA affects MAPK signalling in an anti-inflammatory manner. In contrast, Shi et al. observed that NA increased phosphorylation of p38, ERK1/2 and JNK in RAW264.7 macrophages when co-incubated with the chemoattractant peptide N-formyl-methionyl-leucyl-phenylalanine (fMLF). Increased phosphorylation of the MAPK resulted in the inhibition of inflammatory cell migration (80), which proves that an upregulation of MAPK phosphorylation can also elicit anti-inflammatory effects, however in dependence of the cell type. This underlines the complexity of the MAPK signalling pathways and suggests to continue studies investigating the role of NA and NUA in MAPK signalling.

Furthermore, it was examined if NUA can affect the Akt signalling pathway in human primary monocytes. Results showed no significant differences in p-Akt levels after 5 min treatment with NUA and NA, however 100µM,500µM NUA slightly increased p-Akt levels compared to control. After 15 min stimulation, 100µM NUA revealed significantly decreased p-Akt levels compared to controls which might suggest that NUA affects the Akt signalling pathway in a pro-inflammatory manner. However, an NUA independent downregulation of Akt phosphorylation should be contemplated.

NA also showed a mild reduction in p-Akt levels after 15 min, however without significance. In another working group, it was shown that NA induced Akt signal transduction in murine primary macrophages with a peak at 5 min followed by a reduction to baseline levels after 30 min (54). These time dependent results support the observations of this thesis and indicate that NA and NUA are able to induce p-Akt phosphorylation within 5 min while a longer treatment leads to reduced phosphorylation levels in a compensatory manner. Shi and colleagues reported that co-treatment with NA and fMLF in RAW264.7 macrophages induced significantly increased p-Akt levels after 5 min. After 30 min, even higher p-Akt levels were observed (80). However, this effect could be explained by a slower cell signal transduction in cell-lines compares to primary cells.

Moreover, the effects of NUA on AMPKα phosphorylation in human monocytes were examined. Cell treatment with NUA for 5 min did not show significant differences in p-AMPKα levels, although 100µM NUA slightly increased phosphorylation which might be seen as an anti-inflammatory effect by NUA. However, as for the other kinases, no definitive conclusions can be drawn due to lack of significance. 15 min stimulation revealed a significantly reduced phosphorylation of AMPKα by 100µM NUA which in turn could imply a pro-inflammatory effect in monocytes. These results again assume that NUA elicits signalling peaks in a time dependent manner.

NA showed no differences in AMPKα phosphorylation compared to control groups in both stimulation times. In another study, it was observed that hepatocytes, treated with NA, showed an increased phosphorylation of AMPK followed by reduced lipogenesis (92) which underlines the lipid-modifying characteristics of NA. To my knowledge, this experiment is the first report of NA`s and NUA`s role in AMPKα signalling in human primary monocytes. Therefore, additional investigations are required to determine the effects of NA and NUA on the AMPKα signalling pathway.

Taken together, results showed that NUA reduced phosphorylation of MAPKs, Akt and AMPKα in immune cells in a time and dose dependent manner. However, these results are not sufficient to attribute pro-inflammatory or anti-inflammatory effects to NUA yet. Furthermore, "stimulation-induced waveforms that mask underlying signals of interest", so called artifacts (124), have to be considered into evaluation. Since investigations were performed with immune cells of healthy donors, it is of importance to repeat experiments with immune cells of subjects suffering from obesity or T2D to analyse the effects of NUA on intracellular kinases in present metabolic inflammation.

6.5 Regulation of intracellular Ca^{2+} and cAMP levels by NUA

cAMP and Ca^{2+} are the main second messengers and are present in every cell type (125). In immune cells, several GPR109A agonists, such as NA, are able to regulate cAMP levels as well as intracellular Ca^{2+} mobilization (126, 127). For this reason, it was investigated if NUA also shows effects on intracellular Ca^{2+} and cAMP levels in human neutrophils and monocytes.

It was observed that 100µM,500µM NUA induced intracellular Ca^{2+} signalling in neutrophils which was comparable to the effects of NA with the same dose. These results show for the first time that NUA is able to induce intracellular Ca^{2+} mobilization and confirm results of another

working group who demonstrated that NA increased intracellular Ca^{2+} flux in mature neutrophils (56). Furthermore, 100µM,500µM NUA led to a significant reduction of cAMP levels in human neutrophils compared to controls. However, cAMP levels were not altered after NA treatment which contradicts the findings of Kostylina et al., who showed significantly reduced cAMP levels by NA in neutrophils (56). Although, this is the first report of NUA downregulating cAMP levels, a limitation has to be mentioned that no cytotoxicity assay with human neutrophils has been performed to examine viability of the cells after NUA treatment. Since cAMP levels were significantly decreased by NUA, it would be assumed that this might lead to a reduced cell viability. Therefore, further studies are required to investigate if NUA is also able to induce apoptosis in human neutrophils as NA.

It is to be mentioned that NUA`s effects on Ca^{2+} signalling in human monocytes could not be examined as the high adherence of these cell types on well plates do not allow investigation by flow cytometry. However, it was observed that NUA revealed decreased cAMP levels in human monocytes which suggests that NUA might also be able to act in an anti-inflammatory manner as NA. In contrast, no significant alterations in cAMP levels after NA treatment were observed. These results contradict the findings of another group which showed that NA significantly reduced cAMP levels in macrophages (63). Additionally, these results are of high interest since the reduction of cAMP levels and a temporary Ca^{2+} mobilization belong to the well-known effects of NA`s lipid-modifying characteristics in adipocytes (49, 54). Since results from metabolomics assessment in the FoCus cohort showed a positive association between serum NUA intensities and markers of metabolic inflammation such as BMI, weight and weight circumference, it is of importance to investigate if NUA also exhibits anti-lipolytic properties in adipocytes. A suggestion would be to stimulate adipocytes from obese and lean controls with NUA, followed by the determination of cAMP and Ca^{2+} levels.

6.6 NUA and the GPR109A receptor

Since it is known that NA mediates its lipid-modifying and anti-inflammatory effects via GPR109A (53, 14), it was investigated if NUA also displays an agonist for this receptor. Therefore, NUA`s effects on Ca^{2+} mobilization and cAMP levels in BMD neutrophils of $GPR109A^{+/+}$ and $GPR109A^{-/-}$ mice were examined. Results showed that $GPR109A^{+/+}$ neutrophils stimulated with NUA showed increased intracellular Ca^{2+} mobilization with marginally lower peaks compared to NA, while in $GPR109A^{-/-}$ neutrophils, this effect was abolished. These results additionally show that NUA is able to induce intracellular Ca^{2+} flux in

neutrophils and that NUA mediates this effect via GPR109A. Since NA also induced a Ca^{2+} flux in GPR109A$^{+/+}$ neutrophils, it contradicts the findings of Kostylina et al. who observed no Ca^{2+} flux by NA in BMD neutrophils. They explained by their observations that BMD neutrophils do not express GPR109A due to their immaturity compared to mature blood derived neutrophils (56). However, results from this thesis might suggest that BMD neutrophils express GPR109A however in smaller concentrations as Ca^{2+} levels were lower than in human blood derived neutrophils.

NUA reduced cAMP levels in GPR109A$^{+/+}$ and GPR109A$^{-/-}$ BMD neutrophils which indicates that NUA regulates adenylyl cyclase activation GPR109A-independently. NA showed no effects on cAMP levels which confirms the results of Kostylina et al. Of interest, NUA had no effects on viability of GPR109A$^{+/+}$ BMD neutrophils. An explanation might be that due to a lower GPR109A expression, apoptotic effects could not be induced by NUA. Kostylina and colleagues observed that NA had no apoptotic effects on BMD neutrophils. Therefore, it would be of interest if NUA is able to induce apoptosis in blood derived neutrophils.

Furthermore, it might be assumed that even if NUA is able to induce Ca^{2+} flux und decrease cAMP levels, further downstream signalling, such as BAD, which initiates apoptosis, are not activated. It is therefore recommended to further examine the dephosphorylation of BAD after NUA treatment in mature neutrophils to determine NUA`s potential apoptotic effects.

Moreover, it was investigated if NUA mediates cAMP downregulation in PEMs GPR109A-dependently. GPR109A$^{+/+}$ macrophages stimulated with NUA showed a significant reduction of adenylyl cyclase activation. These results confirm observations from experiments with human monocytes. However, macrophages of GPR109A$^{-/-}$ also revealed reduced cAMP levels as observed in neutrophils. These results further imply that NUA regulates adenylyl cyclase activity via another receptor. Since cAMP synthesis by adenylyl cyclase can be initiated by different GPCRs (128), additional investigations are necessary to identify potential receptors of NUA. GPCRs are the only known receptors for NA with GPR109A as high affinity receptor while GPR109B only reveals low affinity (129). A GPR109B mediated downregulation of cAMP levels by NUA is excluded since GPR109B is not expressed on rodent cell membranes (130). In 2005, it was reported by performing site-directed mutagenesis that NA requires special amino acid residues like Arg111 (TMH3), Ser178 (ECL2), Phe276 (TMH7) to induce internalization of GPR109A (130). This method would also be a possibility to detect critical binding sites of NUA to initiate intracellular signalling pathways via GPR109A and other receptors.

Another working group investigated if NUA evokes flush specific PGD_2 secretion via GPR109A in THP-cells. Since NA mediates Cox-1 activation, which catalyses the conversion of AA to PGD_2, via GPR109 (18), cells were pre-incubated with acetylsalicylate which inhibits COX-1. Results showed that, despite NA/NUA treatment, the PGD_2 secretion in macrophages was abolished compared to controls (131). These results not only suggest that NUA is involved in flushing response but also agree with the results of this thesis that NUA mediates its effects via GPR109A.

In summary, NUA induced Ca^{2+} mobilisation in human neutrophils which was shown to be GPR109A-dependently. cAMP levels were reduced by NUA in neutrophils and macrophages, however this effect was GPR109A-independent. It again raises the question if NUA represents more than a catabolic product and might elicit anti-inflammatory effects. In 1960, this hypothesis has already been set up when they described serum cholesterol lowering effects by NUA in *in vivo* experiments (19). However, data availability is still insufficient. Moreover, future studies of NUA`s role in inflammatory response should also consider NUA`s involvement in flushing response elicited by keratinocytes since this side effect displays a limiting factor in the pharmaceutical application of NA.

6.7 GPR109A expression in hepatic and hypothalamic tissues

GPR109A acts as metabolic sensor for changes in cell signalling involved in energy/lipid metabolism and immunological activity. Adipocytes reveal high amounts of GPR109A and its activation by NA leads to an improvement of lipid profile (52, 49, 48). Recently, differences in expression levels between adipocytes of visceral and subcutaneous fatty tissue in obese subjects were investigated. It was observed that subcutaneous adipocytes had significant higher GPR109A expression levels compared to visceral adipocytes. Furthermore, visceral adipocytes of obese subjects revealed a remarkably higher GPR109A expression than visceral adipocytes of lean controls (unpublished data). These results indicate that GPR109A is involved in anti-inflammatory effects of subcutaneous tissue (132) and GPR109A expression in visceral adipocytes is compensatory upregulated to limit low-grade inflammation.

Primary reports assumed that expression of GPR109A is limited to adipocytes, however further studies confirmed GPR109A expression in other cell types such as monocytes, neutrophils and keratinocytes (133, 50). It is known that the liver plays a major role in metabolic homeostasis which is also related to general GPR109A signalling. However, the expression of this receptor

in the liver is still controversial (134). Results of immunohistochemical analysis showed GPR109A expression in liver cells of $RFP^{+/+}$ mice but not in $GPR109A^{-/-}$ mice which confirms the expression of GPR109A in the liver. Furthermore, GPR109A expression was detected in macrophages of the liver, so called Kupffer cells. However, a limitation of this study is worth noting that the expression of GPR109A in Kupffer cells was determined due to characteristic morphology and therefore only performed by visual evaluation. Another working group investigated GPR109A mRNA expression in specific liver cell types of mice and showed high amounts of GPR109A in Kupffer cells. Other cell types, like hepatocytes and endothelial cells showed lower expression levels (52). These results are in line with observations of this thesis since immunoreactivity for GPR109A in hepatocytes and endothelial cells was either too small for detection or not existent.

Kupffer cells are of high importance in mononuclear phagocytic system since they play a key role in hepatic and systemic response to pathogens (135). Furthermore, Kupffer cells are negatively associated with metabolic diseases such as obesity since a loss in Kupffer cell amounts leads to increased hepatic steatosis and IR (136). With regard to this, it might be assumed that a decline in Kupffer cells is linked to a decreased GPR109A activity in the liver reinforcing metabolic inflammation. However, the specific role of GPR109A in this cell type is still elusive. Therefore, further investigations of the association between GPR109A expression in Kupffer cells and metabolic inflammation are required. Furthermore it is suggested that the effects of NA and NUA on intracellular signalling in Kupffer cells should be included into evaluation, since NA mediates anti-inflammatory effects in blood derived macrophages via GPR109A (14) and NUA also induced alterations in monocytes such as cAMP downregulation. This would be another approach to further classify the role of the two metabolites in the pathophysiology of metabolic inflammation.

Initially, chronic low-grade inflammation was linked to adipose tissue. However, studies confirmed that low-grade inflammation is also present in the hypothalamus leading to leptin resistance and reinforcement of obesity (4). In this thesis, it was examined if GPR109A is expressed in cells of hypothalamic tissue. Results of immunohistochemistry showed remarkable immunoreactivity for GPR109A in $RFP^{+/+}$ mice but not in $GPR109A^{-/-}$ mice which shows that GPR109A is expressed in cells of hypothalamic tissue. These results are in line with the findings of another working group who reported GPR109A expression in primary hypothalamic cells of rats and in the GT1-7 cell line (137). In 2014, it was reported that microglia of murine brain tissues expressed GPR109A but not astrocytes or neurons (138). Therefore, it was investigated

which cell type in hypothalamus expresses GPR109A. Hypothalamic tissues were treated with the microglia cell specific marker Iba-1 and showed a staining of microglia which were identical in morphology to cell types stained with RFP antibody. These results show that GPR109A is not even present in the hypothalamus but also expressed by microglia in the hypothalamus. However, it is to be mentioned that the detection of GPR109A in microglia by visual evaluation displays a limitation of this study.

Taken together, these results show for the first time GPR109A expression in microglia of the hypothalamus. Although further studies are required to validate these results, the presence of the GPR109A in the hypothalamus might be of interest in connection with hypothalamic inflammation. Rahmann et al. showed in a stroke model that GPR109A expression in brain tissues exhibits neuroprotective effects. Furthermore, it was observed that NA reduced the infarct size in ischemic brain via GPR109A (138). Thus, it might be speculated that the anti-inflammatory effects of GPR109A ameliorate hypothalamic inflammation and leptin resistance which would positively affect the pathophysiology of obesity.

6.8 Pharmacokinetics of NUA

In this thesis, it was demonstrated that serum NUA intensities are positively associated with markers of metabolic inflammation. From results of *in vitro* experiments, it can be assumed that NUA affects immune cell signalling GPR109A-dependently. Whether these effects influence the pathophysiology of metabolic inflammation in a beneficial or detrimental manner is still elusive. Planned *in vivo* experiments, using a mouse model of diet-induced obesity and IR, will help to further investigate pro-inflammatory or anti-inflammatory properties of NUA. To facilitate these studies, it is of relevance to ensure that mice intestinally absorb NUA and show detectable NUA levels in the serum. The intestinal absorption of NUA is still elusive. There is one report from 1960, which showed that NUA is gradually excreted via the urine in dependence of oral application dose (19). Therefore, a preliminary *in vivo* experiment was performed to investigate the intestinal absorption of NUA.

A time-dependent experiment with GPR109A$^{+/+}$ and GPR109$^{-/-}$ mice on a TRP/NA free high fat diet was performed. On the one hand, it was examined if NUA is gastrointestinally absorbed and on the other hand, serum NUA levels after application by oral gavage and drinking water were compared to determine the most appropriate application method. Results showed that all groups, except for controls which had received water, revealed serum NUA levels. It confirms

the findings of Miller et al. that NUA is gastrointestinally absorbed after oral application (19). Moreover, it indicates that dietary TRP/NA is the main source for systemic NA metabolism compared to endogenous synthesis (37). Administration of NUA by drinking water showed higher serum NUA levels compared to application by oral gavage. Mice which were treated with drinking water for 72 h showed the highest serum levels. It was reported that NA from immediate formulations are absorbed in a few hours. Therefore, the NAM pathway is saturated very fast and NA is systemically converted into NUA for renal excretion (139, 96). In contrast, administration of sustained NA formulations requires more than 12 h for absorption and shows better utilization via the NAD pathway (139, 140). With this in mind, it might explain why administration by one-time oral gavage, reflecting an immediate NUA formulation, also showed lower NUA serum levels due to faster renal excretion compared to mice which continuously received NUA by drinking water. Groups with drinking water showed remarkably reduced NUA levels after 7 d. Therefore, further studies with NUA administration for more than 7 days are necessary to investigate medium-term absorption of NUA.

Moreover, it was investigated if GPR109A$^{+/+}$ and GPR109$^{-/-}$ mice show differences in the absorption of NUA. Results showed that serum NUA levels of GPR109A$^{+/+}$ and GPR109$^{-/-}$ mice were similar, which indicates that the gastrointestinal absorption of NUA takes place GPR109A-independently.

It was reported that NA is absorbed sodium dependently or via passive diffusion, however specific mechanisms of intestinal absorption and its regulation are widely unknown (37, 141). Nabokina et al. performed several experiments with human-derived Caco-cells to investigate cellular mechanisms of NA uptake in the intestine. They stated that NA uptake requires carrier-mediated systems which are dependent of extracellular acidic pH, temperature and energy state. Interestingly, they observed a sodium independent uptake of NA. Since NA is a monocarboxylic acid and NUA displays a structural analogue of NA, it is assumed that NUA might be absorbed in similar conditions (141).

Taken together, these results show that NUA is gastrointestinally absorbed after oral application and occurs GPR109A-independently.

7 Conclusion/ Outlook

Results of this thesis showed that NUA is linked to metabolic inflammation. In FoCus subjects, serum NUA levels were positively associated with obesity and T2D as well as inflammatory markers while it showed no correlation with other diseases. Furthermore, NUA intensities were evaluated to be independent of nutritional intake and diversity of the gut microbiome.

Results from *in vitro* studies showed that in monocytes, NUA reduced phosphorylation of NF-κB, MAPKs, Akt and AMPKα in a time and a dose dependent manner. Moreover, it was demonstrated that NUA induced intracellular Ca^{2+} flux via GPR109A and decreased cAMP levels in neutrophils and monocytes. Further investigations are necessary to identify other receptors of NUA since cAMP downregulation was mediated GPR109A-independently.

With regard to these results, it can be assumed that NUA is involved in metabolic diseases such as obesity and T2D. Whether elevated serum NUA levels negatively affect these phenotypes or exhibit beneficial effects, representing a reactive compensation mechanism, is still elusive. In a planned *in vivo* study, a diet-induced obesity model with $GPR109A^{+/+}$ and $GPR109A^{-/-}$ mice will give more insights into the pro-inflammatory or anti-inflammatory characteristics of NUA. A preliminary experiment proved that NUA is gastrointestinally absorbed after oral application. In the following study, oral treatment with NUA will show if obese mice exhibit alterations in markers of metabolic inflammation such as glucose levels and inflammatory parameters. The measurement of the adipose tissue specific hormone leptin might provide more information of changes in hypothalamic inflammation by NUA.

In conclusion, data suggest that NUA represents an active metabolite rather than just a degradation product of NA. As NA metabolism is altered in obesity and T2D, it is of importance to get more insights into the inflammatory characteristics of NUA and its role in metabolic inflammation.

8 Literature Cited

1. Xanthakos SA. Nutritional Deficiencies in Obesity and After Bariatric Surgery. Pediatric Clinics of North America 2009; 56(5):1105–21.

2. Khan MAB, Hashim MJ, King JK, Govender RD, Mustafa H, Al Kaabi J. Epidemiology of Type 2 Diabetes – Global Burden of Disease and Forecasted Trends. JEGH 2020; 10(1):107.

3. Dali-Youcef N, Mecili M, Ricci R, Andrès E. Metabolic inflammation: connecting obesity and insulin resistance. Ann Med 2013; 45(3):242–53.

4. Kreutzer C, Peters S, Schulte DM, Fangmann D, Türk K, Wolff S et al. Hypothalamic Inflammation in Human Obesity Is Mediated by Environmental and Genetic Factors. Diabetes 2017; 66(9):2407–15.

5. Çatak J. Determination of niacin profiles in some animal and plant based foods by high performance liquid chromatography: association with healthy nutrition. J Anim Sci Technol 2019; 61(3):138–46.

6. Kirkland JB, Meyer-Ficca ML. Niacin. In: New Research and Developments of Water-Soluble Vitamins. Elsevier; 2018. p. 83–149 (Advances in Food and Nutrition Research).

7. Fangmann D, Theismann E-M, Türk K, Schulte DM, Relling I, Hartmann K et al. Targeted Microbiome Intervention by Microencapsulated Delayed-Release Niacin Beneficially Affects Insulin Sensitivity in Humans. Diabetes Care 2018; 41(3):398–405.

8. Palego L, Betti L, Rossi A, Giannaccini G. Tryptophan Biochemistry: Structural, Nutritional, Metabolic, and Medical Aspects in Humans. J Amino Acids 2016; 2016.

9. Badawy AA-B. Kynurenine Pathway of Tryptophan Metabolism: Regulatory and Functional Aspects. Int J Tryptophan Res 2017; 10:1178646917691938.

10. DGE - Deutsche Gesellschaft für Ernährung e.V. Niacin; 2020 [cited 2020 Apr 16]. Available from: URL: https://www.dge.de/wissenschaft/referenzwerte/niacin/.

11. Christensen MHE, Fadnes DJ, Røst TH, Pedersen ER, Andersen JR, Våge V et al. Inflammatory markers, the tryptophan-kynurenine pathway, and vitamin B status after bariatric surgery. PLoS ONE 2018; 13(2):e0192169.

12. Favennec M, Hennart B, Caiazzo R, Leloire A, Yengo L, Verbanck M et al. The kynurenine pathway is activated in human obesity and shifted toward kynurenine monooxygenase activation. Obesity (Silver Spring) 2015; 23(10):2066–74.

13. Julius U, Fischer S. Nicotinic acid as a lipid-modifying drug – A review. Atherosclerosis Supplements 2013; 14(1):7–13.

14. Digby JE, Martinez F, Jefferson A, Ruparelia N, Chai J, Wamil M et al. Anti-inflammatory effects of nicotinic acid in human monocytes are mediated by GPR109A dependent mechanisms. Arterioscler Thromb Vasc Biol 2012; 32(3):669–76.

15. Huang C-F, Cheng M-L, Fan C-M, Hong C-Y, Shiao M-S. Nicotinuric acid: a potential marker of metabolic syndrome through a metabolomics-based approach. Diabetes Care 2013; 36(6):1729–31.

16. Couturier A, Ringseis R, Most E, Eder K. Pharmacological doses of niacin stimulate the expression of genes involved in carnitine uptake and biosynthesis and improve the carnitine status of obese Zucker rats. BMC Pharmacol Toxicol 2014; 15:37.

17. Piepho RW. The pharmacokinetics and pharmacodynamics of agents proven to raise high-density lipoprotein cholesterol. Am J Cardiol 2000; 86(12A):35L-40L.

18. Bodor ET, Offermanns S. Nicotinic acid: an old drug with a promising future. Br J Pharmacol 2008; 153(S1):S68-S75.

19. Miller ON, Hamilton JG, Goldsmith GA. Investigation of the mechanism of action of nicotinic acid on serum lipid levels in man. Am J Clin Nutr 1960; 8:480–90.

20. La Montserrat-de Paz S, Naranjo MC, Lopez S, Abia R, Muriana FJG, Bermudez B. Niacin and its metabolites as master regulators of macrophage activation. The Journal of Nutritional Biochemistry 2017; 39:40–7.

21. Kil DY, Swanson KS. Endocrinology of obesity. The Veterinary clinics of North America. Small animal practice 2010; 40(2). Available from: URL: https://pubmed.ncbi.nlm.nih.gov/20219484/.

22. Chooi YC, Ding C, Magkos F. The epidemiology of obesity. Metab Clin Exp 2019; 92:6–10.

23. Leitner DR, Frühbeck G, Yumuk V, Schindler K, Micic D, Woodward E et al. Obesity and Type 2 Diabetes: Two Diseases with a Need for Combined Treatment Strategies - EASO Can Lead the Way. Obes Facts 2017; 10(5):483–92.

24. Khaodhiar L, Cummings S, Apovian CM. Treating diabetes and prediabetes by focusing on obesity management. Curr Diab Rep 2009; 9(5):348–54.

25. Laudes M. Role of WNT signalling in the determination of human mesenchymal stem cells into preadipocytes. J Mol Endocrinol 2011; 46(2):R65-72.

26. Khan S, Wang CH. ER stress in adipocytes and insulin resistance: mechanisms and significance (Review). Mol Med Rep 2014; 10(5):2234–40.

27. Ziemke F, Mantzoros CS. Adiponectin in insulin resistance: lessons from translational research1234. Am J Clin Nutr 2009; 91(1):258S-61S.

28. Goodrich JK, Di Rienzi SC, Poole AC, Koren O, Walters WA, Caporaso JG et al. Conducting a Microbiome Study. Cell 2014; 158(2):250–62.

29. Clarke SF, Murphy EF, Nilaweera K, Ross PR, Shanahan F, O'Toole PW et al. The gut microbiota and its relationship to diet and obesity. Gut Microbes 2012; 3(3):186–202.

30. Jenkins TA, Nguyen JCD, Polglaze KE, Bertrand PP. Influence of Tryptophan and Serotonin on Mood and Cognition with a Possible Role of the Gut-Brain Axis. Nutrients 2016; 8(1).

31. Savitz J. The Kynurenine Pathway: A Finger in Every Pie. Mol Psychiatry 2019; 25(1):131–47.

32. Goh J, Goh KP, Abbasi A. Exercise and Adipose Tissue Macrophages: New Frontiers in Obesity Research? Front Endocrinol (Lausanne) 2016; 7:65.

33. Dadvar S, Ferreira DMS, Cervenka I, Ruas JL. The weight of nutrients: kynurenine metabolites in obesity and exercise. J Intern Med 2018; 284(5):519–33.

34. Oxenkrug G. Insulin resistance and dysregulation of tryptophan-kynurenine and kynurenine-nicotinamide adenine dinucleotide metabolic pathways. Mol Neurobiol 2013; 48(2):294–301.

35. Gasperi V, Sibilano M, Savini I, Catani MV. Niacin in the Central Nervous System: An Update of Biological Aspects and Clinical Applications. Int J Mol Sci 2019; 20(4).

36. Biesalski HK, editor. Vitamine und Minerale. Stuttgart: Georg Thieme Verlag; 2016.

37. Surjana D, Halliday GM, Damian DL. Role of nicotinamide in DNA damage, mutagenesis, and DNA repair. J Nucleic Acids 2010; 2010.

38. Mielgo-Ayuso J, Aparicio-Ugarriza R, Olza J, Aranceta-Bartrina J, Gil Á, Ortega RM et al. Dietary Intake and Food Sources of Niacin, Riboflavin, Thiamin and Vitamin B6 in a Representative Sample of the Spanish Population. The ANIBES Study †. Nutrients 2018; 10(7).

39. EFSA. Scientific Opinion on Dietary Reference Values for niacin. EFSA Journal 2014; 12(7):3759.

40. DGE - Deutsche Gesellschaft für Ernährung e.V. Niacin; 2020 [cited 2019 Jul 3]. Available from: URL: https://www.dge.de/wissenschaft/weitere-publikationen/faqs/niacin/#ad5.

41. Savvidou S. Pellagra: a non-eradicated old disease. Clin Pract 2014; 4(1):637.

42. Meyer-Ficca M, Kirkland JB. Niacin12. Adv Nutr 2016; 7(3):556–8.

43. Bechgaard H, Jespersen S. GI absorption of niacin in humans. J Pharm Sci 1977; 66(6):871–2.

44. Kumar JS, Subramanian VS, Kapadia R, Kashyap ML, Said HM. Mammalian colonocytes possess a carrier-mediated mechanism for uptake of vitamin B3 (niacin): studies utilizing human and mouse colonic preparations. Am J Physiol Gastrointest Liver Physiol 2013; 305(3):G207-13.

45. Yoshii K, Hosomi K, Sawane K, Kunisawa J. Metabolism of Dietary and Microbial Vitamin B Family in the Regulation of Host Immunity. Front Nutr 2019; 6:48.

46. Bodor ET, Offermanns S. Nicotinic acid: an old drug with a promising future. Br J Pharmacol 2007; 153(Suppl 1):S68-75.

47. Romani M, Hofer DC, Katsyuba E, Auwerx J. Niacin: an old lipid drug in a new NAD+ dress. J Lipid Res 2019; 60(4):741–6.

48. Martin PM, Ananth S, Cresci G, Roon P, Smith S, Ganapathy V. Expression and localization of GPR109A (PUMA-G/HM74A) mRNA and protein in mammalian retinal pigment epithelium. Mol Vis 2009; 15:362–72.

49. Lukasova M, Hanson J, Tunaru S, Offermanns S. Nicotinic acid (niacin): new lipid-independent mechanisms of action and therapeutic potentials. Trends Pharmacol Sci 2011; 32(12):700–7.

50. Chai JT, Digby JE, Choudhury RP. GPR109A and Vascular Inflammation. Curr Atheroscler Rep 2013; 15(5).

51. Offermanns S, Schwaninger M. Nutritional or pharmacological activation of HCA(2) ameliorates neuroinflammation. Trends Mol Med 2015; 21(4):245–55.

52. Jadeja RN, Jones MA, Fromal O, Powell FL, Khurana S, Singh N et al. Loss of GPR109A/HCAR2 induces aging-associated hepatic steatosis. Aging (Albany NY) 2019; 11(2):386–400.

53. Lukasova M, Malaval C, Gille A, Kero J, Offermanns S. Nicotinic acid inhibits progression of atherosclerosis in mice through its receptor GPR109A expressed by immune cells. J Clin Invest 2011; 121(3):1163–73.

54. Sun H, Li G, Zhang W, Zhou Q, Yu Y, Shi Y et al. Niacin Activates the PI3K/Akt Cascade via PKC- and EGFR-Transactivation-Dependent Pathways through Hydroxyl-Carboxylic Acid Receptor 2. PLoS ONE 2014; 9(11):e112310.

55. Rosales C. Neutrophil: A Cell with Many Roles in Inflammation or Several Cell Types? Front Physiol 2018; 9:113.

56. Kostylina G, Simon D, Fey MF, Yousefi S, Simon HU. Neutrophil apoptosis mediated by nicotinic acid receptors (GPR109A). Cell Death Differ 2008; 15(1):134–42.

57. Oeckinghaus A, Ghosh S. The NF-κB Family of Transcription Factors and Its Regulation. Cold Spring Harb Perspect Biol 2009; 1(4).

58. Sharma D, Parameswaran N. Multifaceted role of β-arrestins in inflammation and disease. Genes Immun 2015; 16(8):499–513.

59. Tak PP, Firestein GS. NF-κB: a key role in inflammatory diseases. J. Clin. Invest. 2001; 107(1):7–11.

60. Witherow DS, Garrison TR, Miller WE, Lefkowitz RJ. -Arrestin inhibits NF- B activity by means of its interaction with the NF- B inhibitor I B. Proceedings of the National Academy of Sciences 2004; 101(23):8603–7.

61. Baker RG, Hayden MS, Ghosh S. NF-κB, Inflammation, and Metabolic Disease. Cell Metabolism 2011; 13(1):11–22.

62. Li Z, McCafferty KJ, Judd RL. Role of HCA2 in Regulating Intestinal Homeostasis and Suppressing Colon Carcinogenesis. Front Immunol 2021; 12:606384.

63. Chai JT, Digby JE, Ruparelia N, Jefferson A, Handa A, Choudhury RP. Nicotinic acid receptor GPR109A is down-regulated in human macrophage-derived foam cells. PLoS ONE 2013; 8(5):e62934.

64. Pike NB. Flushing out the role of GPR109A (HM74A) in the clinical efficacy of nicotinic acid. J Clin Invest 2005; 115(12):3400–3.

65. Cuadrado A, Nebreda AR. Mechanisms and functions of p38 MAPK signalling. Biochem J 2010; 429(3):403–17.

66. English J, Pearson G, Wilsbacher J, Swantek J, Karandikar M, Xu S et al. New insights into the control of MAP kinase pathways. Exp Cell Res 1999; 253(1):255–70.

67. Cargnello M, Roux PP. Activation and Function of the MAPKs and Their Substrates, the MAPK-Activated Protein Kinases. Microbiol Mol Biol Rev 2011; 75(1):50–83.

68. Kyriakis JM, Avruch J. Mammalian MAPK signal transduction pathways activated by stress and inflammation: a 10-year update. Physiol Rev 2012; 92(2):689–737.

69. Kwon WY, Suh GJ, Kim KS, Lee HJ, Jeong KY, Kwak YH et al. Niacin Suppresses the Mitogen-Activated Protein Kinase Pathway and Attenuates Brain Injury After Cardiac Arrest in Rats*. Critical Care Medicine 2013; 41(9):e223-e232.

70. Wang Z-Q, Wu D-C, Huang F-P, Yang G-Y. Inhibition of MEK/ERK 1/2 pathway reduces pro-inflammatory cytokine interleukin-1 expression in focal cerebral ischemia. Brain Research 2004; 996(1):55–66.

71. Schieven G. The Biology of p38 Kinase: A Central Role in Inflammation. Current Topics in Medicinal Chemistry 2005; 5(10):921–8. Available from: URL: http://dx.doi.org/10.2174/1568026054985902.

72. Liu Z, Cao W. p38 Mitogen-Activated Protein Kinase: A Critical Node Linking Insulin Resistance and Cardiovascular Diseases in Type 2 Diabetes Mellitus. EMIDDT 2009; 9(1):38–46.

73. Huang G, Shi LZ, Chi H. Regulation of JNK and p38 MAPK in the immune system: signal integration, propagation and termination. Cytokine 2009; 48(3):161–9.

74. Grimsey NJ, Lin Y, Narala R, Rada CC, Mejia-Pena H, Trejo J. G protein–coupled receptors activate p38 MAPK via a non-canonical TAB1–TAB2– and TAB1–TAB3–dependent pathway in endothelial cells. Journal of Biological Chemistry 2019; 294(15):5867–78.

75. Ganji SH, Kamanna VS, Kashyap ML. Niacin decreases leukocyte myeloperoxidase: Mechanistic role of redox agents and Src/p38MAP kinase. Atherosclerosis 2014; 235(2):554–61.

76. Guo Y-J, Pan W-W, Liu S-B, Shen Z-F, Xu Y, Hu L-L. ERK/MAPK signalling pathway and tumorigenesis (Review). Exp Ther Med 2020.

77. Lu N, Malemud CJ. Extracellular Signal-Regulated Kinase: A Regulator of Cell Growth, Inflammation, Chondrocyte and Bone Cell Receptor-Mediated Gene Expression. Int J Mol Sci 2019; 20(15).

78. Wong E, Xu F, Joffre J, Nguyen N, Wilhelmsen K, Hellman J. ERK1/2 Has Divergent Roles in LPS-Induced Microvascular Endothelial Cell Cytokine Production and Permeability. Shock 2021; 55(3):349–56.

79. Bost F, Aouadi M, Caron L, Even P, Belmonte N, Prot M et al. The Extracellular Signal-Regulated Kinase Isoform ERK1 Is Specifically Required for In Vitro and In Vivo Adipogenesis. Diabetes 2005; 54(2):402–11.

80. Shi Y, Lai X, Ye L, Chen K, Cao Z, Gong W et al. Activated niacin receptor HCA2 inhibits chemoattractant-mediated macrophage migration via Gβγ/PKC/ERK1/2 pathway and heterologous receptor desensitization. Sci Rep 2017; 7(1).

81. McDonald PH, Chow CW, Miller WE, Laporte SA, Field ME, Lin FT et al. Beta-arrestin 2: a receptor-regulated MAPK scaffold for the activation of JNK3. Science 2000; 290(5496). Available from: URL: https://pubmed.ncbi.nlm.nih.gov/11090355/.

82. Zhao H-F, Wang J, To S-ST. The phosphatidylinositol 3-kinase/Akt and c-Jun N-terminal kinase signaling in cancer: Alliance or contradiction? (Review). International Journal of Oncology 2015; 47(2):429–36.

83. Feng J, Lu S, Ou B, Liu Q, Dai J, Ji C et al. The Role of JNk Signaling Pathway in Obesity-Driven Insulin Resistance . DMSO 2020; Volume 13:1399–406.

84. Yin T, Sandhu G, Wolfgang CD, Burrier A, Webb RL, Rigel DF et al. Tissue-specific pattern of stress kinase activation in ischemic/reperfused heart and kidney. J Biol Chem 1997; 272(32):19943–50.

85. Imajo M, Tsuchiya Y, Nishida E. Regulatory mechanisms and functions of MAP kinase signaling pathways. IUBMB Life (International Union of Biochemistry and Molecular Biology: Life) 2006; 58(5-6):312–7.

86. Solinas G, Becattini B. JNK at the crossroad of obesity, insulin resistance, and cell stress response. Mol Metab 2016; 6(2):174–84.

87. Huang X, Liu G, Guo J, Su Z. The PI3K/AKT pathway in obesity and type 2 diabetes. Int. J. Biol. Sci. 2018; 14(11):1483–96.

88. T Weichhart, M D Säemann. The PI3K/Akt/mTOR pathway in innate immune cells: emerging therapeutic applications. Annals of the Rheumatic Diseases 2008; 67(Suppl 3):iii70-iii74. Available from: URL: https://ard.bmj.com/content/67/Suppl_3/iii70.

89. Mihaylova MM, Shaw RJ. The AMPK signalling pathway coordinates cell growth, autophagy and metabolism. Nat Cell Biol 2011; 13(9):1016–23.

90. Sag D, Carling D, Stout RD, Suttles J. Adenosine 5′-Monophosphate-Activated Protein Kinase Promotes Macrophage Polarization to an Anti-Inflammatory Functional Phenotype. J Immunol 2008; 181(12):8633–41.

91. Jeon S-M. Regulation and function of AMPK in physiology and diseases. Exp Mol Med 2016; 48(7):e245-e245.

92. Ye L, Cao Z, Lai X, Shi Y, Zhou N. Niacin Ameliorates Hepatic Steatosis by Inhibiting De Novo Lipogenesis Via a GPR109A-Mediated PKC–ERK1/2–AMPK Signaling Pathway in C57BL/6 Mice Fed a High-Fat Diet. The Journal of Nutrition 2020; 150(4):672–84.

93. Jones Em, Elliot Wh. The synthesis of nicotinuric acid by rat-kidney preparations. Biochem J 1959; 73:706–13.

94. Shen C, Sun Z, Chen D, Su X, Jiang J, Li G et al. Developing urinary metabolomic signatures as early bladder cancer diagnostic markers. OMICS 2015; 19(1):1–11.

95. Pfuhl P, Kärcher U, Häring N, Baumeister A, Tawab MA, Schubert-Zsilavecz M. Simultaneous determination of niacin, niacinamide and nicotinuric acid in human plasma. J Pharm Biomed Anal 2005; 36(5):1045–52.

96. Figge HL, Figge J, Souney PF, Sacks FM, Shargel L, Janosik JE et al. Comparison of excretion of nicotinuric acid after ingestion of two controlled release nicotinic acid preparations in man. J Clin Pharmacol 1988; 28(12):1136–40.

97. Stern RH. The role of nicotinic acid metabolites in flushing and hepatotoxicity. J Clin Lipidol 2007; 1(3):191–3.

98. Hsieh Y, Chen J. Simultaneous determination of nicotinic acid and its metabolites using hydrophilic interaction chromatography with tandem mass spectrometry. Rapid Commun. Mass Spectrom. 2005; 19(21):3031–6.

99. Ding RW, Kolbe K, Merz B, Vries J de, Weber E, Benet LZ. Pharmacokinetics of nicotinic acid-salicylic acid interaction. Clin Pharmacol Ther 1989; 46(6):642–7.

100. Nishida C, Ko GT, Kumanyika S. Body fat distribution and noncommunicable diseases in populations: overview of the 2008 WHO Expert Consultation on Waist Circumference and Waist-Hip Ratio. Eur J Clin Nutr 2010; 64(1):2–5.

101. Heinsen F-A, Fangmann D, Müller N, Schulte DM, Rühlemann MC, Türk K et al. Beneficial Effects of a Dietary Weight Loss Intervention on Human Gut Microbiome Diversity and Metabolism Are Not Sustained during Weight Maintenance. Obes Facts 2016; 9(6):379–91.

102. Mareike Täger, Jonas Peltner Silke Thiele. Evaluation of diet quality by means of the Healthy Eating Index and its modified variants; 2016 [cited 2021 May 5.527Z]. Available from: URL: https://www.ernaehrungs-umschau.de/english-articles/15-06-2016-evaluation-of-diet-quality-by-means-of-the-healthy-eating-index-and-its-modified-variants/.

103. Hanson J, Gille A, Zwykiel S, Lukasova M, Clausen BE, Ahmed K et al. Nicotinic acid–and monomethyl fumarate–induced flushing involves GPR109A expressed by keratinocytes and COX-2–dependent prostanoid formation in mice. J. Clin. Invest. 2010; 120(8):2910–9.

104. Tunaru S, Kero J, Schaub A, Wufka C, Blaukat A, Pfeffer K et al. PUMA-G and HM74 are receptors for nicotinic acid and mediate its anti-lipolytic effect. Nat Med 2003; 9(3):352–5.

105. Morgan AJ, Jacob R. Ionomycin enhances Ca2+ influx by stimulating store-regulated cation entry and not by a direct action at the plasma membrane. Biochem J 1994; 300(Pt 3):665–72.

106. Henderson S, Magu B, Rasmussen C, Lancaster S, Kerksick C, Smith P et al. Effects of Coleus Forskohlii Supplementation on Body Composition and Hematological Profiles in Mildly Overweight Women. J Int Soc Sports Nutr 2005; 2(2):54–62.

107. Bosshart H, Heinzelmann M. THP-1 cells as a model for human monocytes. Ann Transl Med 2016; 4(21):438.

108. Shenoy SK, Lefkowitz RJ. Seven-Transmembrane Receptor Signaling Through -Arrestin. Science Signaling 2005; 2005(308):cm10-cm10.

109. Yu E, Papandreou C, Ruiz-Canela M, Guasch-Ferre M, Clish CB, Dennis C et al. Association of Tryptophan Metabolites with Incident Type 2 Diabetes in the PREDIMED Trial: A Case–Cohort Study. Clinical Chemistry 2018; 64(8):1211–20.

110. Xie G, Ma X, Zhao A, Wang C, Zhang Y, Nieman D et al. The Metabolite Profiles of the Obese Population Are Gender-Dependent. J Proteome Res 2014; 13(9):4062–73.

111. Samad N. Serum levels of leptin, zinc and tryptophan with obesity: A case-control study. Pak J Pharm Sci 2017; 30(5):1691–6.

112. Cussotto S, Delgado I, Anesi A, Dexpert S, Aubert A, Beau C et al. Tryptophan Metabolic Pathways Are Altered in Obesity and Are Associated With Systemic Inflammation. Front Immunol 2020; 11.

113. Brandacher G, Winkler C, Aigner F, Schwelberger H, Schroecksnadel K, Margreiter R et al. Bariatric Surgery Cannot Prevent Tryptophan Depletion Due to Chronic Immune Activation in Morbidly Obese Patients. obes surg 2006; 16(5):541–8.

114. Raheja UK, Fuchs D, Giegling I, Brenner LA, Rovner SF, Mohyuddin I et al. In psychiatrically healthy individuals, overweight women but not men have lower tryptophan levels. Pteridines 2015; 26(2):79–84.

115. Sorgdrager FJH, Naudé PJW, Kema IP, Nollen EA, Deyn PP de. Tryptophan Metabolism in Inflammaging: From Biomarker to Therapeutic Target. Front Immunol 2019; 10.

116. Mangge H, Summers KL, Meinitzer A, Zelzer S, Almer G, Prassl R et al. Obesity-related dysregulation of the tryptophan-kynurenine metabolism: role of age and parameters of the metabolic syndrome. Obesity (Silver Spring) 2014; 22(1):195–201.

117. Matsuoka K, Kato K, Takao T, Ogawa M, Ishii Y, Shimizu F et al. Concentrations of various tryptophan metabolites are higher in patients with diabetes mellitus than in healthy aged male adults. Diabetol Int 2017; 8(1):69–75.

118. Wang TJ, Larson MG, Vasan RS, Cheng S, Rhee EP, McCabe E et al. Metabolite profiles and the risk of developing diabetes. Nat Med 2011; 17(4):448–53.

119. Chen T, Zheng X, Ma X, Bao Y, Ni Y, Hu C et al. Tryptophan Predicts the Risk for Future Type 2 Diabetes. PLoS ONE 2016; 11(9):e0162192.

120. Zuo J, Lan Y, Hu H, Hou X, Li J, Wang T et al. Metabolomics-based multidimensional network biomarkers for diabetic retinopathy identification in patients with type 2 diabetes mellitus. BMJ Open Diab Res Care 2021; 9(1):e001443.

121. Zhou S-S. Vitamin paradox in obesity: Deficiency or excess? WJD 2015; 6(10):1158.

122. Maguire O, O'Loughlin K, Minderman H. Simultaneous assessment of NF-κB/p65 phosphorylation and nuclear localization using imaging flow cytometry. Journal of Immunological Methods 2015; 423:3–11.

123. Bagaev AV, Garaeva AY, Lebedeva ES, Pichugin AV, Ataullakhanov RI, Ataullakhanov FI. Elevated pre-activation basal level of nuclear NF-κB in native macrophages accelerates LPS-induced translocation of cytosolic NF-κB into the cell nucleus. Sci Rep 2019; 9(1).

124. Young D, Willet F, Memberg WD, Murphy B, Walter B, Sweet J et al. Signal processing methods for reducing artifacts in microelectrode brain recordings caused by functional electrical stimulation. J Neural Eng 2018; 15(2):026014-.

125. Halls ML, Cooper DMF. Regulation by Ca2+-Signaling Pathways of Adenylyl Cyclases. Cold Spring Harb Perspect Biol 2011; 3(1).

126. Gautam J, Banskota S, Shah S, Jee J-G, Kwon E, Wang Y et al. 4-Hydroxynonenal-induced GPR109A (HCA2 receptor) activation elicits bipolar responses, Gαi -mediated anti-inflammatory effects and Gβγ -mediated cell death. Br J Pharmacol 2018; 175(13):2581–98.

127. Gaidarov I, Chen X, Anthony T, Maciejewski-Lenoir D, Liaw C, Unett DJ. Differential tissue and ligand-dependent signaling of GPR109A receptor: implications for anti-atherosclerotic therapeutic potential. Cell Signal 2013; 25(10):2003–16.

128. Sassone-Corsi P. The cyclic AMP pathway. Cold Spring Harb Perspect Biol 2012; 4(12).

129. Li G, Shi Y, Huang H, Zhang Y, Wu K, Luo J et al. Internalization of the Human Nicotinic Acid Receptor GPR109A Is Regulated by Gi, GRK2, and Arrestin3*. J Biol Chem 2010; 285(29):22605–18.

130. Tunaru S, Lättig J, Kero J, Krause G, Offermanns S. Characterization of determinants of ligand binding to the nicotinic acid receptor GPR109A (HM74A/PUMA-G). Mol Pharmacol 2005; 68(5):1271–80.

131. Meyers CD, Liu P, Kamanna VS, Kashyap ML. Nicotinic acid induces secretion of prostaglandin D2 in human macrophages: an in vitro model of the niacin flush. Atherosclerosis 2007; 192(2):253–8.

132. Mittal B. Subcutaneous adipose tissue & visceral adipose tissue. Indian J Med Res 2019; 149(5):571–3.

133. Gambhir D, Ananth S, Veeranan-Karmegam R, Elangovan S, Hester S, Jennings E et al. GPR109A as an Anti-Inflammatory Receptor in Retinal Pigment Epithelial Cells and Its Relevance to Diabetic Retinopathy. Invest Ophthalmol Vis Sci 2012; 53(4):2208–17.

134. Jadeja RN, Martin PM. GPR109A activation and aging liver. Aging (Albany NY) 2019; 11(19):8044–5.

135. Dixon LJ, Barnes M, Tang H, Pritchard MT, Nagy LE. Kupffer Cells in the Liver. Compr Physiol 2013; 3(2):785–97.

136. Clementi AH, Gaudy AM, van Rooijen N, Pierce RH, Mooney RA. Loss of Kupffer cells in diet-induced obesity is associated with increased hepatic steatosis, STAT3 signaling, and further decreases in insulin signaling. Biochim Biophys Acta 2009; 1792(11):1062–72.

137. Fu S-P, Liu B-R, Wang J-F, Xue W-J, Liu H-M, Zeng Y-L et al. β-Hydroxybutyric acid inhibits growth hormone-releasing hormone synthesis and secretion through the GPR109A/extracellular signal-regulated 1/2 signalling pathway in the hypothalamus. J Neuroendocrinol 2015; 27(3):212–22.

138. Rahman M, Muhammad S, Khan MA, Chen H, Ridder DA, Müller-Fielitz H et al. The β-hydroxybutyrate receptor HCA2 activates a neuroprotective subset of macrophages. Nat Commun 2014; 5:3944.

139. Inamadugu JK, Damaramadugu R, Mullangi R, Ponneri V. Simultaneous determination of niacin and its metabolites--nicotinamide, nicotinuric acid and N-methyl-2-pyridone-5-

carboxamide--in human plasma by LC-MS/MS and its application to a human pharmacokinetic study. Biomed Chromatogr 2010; 24(10):1059–74.

140. Berns JS. Niacin and related compounds for treating hyperphosphatemia in dialysis patients. Semin Dial 2008; 21(3):203–5.

141. Nabokina SM, Kashyap ML, Said HM. Mechanism and regulation of human intestinal niacin uptake. Am J Physiol Cell Physiol 2005; 289(1):C97-103.

9 Supplemental Information

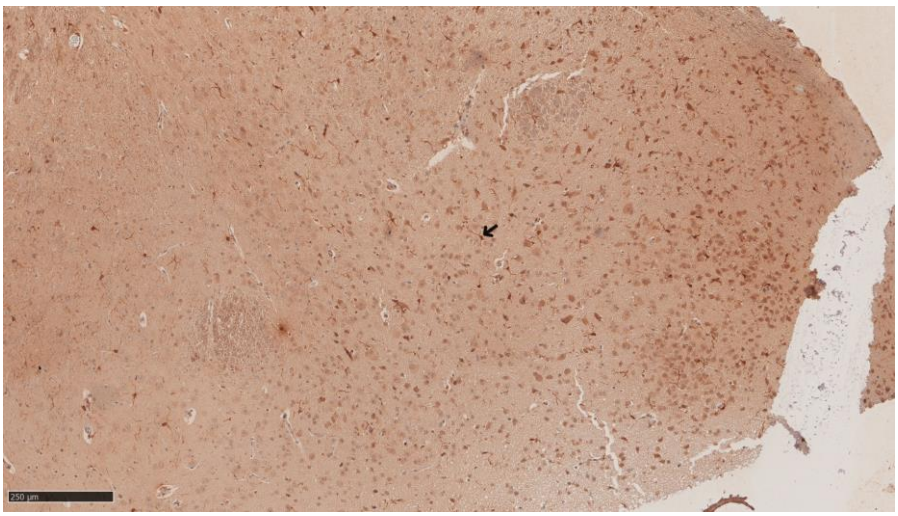

Figure S1: Immunohistochemical detection of microglia in hypothalamic tissue of RFP$^{+/+}$ mice: 5µm hypothalamic tissue samples were stained with Iba1 monoclonal antibody (1:500); scale=250µm; This shows one representative example out of two experiments.

Table S1: A high-fat diet (60% kcal from fat (lard)) (D12492) was used to induce obesity (DIO) in GPR109A$^{+/+}$ and GPR109A$^{-/-}$ mice. This diet was modified by the exclusion of TRP and NA.

Ingredient **Product number**	**U**	**HF, 0% Tryptophan, 0 ppm Niacin** **S8728-E714**
Corn starch, pre-gelatinized	%	12.000
Maltodextrin	%	7.000
Sucrose	%	18.450
Cellulose powder	%	4.200
L-Lysine HCl	%	1.800
DL-Methionine	%	0.700
L-Cystine	%	0.350
L-Threonine	%	0.900
L-Tryptophan	%	——
L-Arginine, free base	%	1.000
L-Histidine, base	%	0.450
L-Valine	%	0.900
L-Isoleucine	%	0.820
L-Leucine	%	1.200
L-Phenylalanine	%	0.750
L-Tyrosine	%	0.500
Glycine	%	2.500
L-Glutamic acid	%	3.000
L-Glutamine	%	1.000
L-Aspartic acid	%	0.350
L-Asparagine	%	1.000
L-Proline	%	0.400
L-Serine	%	0.350
L- Alanine	%	0.400
Vitamin premix	%	1.000

Mineral & trace element premix	%	3.500
Niacin	%	——
Na bicarbonate	%	0.200
Calcium phosphate, dibasic	%	0.400
Choline Cl	%	0.250
Soybean oil	%	1.000
Pork lard [1)]	%	18.000
Palm oil [1)]	%	16.000
Dye [yellow / green]	%	0.030
Proximate contents		
Crude protein (AA, N x 6.25)	%	16.2
Crude fat	%	35.0
Crude fibre	%	4.2
Crude ash	%	3.7
Starch	%	11.5
Sugar	%	19.4
Dextrin	%	6.9
Lysine	%	1.40
Methionine	%	0.68
Cystine	%	0.35
Threonine	%	0.88
Tryptophan	%	——
Niacin	mg/kg	——
Calcium	%	0.65
Phosphorus	%	0.40
Sodium	%	0.19
Magnesium	%	0.08
Potassium	%	0.52
Fatty acids		
C 12:0	%	0.04
C 14:0	%	0.39
C 16:0	%	11.47
C 18:0	%	3.20
C 16:1	%	0.56
C 18:1	%	14.08
C 18:2	%	3.69
C 18:3	%	0.26
Energy (Atwater) [2)]	MJ/kg	22.7
Protein	kcal%	12
Fat	kcal%	58
Carbohydrates	kcal%	30

[1)] Fat sources can be exchanged or varied

[2)] Physiological fuel value

Table S2: Kinetic pre-experiment: Effects of 100µM NUA on NF-κB p50 protein expression in THP-1 cells after 30min, 2 h, 4 h, 8 h or 24 h: Raw data of densitometry for NF-κB p50 protein expression after normalization (GAPDH).

NF-κB p50	**100µM NUA**				
Replication	**30min**	**2h**	**4h**	**8h**	**24h**
Control V1	100	100	100	100	100
Control V2	100	100	100	100	100
100µM NUA V1	126.190	68.726	101.995	90.795	77.197
100µM NUA V2	37.741	56.436	74.552	96.044	119.394

Table S3: Dose-response experiment: NF-κB p50 protein expression in THP-1 cells dependent on different doses of NUA (100µM, 500µM, 1mM, 5mM, 10mM) after 2h stimulation: Raw data of densitometry for NF-κB p50 protein expression after normalization (GAPDH).

NF-κB p50	2h					
Replication	**Control**	**100µM NUA**	**500µM NUA**	**1mM NUA**	**5mM NUA**	**10mM NUA**
V1	100	116.606	137.692	99.375	123.577	129.763
V2	100	87.545	111.904	175.678	185.659	128.223
V3	100	98.067	84.936	81.965	59.575	64.104
V4	100	137.946	175.503	192.474	150.656	143.771

Table S4: β-Arrestin1 phosphorylation, NF-κB p65 protein expression and phosphorylation in human primary monocytes after 100µM, 500µM NUA treatment (5min; 15min): Raw data of densitometry after normalization (β-Actin).

	5 min				15 min			
p-βArrestin1								
Replication	**Control**	**100µM NA**	**100µM NUA**	**500µM NUA**	**Control**	**100µM NA**	**100µM NUA**	**500µM NUA**
V1	100	418.012	245.041	703.443	100	0.000	19.737	38.180
V2	100	32.536	35.101	83.512	100	135.437	9.497	10.756
V3	100	427.015	664.460	1404.175	100	60.969	21.879	9.496
V4	100	173.812	309.355	17.194	100	231.422	57.524	103.598
NF-κB p65								
Replication	**Control**	**100µM NA**	**100µM NUA**	**500µM NUA**	**Control**	**100µM NA**	**100µM NUA**	**500µM NUA**
V1	100	232.610	199.307	243.098	100	78.761	47.952	82.505
V2	100	83.166	68.099	97.512	100	82.965	36.561	82.248
V3	100	223.584	265.626	168.874	100	103.933	77.711	88.552
V4	100	93.356	163.223	149.112	100	110.146	74.687	53.767
V5	100	79.649	101.999	99.356	100	102.117	48.666	65.185
p-NF-κB p65								
Replication	**Control**	**100µM NA**	**100µM NUA**	**500µM NUA**	**Control**	**100µM NA**	**100µM NUA**	**500µM NUA**
V1	100	230.046	196.722	220.469	100	62.330	40.678	69.515
V2	100	76.914	67.097	102.216	100	190.681	71.272	183.702
V3	100	332.066	270.109	165.885	100	189.570	107.294	125.233
V4	100	163.646	277.477	233.524	100	71.470	48.404	25.380
V5	100	118.007	133.143	142.133	100	84.310	68.245	100.305

Table S5: Phosphorylation of the MAPKs p38, ERK1/2 and JNK[46/54] in human primary monocytes after 100µM, 500µM NUA treatment (5min; 15min): Raw data of densitometry after normalization (β-Actin).

	5 min				15 min			
p-p38								
Replication	**Control**	**100µM NA**	**100µM NUA**	**500µM NUA**	**Control**	**100µM NA**	**100µM NUA**	**500µM NUA**
V1	100	288.230	250.679	309.850	100	83.053	63.953	93.321
V2	100	89.720	79.316	117.973	100	69.304	25.996	84.694
V3	100	360.517	215.649	234.635	100	95.170	105.665	129.106
V4	100	102.272	527.219	172.802	100	65.562	54.010	36.247
V5	100	98.026	93.221	110.130	100	124.533	81.717	97.246
p-ERK1/2								
Replication	**Control**	**100µM NA**	**100µM NUA**	**500µM NUA**	**Control**	**100µM NA**	**100µM NUA**	**500µM NUA**
V1	100	361.659	237.741	334.065	100	72.842	50.157	97.422
V2	100	95.145	81.902	151.216	100	70.232	25.456	86.342
V3	100	214.291	173.714	161.063	100	97.637	95.319	135.174
V4	100	122.554	180.702	70.216	100	127.483	53.468	45.374
V5	100	95.700	101.216	96.118	100	130.533	72.320	99.049

p-JNK[46]								
Replication	**Control**	**100µM NA**	**100µM NUA**	**500µM NUA**	**Control**	**100µM NA**	**100µM NUA**	**500µM NUA**
V1	100	199.948	108.855	222.913	100	59.840	50.765	220.542
V2	100	102.111	80.695	197.884	100	141.967	23.924	106.093
V3	100	98.906	63.227	183.700	100	152.790	50.547	160.022
V4	100	134.352	227.109	78.950	100	65.946	46.476	56.601
p-JNK[54]								
Replication	**Control**	**100µM NA**	**100µM NUA**	**500µM NUA**	**Control**	**100µM NA**	**100µM NUA**	**500µM NUA**
V1	100	181.848	157.026	341.169	100	71.248	65.243	136.797
V2	100	118.968	176.607	166.930	100	80.834	32.785	59.384
V3	100	134.219	91.845	230.100	100	118.525	70.341	153.948
V4	100	50.739	127.174	81.269	100	25.811	59.452	22.846

Table S6: Phosphorylation of Akt in human primary monocytes after 100µM, 500µM NUA treatment (5min; 15min): Raw data of densitometry after normalization (β-Actin).

	5 min				**15 min**			
p-Akt								
Replication	**Control**	**100µM NA**	**100µM NUA**	**500µM NUA**	**Control**	**100µM NA**	**100µM NUA**	**500µM NUA**
V1	100	188.742	257.093	409.733	100	112.557	63.593	49.957
V2	100	89.309	74.379	133.236	100	46.834	13.773	71.912
V3	100	218.301	114.096	57.618	100	10.141	17.587	98.097
V4	100	73.217	310.009	78.861	100	64.197	36.930	30.868
V5	100	32.961	84.344	110.642	100	127.352	93.714	71.249

Table S7: Phosphorylation of AMPKα in human primary monocytes after 100µM, 500µM NUA treatment (5min; 15min): Raw data of densitometry after normalization (β-Actin).

	5 min				**15 min**			
p-AMPKα								
Replication	**Control**	**100µM NA**	**100µM NUA**	**500µM NUA**	**Control**	**100µM NA**	**100µM NUA**	**500µM NUA**
V1	100	254.267	203.699	334.764	100	94.828	56.473	98.577
V2	100	95.122	54.054	87.412	100	97.612	24.418	129.145
V3	100	518.719	349.871	261.340	100	105.688	89.923	168.610
V4	100	104.146	432.336	91.215	100	20.357	52.440	26.056
V5	100	52.213	40.815	54.830	100	74.460	49.120	45.737

10 Danksagung

Zu allererst gilt mein Dank Herrn Prof. Matthias Laudes, der es mir ermöglicht hat dieses spannende Projekt durchzuführen. In den 3 Jahren, der produktiven Zusammenarbeit, hatte er immer ein offenes Ohr für mich und hat es ermöglicht, dass dieses Projekt aus unterschiedlichen Blickwinkeln betrachtet wird, was es zu einer facettenreichen Arbeit gemacht hat, die mir viel Freude bereitet hat.

Mein weiterer Dank gilt natürlich allen meinen Kollegen aus unserer Arbeitsgruppe. Es hat mir sehr viel Spaß mit ihnen gemacht und wir konnten uns immer gegenseitig unterstützen. Hierbei natürlich vor allem ein Dank an Frau Kathrin Türk und ihr Organisationstalent. Auch möchte ich Herrn Prof. Dominik Schulte für den tollen Austausch im Montagskolloquium und seine Unterstützung danken.

Ein besonderer Dank gilt vor allem Frau Katharina Hartmann, Frau Dr. Kristina Schlicht und Frau Dr. Ina Suhrkamp, welche sehr geduldig mit mir waren und mir sehr viel beigebracht haben. Ob es sich um die 1 Millionste Frage zu Konzentrationsrechnungen, Statistik oder die Korrektur dieser Arbeit handelte – sie standen mir stets zur Seite.

Des Weiteren möchte ich mich bei Herrn Prof. Ulrich Mrowietz für die Kooperation bedanken und natürlich auch bei Herrn Prof. Gerhard Schultheiß und Frau Sarah Vieten für ihre Unterstützung im Mausprojekt. Auch gilt mein Dank Frau Prof. Karin Schwarz, Herrn Dr. Tobias Demetrowitsch und Herrn Fynn Brix für die tolle Kooperation im Metabolomics-Projekt. Außerdem möchte ich Herrn Prof. Philip Rosentiel und Frau Maren Reffelmann aus dem IKMB, als auch Herrn Prof. Ralph Lucius und Frau Katrin Masuhr aus dem Institut für Anatomie für die super Zusammenarbeit danken.

Mein weiterer Dank gilt dem RTG, welches mich stets in meiner wissenschaftlichen Arbeit unterstützt und gefördert hat.

Ein großer Dank gilt vor allem auch meiner lieben Familie und meinen Freunden welche mir immer Kraft gegeben und Mut zugesprochen haben.